



1990

Purification and Characterization of Two Oxidoreductases Involved in Bile Acid Modification by the Intestinal Anaerobe *Eubacterium* sp. VPI 12708

Clifton Franklund

Follow this and additional works at: <https://scholarscompass.vcu.edu/etd>

 Part of the [Medicine and Health Sciences Commons](#)

© The Author

Downloaded from

<https://scholarscompass.vcu.edu/etd/5597>

This Dissertation is brought to you for free and open access by the Graduate School at VCU Scholars Compass. It has been accepted for inclusion in Theses and Dissertations by an authorized administrator of VCU Scholars Compass. For more information, please contact libcompass@vcu.edu.

School of Basic Health Sciences
Virginia Commonwealth University

This is to certify that the dissertation prepared by Clifton Victor Franklund entitled "The Purification and Characterization of Two Oxidoreductases Involved in Bile Acid Modification by *Eubacterium* sp. VPI 12708" has been approved by his committee as satisfactory completion of the dissertation requirement for the degree of Doctor of Philosophy.


Director of Dissertation


Committee Member


Committee Member


Committee Member


Committee Member and
Department Chairman


Chairman of Graduate Committee


School Dean

December 20 1990

Date

Purification and Characterization of Two Oxidoreductases Involved in Bile Acid
Modification by the Intestinal Anaerobe *Eubacterium* sp. VPI 12708.

A dissertation submitted in partial fulfillment of the
requirements for the degree of Doctor of Philosophy
at Virginia Commonwealth University

by

Clifton Victor Franklund
B.A., Concordia College, 1984
M.S., North Dakota State University, 1986

Director: Dr. Phillip B. Hylemon, Professor,
Department of Microbiology and Immunology

Virginia Commonwealth University
Richmond, Virginia
December, 1990

DEDICATION

For my family, Carrie and Jennifer.

Their unflagging support, and love have seen me through the most difficult times, and encouraged me when I thought I could not go on. Any accolades or sense of achievement that may come as a result of the completion of this work are not mine, but ours.

ACKNOWLEDGEMENTS

I wish to express my deepest appreciation to my advisor, Dr. Phillip Hylemon, for his patience and guidance during the time I have spent in his laboratory. He has set an example of a research and teaching setting that I shall spend a career in an effort to emulate. Also, a heartfelt thanks to my committee members, Drs. Jan Chlebowski, John Monaco, Frank Macrina, and Richard Carchman for their time, effort and helpful suggestions. I am very indebted to Paloma de Prada and Dr. Steve Baron for their work on the kinetic characterization, and sequence analysis of the 7 α -HSDH, respectively. I also wish to thank all of the technicians in Dr. Hylemon's lab, but especially Elaine Studor for her help in handling the rabbits used in this work and in collecting polyclonal antibodies, and Pam Melone and Emily Gurley for always being there when I, or anyone, needed a little help and for keeping the lab running smoothly. I wish to recognize Tom Reynolds and the Molecular Biology Core Facility, who synthesized all of the oligonucleotides used in this study, and Dr. Bryan White who derived the N-terminal amino acid sequences of the two proteins described herein. Finally, I want to thank both Dr. Phillip Hylemon and the Department of Microbiology for the financial aid that they have extended to me. Without these resources (personal, physical, and financial) I could not have undertaken this work; I am deeply grateful for all their help.

TABLE OF CONTENTS

	Page
List of Tables	viii
List of Figures	ix
List of Abbreviations	xiii
Abstract	xvii
INTRODUCTION	1
The Gastrointestinal Tract and Its Microflora	1
Physiological Impact of the Intestinal Microflora on the Host	5
Bile Acid Structure, Nomenclature and Properties	7
Bile Acid Biosynthesis	11
Enterohepatic Circulation of Bile Acids	15
Microbial Modifications of Bile Acids	16
Physiological Significance of Bile Acid Biotransformations	32
STATEMENT OF PROBLEM AND OBJECTIVES	35
EXPERIMENTAL PROCEDURES	37
MATERIALS	37
Bile Acids	37
Radiochemicals	37

Enzymes	37
Chemicals and Other Supplies	37
Bacterial Strains and Bacteriophage	38
METHODS	39
Bacterial Culture Conditions	39
Enzyme Assay Conditions	39
Preparation of Cell Free Extracts	40
Purification of the 7 α -HSDH	40
Purification of the NADH:FOR	43
Electrophoresis Conditions	45
Native Molecular Mass Determinations	46
Characterization of Substrates and Inhibitors	46
Determination of Apparent Kinetic Constants	46
Amino Terminal Amino Acid Sequence Determination	47
Generation of Polyclonal Antibodies	47
Western Blot Analysis	48
Immunoinhibition Studies	48
Generation of Restriction Maps	49
Cloning of the 7 α -HSDH	49
Sequencing the 7 α -HSDH Gene	50
Northern Blot Analysis	50
Primer Extension Analysis	51

Protein and DNA Sequence Analysis	51
RESULTS	53
Purification of the 7 α -HSDH	53
Bile Acid Substrate and Pyridine Nucleotide Cofactor Specificity of the 7 α -HSDH	61
Apparent Kinetic Constants for the Purified 7 α -HSDH	65
Optimizing the pH for 7 α -HSDH Catalysis	68
Inhibitors of 7 α -HSDH Activity	68
Use of the Purified 7 α -HSDH for the Quantitation of Bile Acids	72
N-Terminal Amino Acid Sequence Analysis of the 7 α -HSDH	72
Cloning the Gene Encoding the 7 α -HSDH	72
Expression of the 7 α -HSDH in <i>Eubacterium</i> sp. VPI 12708 and <i>Escherichia coli</i>	87
Sequence Homology Between the 7 α -HSDH and Several Other Alcohol/Polyol Dehydrogenases	97
Purification of the NADH:FOR	113
Expression of the NADH:FOR in <i>Eu.</i> sp. VPI 12708	123
Effect of Various Compounds Upon NADH:FOR Activity	129
N-Terminal Amino Acid Sequence Analysis of the NADH:FOR	136
DISCUSSION	141
Purification and Characterization of the 7 α -HSDH	141
Cloning and Sequencing the 7 α -HSDH Gene	152
Purification and Characterization of the NADH:FOR	155

LITERATURE CITED	163
APPENDIX	
Structures of Bile Acids Used in This Study	181
VITA	185

LIST OF TABLES

Number	Title	Page
1	Purification of the 7α -HSDH	54
2	Bile Acid Substrate Specificity of the 7α -HSDH	63-64
3	Apparent Kinetic Constants for the Purified 7α -HSDH	67
4	Product Inhibition Patterns for the Purified 7α -HSDH	69
5	Effect of Sulfhydryl-Reactive and Metal Chelating Compounds Upon 7α -HSDH Activity	71
6	Activity of the 7α -HSDH Expressed in <i>Eu. sp</i> VPI 12708 and <i>E. coli</i>	88
7	Alignment Metrics for the Alcohol/Polyol Dehydrogenases as Compared to the Derived 7α -HSDH Sequence Using GAPS (UWGCG)	106
8	Purification of the NADH:FOR	114
9	Effect of Several Different Compounds Upon NADH:FOR Activity	135

LIST OF FIGURES

Number	Title	Page
1	Distribution of the Microflora in the Human GI Tract	3
2	The Structure of Bile Acids	9
3	The Pathway for Bile Acid Biosynthesis in Humans	14
4	Common Microbial Modifications of Bile Acids	18
5	The Samuelson Model for 7α -Dehydroxylation of Bile Acids	22
6	A Model for Bile Acid 7α -Dehydroxylation Involving an Initial Two-Step Oxidation	25
7	TLC Analysis of Bile Acid Products Formed by <i>Eu. sp. VPI 12708</i>	28
8	A New Model for 7α -Dehydroxylation in <i>Eu. sp. VPI 12708</i> Which Accounts for Allo-Bile Acid Formation	31
9	7α -HSDH DEAE-Cellulose Elution Profile	55
10	7α -HSDH Phenyl Sepharose Elution Profile	56
11	7α -HSDH Reactive Red Agarose Elution Profile	57
12	7α -HSDH DEAE-HPLC Elution Profile	58

13	SDS-PAGE of Protein Aliquots from the Purification of the 7 α -HSDH	60
14	Gel Filtration Elution Profile and Native Molecular Mass Determination of the Purified 7 α -HSDH	62
15	Hanes Plots of 7 α -HSDH Saturation Kinetics	66
16	Optimization of pH for the Activity of the Purified 7 α -HSDH	70
17	Quantitation of Free and Conjugated Bile Acids Using the 7 α -HSDH	74
18	N-Terminal Amino Acid Sequence of the Purified 7 α -HSDH and Homology to Several Other Alcohol/Polyol Dehydrogenases	76
19	Synthetic Oligonucleotide Probes and Chromosomal Restriction Map for the 7 α -HSDH	78
20	Determination of the 7 α -HSDH Gene Sequence	81-84
21	Calculated Structure for the Putative Terminator Region	86
22	SDS- and Native-PAGE of the 7 α -HSDH Expressed in <i>Eu. sp.</i> VPI 12708 and <i>E. coli</i>	90
23	Immunoinhibition of the Purified 7 α -HSDH Enzymatic Activity by Rabbit Polyclonal Antisera	92
24	Western Analysis of 7 α -HSDH Expression in <i>Eu. sp.</i> VPI 12708 and <i>E. coli</i>	94
25	Northern Analysis of 7 α -HSDH Transcription in <i>Eu. sp.</i> VPI 12708 and <i>E. coli</i>	96
26	Primer Extension Analysis of the 7 α -HSDH Start of Transcription	99

27	Alignment of the Derived Amino Acid Sequence for the 7 α -HSDH with Nine Other Alcohol/Polyol Dehydrogenases Using LINEUP/GAPS/PRETTY (UWGCG)	101-103
28	Relative Identity Between Several Alcohol/Polyol Dehydrogenases	104
29	Alignment of the Deduced Amino Acid Sequence for the 7 α -HSDH With Several Other Alcohol/Polyol Dehydrogenases Using COMPARE/DOTPLOT (UWGCG)	108-112
30	DEAE-Cellulose Elution Profile for the NADH:FOR	115
31	Cibacron Blue A Elution Profile for the NADH:FOR	117
32	DEAE-HPLC Elution Profile for the NADH:FOR	118
33	Phenyl-HPLC Elution Profile for the NADH:FOR (Form I)	119
34	SDS-PAGE of the NADH:FOR	121
35	Gel Filtration Elution Profile and Native Molecular Mass Determinations for the Purified NADH:FOR	122
36	Effect of the Purification Protocol Upon the DEAE-HPLC Elution Profile of the NADH:FOR	125
37	Phenyl-HPLC Elution Profile of the NADH:FOR (Form III)	126
38	Absorbance Spectra of Purified NADH:FOR Forms I and III	128
39	Native Gel Electrophoresis of the NADH:FOR	131
40	Western Analysis of NADH:FOR Expression in <i>Eu. sp. VPI 12708</i>	133

41	Immunoinhibition of the NADH:FOR Catalytic Activity by Rabbit Polyclonal Antisera	134
42	Similarities Between the N-Terminal Amino Acid Sequences and Proposed Reaction Mechanisms for the NADH:FOR and Enoate Reductase	138
43	Synthetic Oligonucleotide Probes and Chromosomal Restriction Map for the NADH:FOR	140
44	A Model for the Interaction Between the 7α -HSDH and 7α -Dehydroxylation in <i>Eu.</i> sp. VPI 12708	146
45	A Possible Model for the Presence of Multiple Forms of NADH:FOR Upon Elution From DEAE-HPLC	159

LIST OF ABBREVIATIONS

ATP	Adenosine 5'-Triphosphate
CFE	Cell Free Extract
CoA	Coenzyme A
CTP	Cytosine 5'-Triphosphate
DEAE	Diethylaminoethyl
DNA	Deoxyribonucleic Acid
DTT	Dithiothreitol
EDTA	Ethylenediamine-Tetraacetic Acid
EGTA	[Ethylenbis(oxyethylenē-nitrilo)]Tetraacetic Acid
FAD(H ₂)	Flavin Adenine Dinucleotide (Reduced)
FMN(H ₂)	Flavin Mononucleotide (Reduced)
FOR	Flavin Oxidoreductase
GI	Gastrointestinal
HPLC	High Performance Liquid Chromatography
HMG	β -Hydroxy- β -methylglutarate
HSDH	Hydroxysteroid Dehydrogenase
Kb	Kilo base pairs
MOPS	4-Morpholine Propanesulfonic Acid

NAD(H)	Nicotinamide Adenine Dinucleotide (Reduced Form)
NADP(H)	Nicotinamide Adenine Dinucleotide Phosphate (Reduced Form)
NBT	Nitro Blue Tetrazolium Dye
NEM	N-Ethylmaleimide
PAGE	Polyacrylamide Gel Electrophoresis
pCMB	Para-Chloromercuribenzoate
pCMS	Para-Chloromercuriphenyl Sulfonic Acid
PMS	Phenazine Methyl Sulfate
RNA	Ribonucleic Acid
SDS	Sodium Dodecyl Sulfate
Tris	Tris [hydroxymethyl] amino-methane

ENZYMES

ABBREV.	ENZYME NAME	SOURCE
<i>Eu7α</i> -HSDH	7 α -hydroxysteroid dehydrogenase	<i>Eubacterium</i> sp. VPI 12708 This study
<i>Eu</i> NADH:FOR	NADH:flavin oxidoreductase	<i>Eubacterium</i> sp. VPI 12708 This study
<i>Eu27K-1</i>	27 kDa cholate-inducible protein	<i>Eubacterium</i> sp. VPI 12708 Coleman <i>et al</i> [28]

- Eu27K-2* Possible isomer of 27K-1 *Eubacterium* sp. VPI 12708
White *et al* [179]
- Ca7 α -HSDH* 7 α -hydroxysteroid dehydrogenase *Clostridium absonum*
Dr. James Coleman
East Carolina University
(personal communication)
- BmGDH-A* Glucose dehydrogenase-A *Bacillus megaterium*
Heilmann *et al* [74]
- BmGDH-B* Glucose dehydrogenase-B *Bacillus megaterium*
Jany *et al* [89]
- Sh20 β -HSDH* 20 β -hydroxysteroid dehydrogenase *Streptomyces hydrogenans*
Marekov *et al* [120]
- Hs17 β -HSDH* 17 β -hydroxysteroid dehydrogenase Human placenta
Peltoketo *et al* [141]
- Hs15-HPGDH* 15-hydroxyprostaglandin dehydrogenase Human placenta
Krook *et al* [103]
- KaRDH* Ribitol dehydrogenase *Klebsiella aerogenes*
Dothie *et al* [36]
- DmADH* Alcohol dehydrogenase *Drosophila melanogaster*
Thatcher [170]
- Ck2-ENR* 2-enoate reductase *Clostridium kluyveri*
Kuno *et al* [104]

BILE ACIDS AND INTERMEDIATES

- Cholic Acid 3 α ,7 α ,12 α -trihydroxy-5 β -cholanoic acid
- Deoxycholic Acid 3 α ,12 α -dihydroxy-5 β -cholanoic acid
- Lithocholic Acid 3 α -hydroxy-5 β -cholanoic acid
- 7-oxo-Cholic Acid 3 α ,12 α -dihydroxy-7-oxo-5 β -cholanoic acid
- 7-oxo-Chenodeoxycholic Acid 3 α -hydroxy-7-oxo-5 β -cholanoic acid

3-oxo-Chenodeoxycholic Acid	7 α -hydroxy-3-oxo-5 β -cholanoic acid
3-oxo-Cholic Acid	7 α ,12 α -dihydroxy-3-oxo-5 β -cholanoic acid
3-oxo- Δ^4 -Cholic Acid	7 α ,12 α -dihydroxy-3-oxo-4-cholenoic acid
3-oxo- Δ^4 -Deoxycholic Acid	12 α -hydroxy-3-oxo-4-cholenoic acid
3-oxo- $\Delta^{4,6}$ -Deoxycholic Acid	12 α -hydroxy-3-oxo-4,6-choldienoic acid
Allo-Deoxycholic Acid	3 α ,12 α -dihydroxy-5 α -cholanoic acid
3-oxo-Allo-Deoxycholic Acid	12 α -hydroxy-3-oxo-5 α -cholanoic acid
Hyocholic Acid	3 α ,6 α ,7 α -trihydroxy-5 β -cholanoic acid
Ursocholic Acid	3 α ,7 β ,12 α -trihydroxy-5 β -cholanoic acid
Ursodeoxycholic Acid	3 α ,7 β -dihydroxy-5 β -cholanoic acid
3-Deoxycholic Acid	7 α ,12 α -dihydroxy-5 β -cholanoic acid
α -Muricholic Acid	3 α ,6 β ,7 α -trihydroxy-5 β -cholanoic acid
β -Muricholic Acid	3 α ,6 β ,7 β -trihydroxy-5 β -cholanoic acid

Glycine and taurine conjugates of these bile acids would retain the nomenclature for the bile acid nucleus described above, but would be referred to as cholan-24-N-(carboxymethyl)-amides, and cholan-24-N-(2-sulfoethyl)-amides, respectively, in place of cholanoic acid, which is used to denote free bile acids.

Purification and Characterization of Two Oxidoreductases Involved in Bile Acid Modification by Eubacterium sp. VPI 12708.

ABSTRACT

A dissertation submitted in partial fulfillment of the requirements for the degree of Doctor of Philosophy at Virginia Commonwealth University.

Clifton Victor Franklund

Virginia Commonwealth University

Advisor: Dr. Phillip B. Hylemon

Two enzymes, a 7α -hydroxysteroid dehydrogenase (7α -HSDH) and an NADH-dependent flavin oxidoreductase (NADH:FOR), have been purified to apparent electrophoretic homogeneity from the intestinal anaerobe *Eubacterium* sp. VPI 12708. Using a protocol consisting of four chromatographic separations, the 7α -HSDH was purified by a factor of over 1200-fold with more than a 30% final recovery. Subunit molecular mass was estimated to be 32 Kdal by SDS-PAGE, while native molecular mass estimates from gel filtration were 124 Kdal. The purified 7α -HSDH was able to utilize a variety of bile acids containing an unhindered 7α -hydroxy moiety as substrates, existing either as free acids or glycine or taurine conjugates. The presence of an oxo moiety at position 3 or 12 profoundly altered the kinetic values for this enzyme.

The structural gene for the 7α -HSDH was cloned on a 3.8 Kb *KpnI-PstI* fragment and was sequenced using the dideoxy chain termination method. An open reading frame of 798 bp encoding a 266 amino acid protein was detected. The N-

terminal amino acid sequence of the purified protein was identical to the first 22 amino acids predicted from the open reading frame. Putative transcriptional promotor and terminator regions along with a tentative ribosome binding site were also located. Northern blot analysis indicated that this protein was expressed constitutively on an approximately 1 Kb monocistronic message. During sequence analysis, the 7 α -HSDH was found to be highly homologous to several members of the short-chain, non-zinc alcohol/polyol dehydrogenase superfamily.

Using a five step protocol, the NADH:FOR was also purified to homogeneity. A final purification of greater than 500-fold with an 11% recovery was obtained. The purified protein had a subunit molecular mass of 72 Kdal and a native mass of 210 Kdal, suggesting that it exists either as a dimer or a trimer. Northern blot, Western blot, and activity stains of native gels all indicated that the NADH:FOR is a cholate-inducible protein. N-terminal amino acid sequence determination revealed a significant homology to enoate reductase from *Clostridium kluveri*. Since the enoate reductase is involved in the reduction of a variety of α/β unsaturated carboxylates, this homology may be indicative of the physiological function of the NADH:FOR in *Eu. sp* VPI 12708.

INTRODUCTION

The Microflora of the Gastrointestinal Tract: The gastrointestinal (GI) tract may be viewed as an open ecosystem existing under steady-state conditions. As in all biological systems, the GI tract is referred to as open because materials and energy are exchanged between the internal and external environment. This exchange process can be represented either by ingestion of food stuffs and elimination of waste products in the feces, or secretion of digestive fluids into the GI lumen and absorption of water, electrolytes, and nutrients from the lumen by the host organism. Since each physiologically distinct area of the GI tract is maintained at relatively constant physical conditions (ie. pH, temperature, osmotic pressure, and flow rate), the system may be considered to be steady-state. As a consequence of ingesting non-sterile substances, the GI tract is exposed to a variety of bacterial species, some of which are able to colonize specific regions. The normal, mature human GI tract contains an immense and diverse microbial population which is capable of interacting both with the material within the GI lumen and the host tissues themselves. Indeed, of the 10^{14} cells which comprise the adult human organism 9×10^{13} , or 90%, are bacteria [151]. The vast majority of these bacterial cells are distributed throughout the GI tract.

The GI tract is composed of five physiologically distinct regions: the

esophagus, stomach, small intestine, cecum, and large intestine [165]. In humans and other omnivorous/carnivorous mammals, however, the cecum is very underdeveloped and is generally not physiologically significant. Due to differences in physical conditions, each of the digestive regions harbors a microbial community which is unique both in size and composition. As shown in Figure 1, bacteria can be recovered from the luminal contents throughout the entire GI tract. In comparison to the upper GI (stomach, and small intestine), though, the lower GI tract (colon and rectum) contains the far greater fraction of the total bacterial population. However, the mere presence of colony-forming units at a site within the GI tract is not necessarily an indication of the autochthonous (indigenous) flora at that location. In assessing the flora at any site within the GI tract, it is necessary to distinguish between autochthonous bacteria and allochthonous (transient) bacteria, which do not contribute to the overall economy of the ecosystem. The autochthonous bacteria of the intestine are defined as those species capable of growing anaerobically, always found in normal subjects, located in a specific region, colonizing their habitat during succession in infant hosts, capable of maintaining a constant population in a climax community, and able to associate with the intestinal mucosa [5,40,150,160]. When using these criteria, the stomach is found to be essentially devoid of any indigenous bacteria [38]. The bacteria cultured from stomach contents, such as illustrated in Figure 1, are all considered to be allochthonous. This assertion is confirmed by the magnitude of the error bar (suggesting a large variation in population size), and the fact that the types of bacteria cultured differed substantially between individuals [127]. Likewise, the upper portions of the small intestine (duodenum and jejunum)

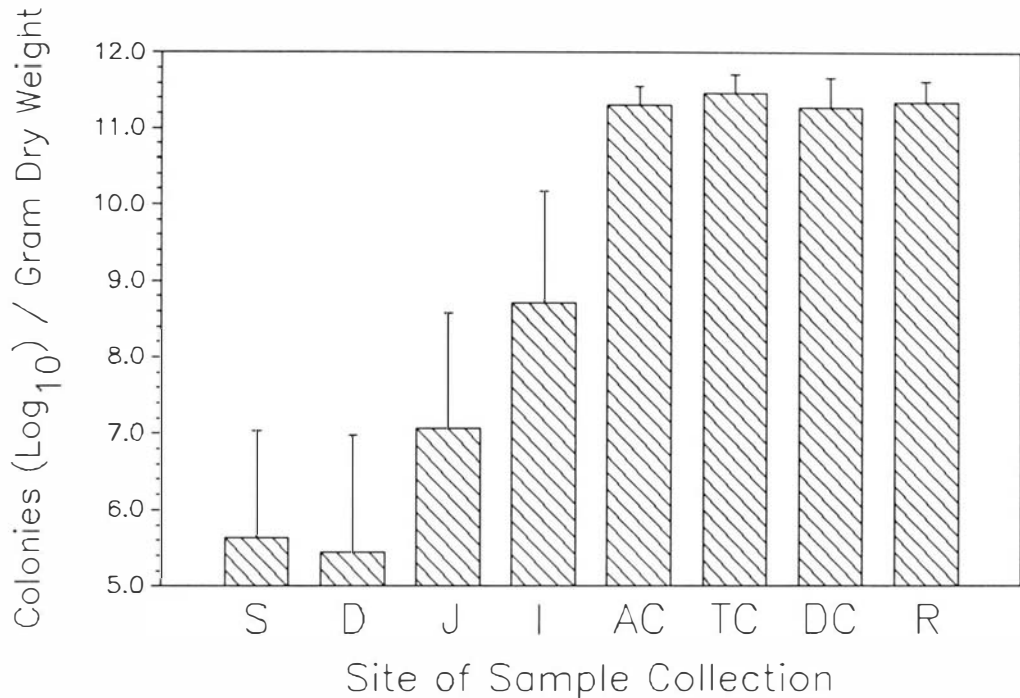


Figure 1: Distribution of the Microflora in the Human GI Tract. The anaerobic microbial population present in the luminal space at each region of the digestive tract was determined from five "healthy" individuals, within 4 hours of expiring. The areas of the GI tract are abbreviated as follows:

S: Stomach, D: Duodenum, J: Jejunum, I: Ileum, AC: Ascending Colon, TC: Transverse Colon, DC: Descending Colon, R: Rectum.

Data were taken from Moore *et al* [127], page 9. The values are represented as averages from five individuals ± Standard Deviation.

are also sparsely populated by bacteria. The species most frequently isolated from the duodenum and jejunum include *Streptococci*, *Staphylococci*, and *Lactobacilli* [151]. In contrast, the ileal bacterial population is more like that of the large bowel. The number of bacteria present has consistently been found to be greater than in either the duodenum or jejunum [37,38,56]. Furthermore, *Bacteroides*, *Bifidobacteria*, and enteric organisms are the predominant organisms cultured, with fewer *Streptococci* and *Lactobacilli* present [56]. The large intestine harbors, by far, the greatest proportion of the GI tract microflora and has received the most attention. For many years, the microflora of the large bowel was thought to be comprised of *Escherichia coli*, *Lactobacilli*, and a few facultative anaerobes. However, after the advent of techniques for the cultivation of strictly anaerobic bacteria, it is now recognized that the majority of the intestinal bacteria are indeed anaerobes, with facultative anaerobes such as *E. coli* constituting less than 1% of the total population [56]. The colon and rectum contain a very stable, climax community of microorganisms. The size of the population (approx 1×10^{11} bacteria per gram dry weight) and relative distribution of bacterial genera is constant over the length of this region. Using anaerobic techniques, several investigators have enumerated and identified the bacteria present in the large bowel [56,65,81,126]. Moore and Holdeman [126] estimated that over 400 species of bacteria are present in the feces of healthy humans. A preponderance of the bacteria identified were from the genera of *Bacteroides*, *Fusobacterium*, *Bifidobacterium*, *Eubacterium*, and *Peptostreptococcus* (all greater than 10^{10} colonies per gram). Lesser populations of *Clostridia*, and facultative anaerobes were also detected (10^8 to 10^9 colonies per gram). These bacteria most

likely encompass the majority of the autochthonous species present in the large intestine. Other significant indigenous populations of bacteria, however, may be associated with the intestinal epithelium and thus be underestimated by these studies.

Physiological Impact of the Intestinal Microflora on the Host: Although the size and composition of the intestinal microflora has been determined, the impact this community has upon the human host is largely unknown. Unlike the situation in ruminants and monogastric herbivores, the human microbial flora does not provide a significant contribution to the digestion of food stuffs for the host. The best data pertaining to the functions of the autochthonous microflora have come from studies using gnotobiotic (germ-free) animals. The absence of a bacterial population in the GI tract has a number of striking effects upon the host organism. The intestinal epithelial cell turnover rate is decreased in germ-free as compared to conventional mice (4 days vs. 2 days) [1], resulting in the formation of elongated intestinal villi. This may partially explain why the presence of a normal microflora impedes the growth rate of many animals. Epithelial cell functions are also altered by the microflora. The levels of several mucosal enzymes are depressed [32,144,180], and the absorption of nutrients [58,75], vitamins [58], and minerals [145] are decreased in conventional, as compared to germ-free animals. Overall intestinal motility is affected as well, being accelerated by the presence of the normal flora [2].

The development of the host immune system is also influenced by the presence of the intestinal flora. The secondary lymphatic tissues, such as the spleen and lymph nodes [12], of gnotobiotic animals tend to be under-developed. The Peyer's patches [1] and lamina propria [30,134] of germ-free animals are also

diminished in size and complexity. Additionally, secretory and serum immunoglobulin levels are depressed in germ-free animals by up to 10-fold [30]. All of these deficiencies are corrected by the colonization of germ-free animals by the indigenous microflora. The cell-mediated immune system functions, in contrast, are not affected by the presence or absence of the intestinal bacteria [13,59,161].

The presence of the autochthonous microflora also serves to protect against infection of the intestinal tract by potential pathogenic strains of bacteria. This was dramatically illustrated by Bohnhoff *et al.* [18]. After using streptomycin to eliminate a portion of the indigenous microflora, an increase in sensitivity to infection by *Salmonella* was observed; the ID₅₀ for the antibiotic treated animals decreased from 1,000,000 bacteria to just 10 bacteria per animal. The manner in which the normal flora exert this protective effect is not known. Several possible mechanisms have been suggested; including competition for carbon and energy sources or epithelial binding sites, and the production of bacteriocins or other toxic products by the members of the indigenous microflora.

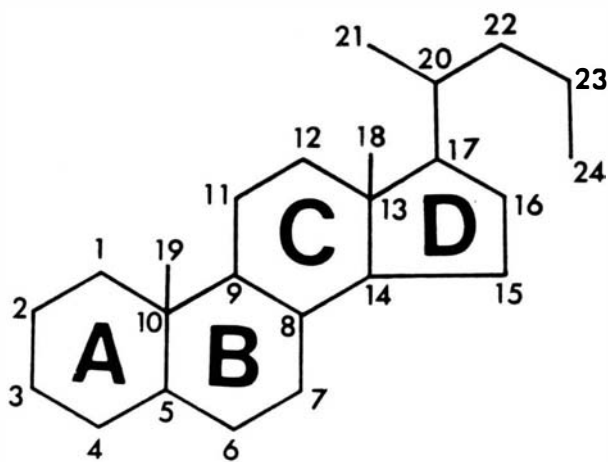
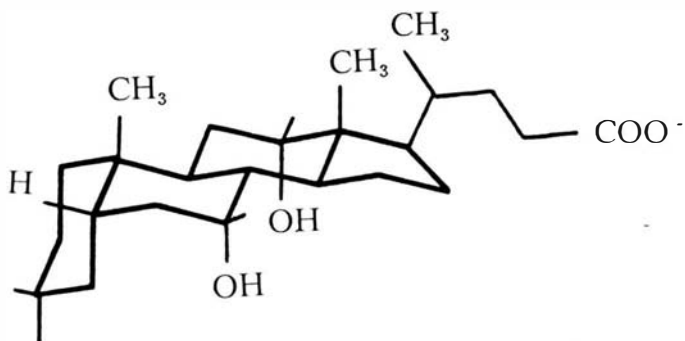
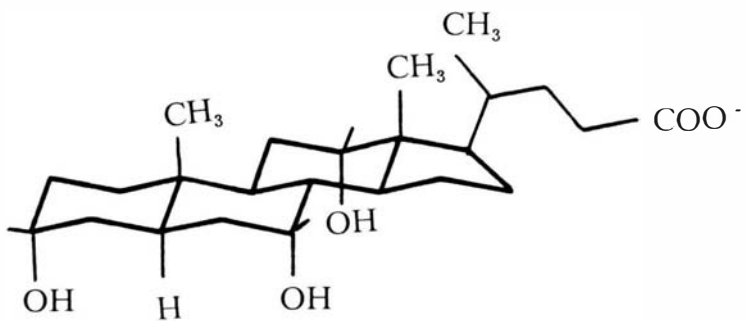
Finally, the members of the indigenous microflora are capable of chemically modifying a variety of compounds in the intestinal lumen. These modifications may result in the formation of new compounds which differ, both in their physicochemical properties and physiological effects, from their parent molecules. Several drugs and other xenobiotic compounds are known to be affected by microbial action in the intestine. Some drugs, such as sulfasalazine, are converted to a biologically active form by microbial action [142], while others, like digoxin, are inactivated [107]. Exogenous compounds derived from the diet may also be altered to form more toxic

products; this is exemplified by the production of nitrosamines from nitrites [100] and cyclohexamine from cyclamate [39]. Compounds of biological origin are also susceptible to microbial biotransformations. Cholesterol and other neutral steroids [19,109] are known to be extensively modified by the bacterial flora. Bile acids, too, are modified in the intestine, resulting in the formation of over 20 different metabolites [72,124]. Some of metabolites formed as a result of these modifications play an important role in the physiology of the host organism.

Bile Acid Structure, Nomenclature, and Properties: Bile acids are a class of steroids derived from cholesterol. Although bile acids comprised of 26, 27, or 28 carbons exist, the predominant series found in healthy human individuals and other higher mammals contains 24 carbons [70,121] and these shall be discussed exclusively in this dissertation. The bile acid nucleus is a saturated, four-ring structure comprised of three fused six carbon rings and one five carbon ring in a cyclopentanoperhydrophenanthrene arrangement. Projecting from this nucleus at carbons 10 and 13 are two methyl groups, and a five-carbon side chain which terminates with a carboxyl group at C-24 extends from carbon 17 (Figure 2A) [87,88]. The orientation of the methyl groups relative to the 4-ring nucleus is defined by convention as β ; adducts in this orientation should be thought of as projecting above the plane of the ring structure. Side groups in the opposite orientation are termed α , and are illustrated as broken or dotted lines as opposed to β , which are drawn as solid lines. Bile acids contain several chiral carbons and, therefore, are able to assume many stereoisomeric forms. Of particular importance is the orientation about carbon 5. If the hydrogen at C-5 is on the same face of the ring structure as the methyl group attached to C-10

FIGURE 2: The Structure of Bile Acids.

- A: A planar representation of the bile acid carbon skeleton. Carbons are numbered as previously assigned [87,88]. Each of the four rings are referred to by their corresponding letter.
- B: A Fisher representation of the 5β -bile acid, cholic acid.
- C: A Fisher representation of the 5α -bile acid, allo-cholic acid.

A**B****C**

(5- β cholane) the ring fusion is termed A/B *cis*. Conversely, when the hydrogen at C-5 is on the opposite face (5- α cholane) the ring fusion is A/B *trans*. All other ring fusions in the bile acid structure are *trans*. The overall difference of the structure of these stereoisomers may be seen in Figure 2B and C. The 5 β -bile ring structure, when viewed as a Fisher model, shows a sharp bend, bringing the hydroxyl groups into closer proximity to each other as compared to the 5 α -bile acids. The vast majority of bile acids formed in humans are 5 β bile acids. The 5 α -bile acids, termed allo-bile acids, assume a more planar conformation and are subsequently less polar. These bile acids account for less than 1% of the total bile acid pool in humans [48].

The bile acids are differentiated primarily by the number, position, and orientation of hydroxy groups on the basic ring structure described above, and the identity of any groups conjugated to the carboxyl group at C-24. The bile acids used in this dissertation will be primarily referred to by their trivial or common names. These names usually are derived from the Greek or Latin roots related to the origin or function of the molecule [73]. Examples of this include: ursocholic acid, urso=bear; hyocholic acid, hyo=pig; chenodeoxycholic acid, cheno=goose; and muricholic acid, murine=mouse. Bile acids conjugated to glycine or taurine at C-24 are given the prefixes glyco and tauro, respectively. Other prefixes are given to specific groups of bile acids; for example the names of the 5 α -bile acids are preceded by allo, while iso is used to identify 3 β -hydroxy bile acids. All trivial bile acid names used in this dissertation, along with their corresponding systematic names, are given in the List of Abbreviations. Planar representations of all bile acids and intermediates mentioned in the text are given in the Appendix.

As can be seen in Figure 2B and C, regardless of the orientation of the C-5 hydrogen, all the hydroxy groups of cholic acid lie on the opposite face of the ring structure from the methyl groups attached at C-10 and C-13. This spatial separation of hydrophilic and hydrophobic domains gives the bile acids the amphiphilic character essential for their role in lipid emulsification. As amphiphiles, bile acids are capable of forming both pure and mixed micelles under the appropriate physical conditions [48,159]. Most of the physicochemical properties of the bile acids, including the critical micellar concentration, critical micellar temperature, solubility, and relative hydrophobicity, are profoundly affected by the position and orientation of the hydroxy groups present [22,79]. The ionization state of bile acids is likewise affected by conjugation at C-24. Free bile acids have been determined to have a pK_a of about 5.0, while bile acids conjugated to glycine and taurine have pK_a values of 2.6 and <1 , respectively [22]. The bile acids, therefore, will be nearly completely deprotonated under most physiological conditions (approx pH 7). These physicochemical properties directly impact upon the physiological functions of the bile acids *in vivo* [80].

Bile Acid Biosynthesis: Since bile acids are synthesized from cholesterol by the liver cells, the formation and regulation of this precursor pool is important to the understanding of bile acid biosynthesis. The process by which acetate is converted into cholesterol can be divided into three stages [34]. In the first set of reactions acetyl coenzyme A (CoA) is converted to β -hydroxy- β -methylglutaryl-CoA (HMG-CoA). Up to this point the pathway is not committed to the formation of cholesterol. The committed, and rate limiting step in cholesterol biosynthesis is HMG-CoA

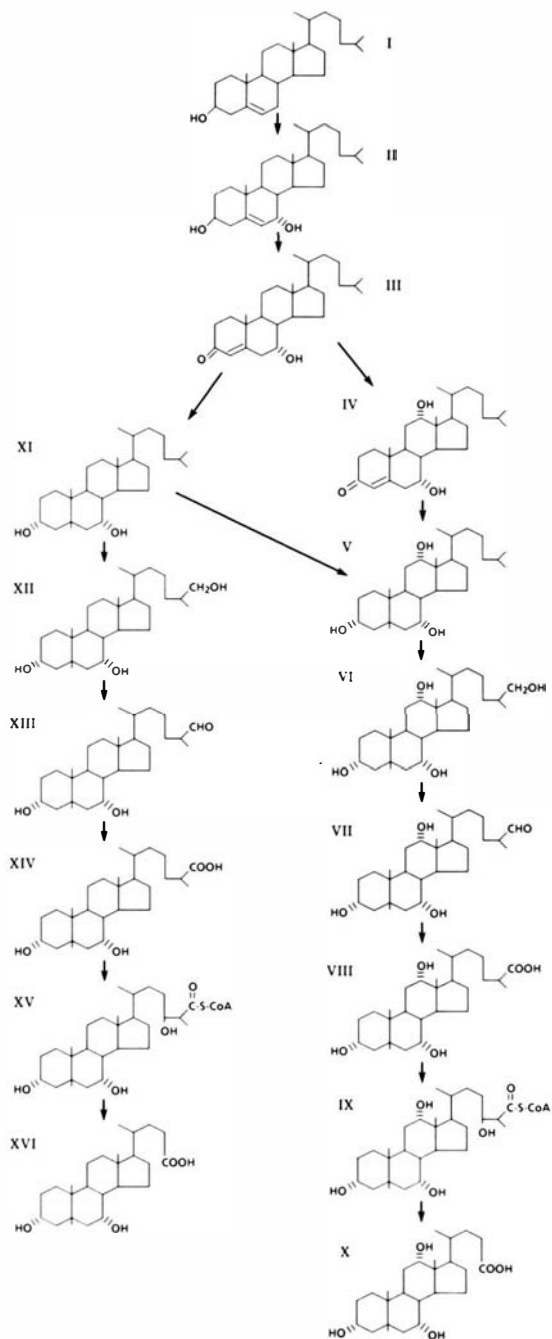
reductase, which cleaves the CoA and reduces HMG to mevalonate [147]. This enzyme is subject to exquisite regulation and has been extensively investigated. In addition to its role in cholesterol synthesis, mevalonate may serve as a precursor for the formation of docitol, ubiquinone, and isopentenyl adenine [181]. The second set of reactions involves the formation of squalene from mevalonate through a series of phosphorylation-condensation reactions. In the final set of reactions, squalene is converted into cholesterol by several membrane bound enzymes.

The pathways for the biosynthesis of the primary bile acids, cholic acid and chenodeoxycholic acid, are shown in Figure 3. The first, and rate limiting, step in bile acid formation is the introduction of a 7α -hydroxy group by cholesterol 7α -hydroxylase. This enzyme is a cytochrome P450-dependent monooxygenase [130] whose activity, like that of HMG-CoA reductase, is highly regulated. The 3β -hydroxy moiety of 7α -hydroxycholesterol is oxidized and the Δ^5 bond migrates to give a $3\text{-oxo-}\Delta^4$ -intermediate. An additional hydroxyl group may be added at position 12 by the action of a microsomal cytochrome P450 12α -hydroxylase [16]. A subsequent two step reduction results in epimerization of the hydroxyl at C-3 to yield either 5β -cholestane- $3\alpha,7\alpha$ -diol or 5β -cholestane- $3\alpha,7\alpha,12\alpha$ -triol. Finally, the aliphatic side chain is shortened through a multi-stepped oxidative cleavage process yielding the primary bile acids, cholic acid and chenodeoxycholic acid.

Bile acid biosynthesis is primarily regulated at two points: the 7α -hydroxylation of cholesterol, and the formation of cholesterol precursor molecules at HMG-CoA reductase. The regulation of these enzymes is similarly affected by many different physiological conditions [172]. Bile acids have long been thought to also be

FIGURE 3: Pathway for Bile Acid Biosynthesis in Humans. The mechanism for bile acid synthesis in humans is illustrated. Figure adapted directly from Vlahcevic *et al.* [172]. The steroid intermediates and products shown are:

I	cholesterol
II	7 α -hydroxycholesterol
III	7 α -hydroxy-4-cholesten-3-one
IV	7 α ,12 α -dihydroxy-4-cholesten-3-one
V	5 β -cholestane-3 α ,7 α ,12 α -triol
VI	5 β -cholestane-3 α ,7 α ,12 α ,26-tetrol
VII	3 α ,7 α ,12 α -trihydroxy-5 β -cholestanol-26-al
VIII	3 α ,7 α ,12 α -trihydroxy-5 β -cholestanoic acid
IX	3 α ,7 α ,12 α ,24-tetrahydroxy-5 β -cholestanoyl-CoA
X	cholic acid
XI	5 β -cholestane-3 α ,7 α -diol
XII	5 β -cholestane-3 α ,7 α ,26-triol
XIII	3 α ,7 α -dihydroxy-5 β -cholestanol-26-al
XIV	3 α ,7 α -dihydroxy-5 β -cholestanoic acid
XV	3 α ,7 α ,26-trihydroxy-5 β -cholestanoyl-CoA
XVI	chenodeoxycholic acid



involved in regulating their own biosynthesis through feedback inhibition. This argument has been strengthened by several recent bile acids feeding studies [76,77]. In these papers, the hydrophobic bile acids were demonstrated to inhibit 7α -hydroxylase and HMG-CoA reductase activities, as a function of their hydrophobicity. In contrast, the hydrophilic bile acids had no effect upon the activity of these enzymes.

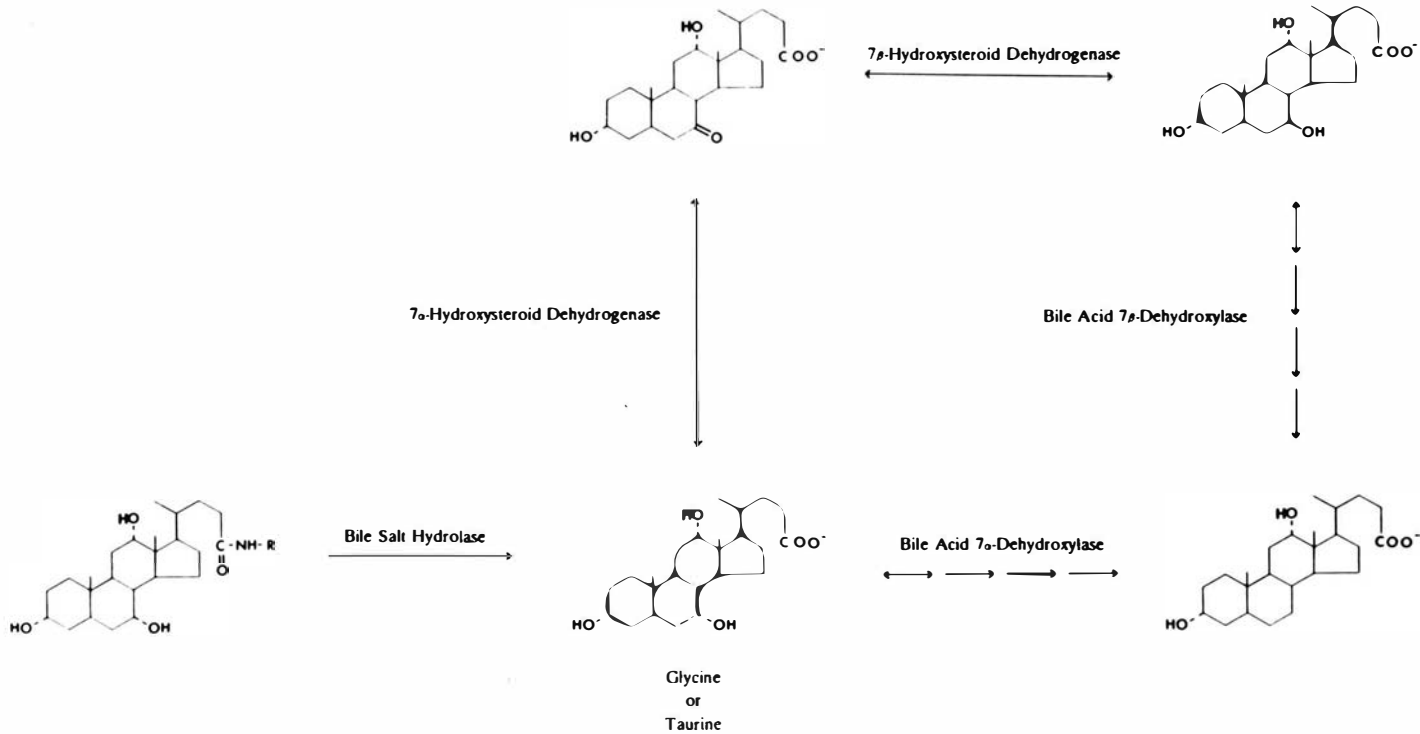
Enterohepatic Circulation of Bile Acids: After synthesis in the liver, bile acids are conjugated at C-24 to either glycine or taurine, and secreted with other substances into the hepatic biliary duct system. The hepatic bile is comprised of bile acids, cholesterol, phospholipids, bilirubin, and electrolytes in an aqueous solution [23]. The bile acids are the most abundant solute, being present at 20 to 30 mM concentrations [23]. This bile is subsequently stored and concentrated in the gallbladder. During digestion, as a result of physical and hormonal stimulation, the contents of the gallbladder are released into the duodenal lumen. In the duodenum and jejunum, bile acids aid in the solubilization and degradation of fatty materials. Conjugated bile acids are efficiently reabsorbed in the terminal ileum by an sodium-dependent, active transport system [60,82], while free bile acids are absorbed by simple diffusion throughout the intestinal tract. Although small amounts (400 to 600 mg/day) of bile acids are not absorbed and pass into the large intestine, the majority (> 95%) are absorbed by these processes during each passage through the intestine. Following absorption, the bile acids are returned to the liver by way of the portal hepatic vein. In the liver, hepatocytes efficiently extract the bile acids from the portal blood so that the total bile acid level in the systemic circulatory system is very

low [8]. The hepatocytes then reduce and re-conjugate any bile acid intermediates that may have been formed by microbial action. As a result of this enterohepatic circulation, the bile acid pool may be reused several times per day with relatively little resultant turnover.

Microbial Modifications of Bile Acids: During their transit through the intestinal tract, the primary bile acids come into intimate contact with the indigenous microbial flora. Using germ-free animals, it has been shown that these bacteria are responsible for the transformation of the primary bile acids into a number of metabolites [98,99]. The nature of the bacterial modifications are necessarily restricted by the reducing nature of the intestinal contents. The major types of reactions are represented in Figure 4, and include hydrolysis of the bile acid conjugate amide bond, the reversible oxidation and reduction of hydroxy groups, possibly resulting in their epimerization, and dehydroxylation (see references 72,83,85, and 109 for reviews).

The conjugated bile acids are remarkably resistant to enzymatic cleavage by the intestinal proteases. A wide variety of bacteria, however, possess the ability to cleave this amide bond to produce free bile acids and glycine or taurine. Bile salt hydrolase activity has been detected in the genera *Bacteroides*, *Bifidobacterium*, *Fusobacterium*, *Clostridium*, *Lactobacillus*, *Peptostreptococcus*, and *Streptococcus* [61,101,125,155], although its presence varies substantially between species. While most of these enzymes are able to utilize both glycine and taurine conjugates, some enzymes exhibiting specificity for the amino acid, or bile acid have been demonstrated [63,97,101,163]. Although bile salt hydrolases have been characterized in whole cells and cell-free extracts from several organisms, relatively few have been

FIGURE 4: Common Microbial Modifications of Bile Acids.



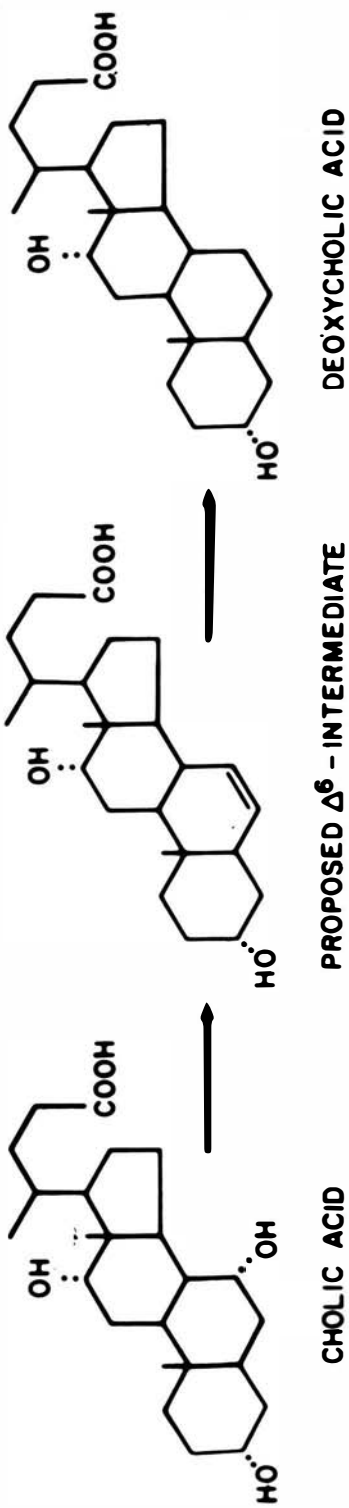
purified to homogeneity [63,97,163].

Many members of the intestinal microflora are also possess the ability to oxidize the hydroxy groups of bile acids in a pyridine nucleotide-dependent manner. Genera which have been found to express hydroxysteroid dehydrogenase (HSDH) activities include *Bacteroides*, *Bifidobacteria*, *Escherichia*, *Clostridia*, *Fusobacteria*, *Eubacterium*, and *Peptostreptococcus* [9,41,47,53,54,78,86,113,118]. These enzymes may be viewed as highly specialized secondary alcohol dehydrogenases. As a whole the HSDH's are extremely regio- and stereo-specific with respect to the hydroxy group oxidized. However, a broad range of substitutions are generally tolerated at other positions of the bile acid substrate. Bacteria have been isolated which produce enzymes capable of oxidizing bile acids at positions 3, 6, 7, and 12 in both the α and β orientations (for examples, see [3,44,51,69,112,171]). The 7α -HSDH, however, appears to be the most widely distributed representative [9]. This may reflect the fact that the 7α -hydroxy group is the most chemically reactive of these substitutions. The combined action of two HSDH's with the same regio- but opposite stereo-specificities (eg. 7α -HSDH and 7β -HSDH) can result in the epimerization of the hydroxy group. This has been demonstrated to occur both when a single bacterial strain expresses both enzymes [42,43] and in mixed cultures where these enzymes are possessed by different bacteria [111]. Like the bile salt hydrolases, few HSDH's have been purified to homogeneity. The HSDH's which have been characterized to date vary substantially with respect to subunit and native molecular mass, kinetic properties, cofactor specificity, and regulation. Therefore, it is not presently clear whether these enzymes are all related members of a secondary alcohol/polyol

dehydrogenase family or if, through convergent evolution, several different enzymes have arisen which are able to perform similar reactions.

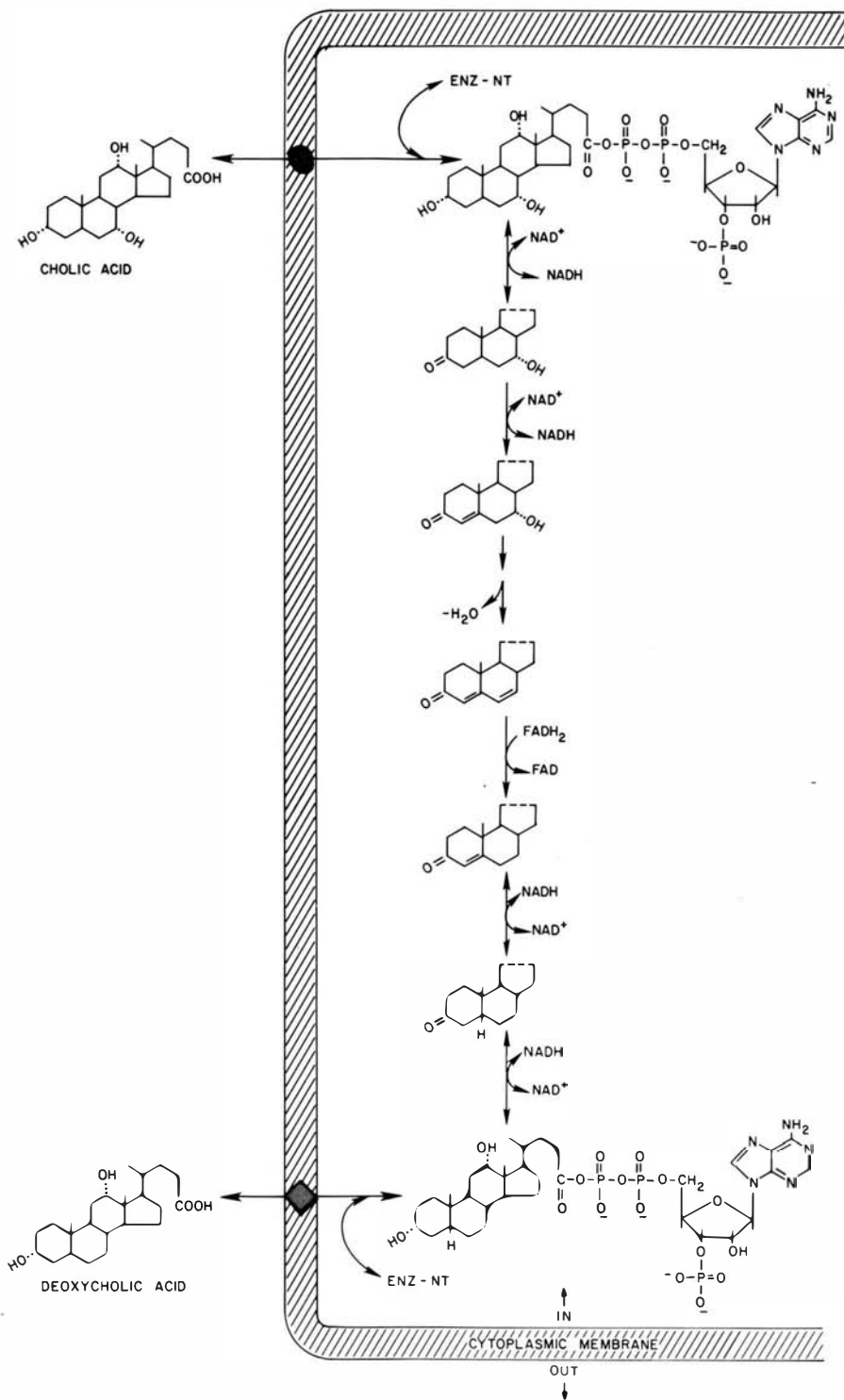
Arguably, the most physiologically important biotransformation of bile acids involves the removal of one of the hydroxy groups. In humans, bacterial 7 α -dehydroxylation of cholate and chenodeoxycholate is the sole pathway for the formation of the secondary bile acids deoxycholate and lithocholate, respectively. These two secondary bile acids have been demonstrated to account for up to 25% of the total human bile acid pool [157]. When compared to bile salt hydrolase and HSDH distribution, the number of intestinal bacteria able to 7-dehydroxylate bile acids is relatively small (10^3 to 10^5 bacteria per gram of feces) [54,164]. All of the known 7-dehydroxylating bacteria are Gram-positive, belonging to the genera *Eubacterium* and *Clostridium*. The reaction mechanism of 7 α -dehydroxylation was first examined by Samuelsson [148], using doubly labelled bile acids fed to conventional rats. Based upon the loss of radiolabel at the 6 β position, he proposed the two step model for dehydroxylation illustrated in Figure 5. The first step involves the *trans* elimination of water (*via* the loss of the 7 α -hydroxy and 6 β -hydrogen) to yield an unsaturated, Δ^6 bile acid intermediate. In the second step, the double bond is reduced, epimerizing the original hydrogens at positions 6 and 7, and yielding the appropriate secondary bile acid. *In vitro* support for this mechanism was provided by the demonstration that cell-free extracts of *Clostridium bifermentans* [55] and *Eubacterium* sp. VPI 12708 [174] were able to reduce chemically synthesized Δ^6 -intermediate to deoxycholic acid. The most detailed analysis of 7 α -dehydroxylation has been performed using *Eu.* sp. VPI 12708, which possesses a cholic acid-inducible

FIGURE 5: The Samuelsson Model for 7 α -Dehydroxylation of Bile Acids [148].



7-dehydroxylation activity [84]. Preliminary examination of the cofactor requirements of this reaction *in vitro* gave somewhat unexpected results [174,177]. The reduced pyridine nucleotide NADH inhibited the reaction, rather than stimulating the activity as expected. Moreover, NAD⁺ was found to stimulate both the reduction of the Δ^6 -intermediate and overall dehydroxylation. The reduction of the Δ^6 intermediate was also found to be stimulated by free, reduced flavins. These results suggest that one or more oxidative steps may be involved in this reaction, prior to the reduction of the Δ^6 unsaturated bile acid intermediate. Upon further examination of 7 α -dehydroxylation by cell free extracts, using radiolabeled bile acids, a water soluble, bile acid-nucleotide conjugate was discovered [27]. The nucleotide portion of this unique conjugate was shown to be ADP, while the bile acid moiety was identified by gas chromatography-mass spectrometry to be 3-oxo- Δ^4 deoxycholic acid. Based upon these results, a new reaction mechanism was proposed for 7 α -dehydroxylation (Figure 6). In this model, dehydroxylation is thought to involve an initial two step oxidation of cholic acid, forming 3-oxo-cholic acid, and 3-oxo- Δ^4 -cholic acid. A subsequent *trans* elimination of water would then result in the production of 3-oxo- $\Delta^{4,6}$ -deoxycholic acid. Following a three step reduction, the secondary bile acid, deoxycholic acid, would be formed. This model serves to explain both the enigmatic stimulation of dehydroxylation by oxidized NAD and the formation of the 3-oxo- Δ^4 -deoxycholic acid intermediate. It should also be pointed out that this reaction mechanism is completely compatible with the results reported by Samuelsson. Further evidence for the formation of a 3-oxo- Δ^4 -intermediate *in vitro* came from experiments using doubly labeled (either ¹⁴C-24, ³H-3 β , or ¹⁴C-24, ³H-5 β) cholic acid

FIGURE 6: A Model for Bile Acid 7 α -Dehydroxylation Involving an Initial Two-Step Oxidation [27].

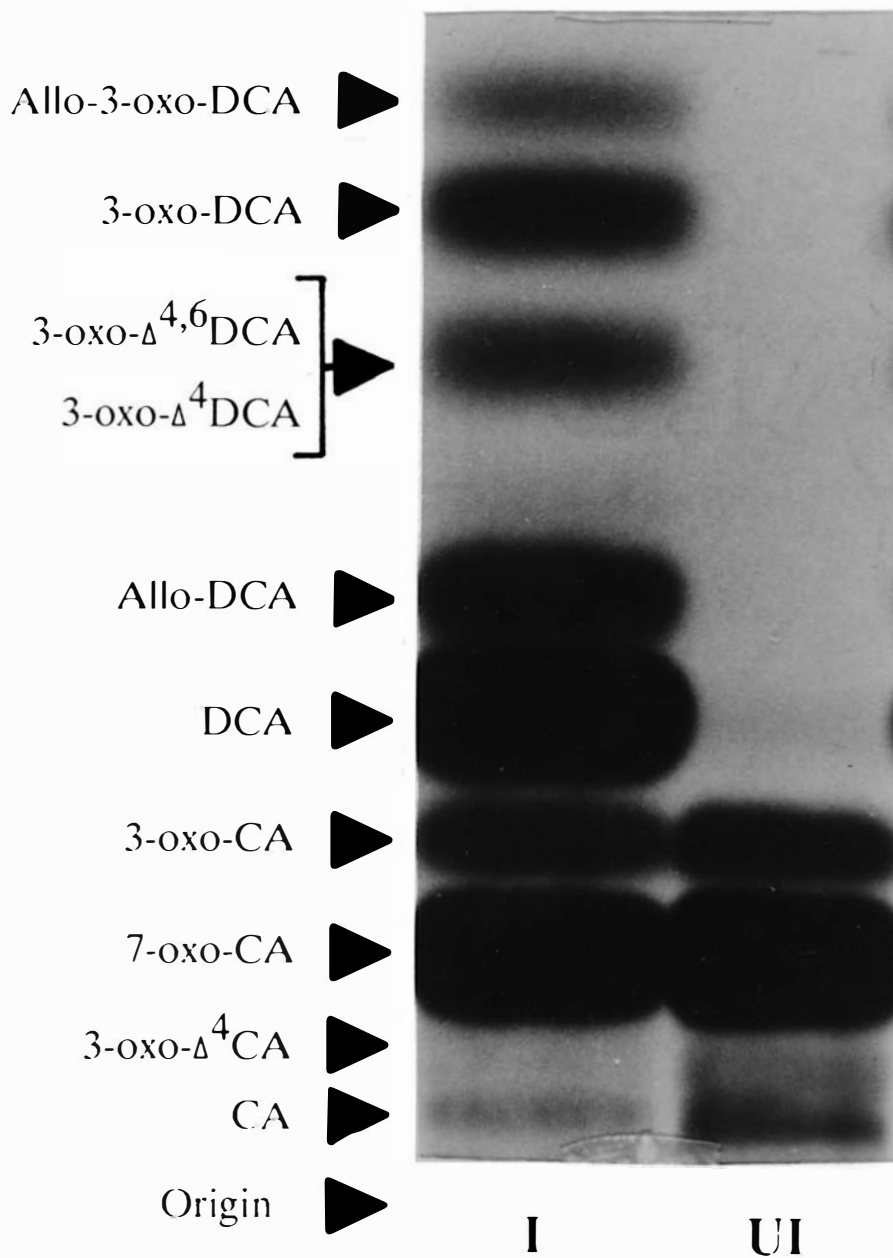


by whole cells and cell-free extracts of *Eu. sp.* VPI 12708. Dehydroxylation was reported to result in the loss of 80 to 85% of tritium at both the 3 β - and 5 β -positions [17]. In addition, cell-free extracts of *Eu. sp.* VPI 12708 were also demonstrated to be capable of forming deoxycholic acid *in vitro* when provided with each of the intermediates proposed in this pathway (Hylemon *et al.* accepted for publication *J. Lipid Res.* 1/91). The presence of a 3-oxo- Δ^4 -steroid structure is by no means unique to either 7 α -dehydroxylation or this particular intestinal anaerobe. Indeed, a similar intermediate is reported to be formed during the hepatic biosynthesis of bile acids (see Figure 3). The ability to reduce 3-oxo- Δ^4 -steroids has previously been demonstrated with both whole cells [10] and cell-free extracts [166] of other intestinal isolates. Additionally, several aerobic organisms have been shown to form 3-oxo- Δ^4 -cholic acid and 3-oxo- $\Delta^{4,6}$ -deoxycholic acid during the oxidative degradation of cholic acid [72,106]. Evidence for the importance of this mechanism of bile acid dehydroxylation *in vivo* was also obtained using doubly labeled cholic acid, after ingestion by human volunteers [17]. Based upon the loss of label at the 3 β - and 5 β -position it was estimated that at least 80 to 90% of the conversion of cholic acid to deoxycholic acid by the human intestinal microflora involves the formation of a 3-oxo- Δ^4 -intermediate.

During TLC analysis of 7 α -dehydroxylation bile acid end-products formed by this organism, several intermediates of unknown structure were discovered (Figure 7). Enzymatic analysis, combined with gas chromatography-mass spectroscopy, identified these products as allo-3-oxo-deoxycholic acid, and allo-deoxycholic acid. The presence of these allo-bile acid intermediates suggests that the hydrogen at C-5

FIGURE 7: TLC Analysis of the Bile Acid Products Formed by *Eu. sp.* VPI 12708. ¹⁴C-24 cholic acid was treated with either uninduced (UI) or cholic acid-induced (I) cell free extract as previously described [174]. The bile acid products were separated on TLC using solvent system S-1 of Eneroth [49].

The full names for the intermediates indicated are given in the List of Abbreviations. The structures for all bile acids and intermediates are illustrated in the Appendix.



can be epimerized during reduction of 3-oxo- Δ^4 -deoxycholic acid. Although the microbial production of allo-bile acids *via* this intermediate has been proposed previously [95,96], this represents the first demonstration of production of these bile acids as a result of dehydroxylation. The model for 7 α -dehydroxylation in this organism, as modified to account for this reaction is illustrated in Figure 8. This pathway may represent the primary source of human allo-bile acids. However, liver cells too, are capable of reducing 3-oxo- Δ^4 -bile acid intermediates undergoing enterohepatic circulation, and could be responsible for all-bile acid production in the human as well.

The 7 α -dehydroxylation of bile acids, as now proposed, should involve the coordinated activity of at least five or six specific enzymes. In *Eu. sp.* VPI 12708, several cholic acid-inducible polypeptides have been reported [174] which are thought to be involved in this process. Two of these, with molecular masses of 27 and 45 kDa, have been purified to homogeneity [26,137]. The 27 kDa protein was shown, by immunoinhibition, to be important for 7 α -dehydroxylation activity. The N-terminal amino acid sequence of this protein suggested that it was related to an alcohol/polyol dehydrogenase superfamily. Based upon these results, it has been proposed that the 27 kDa product is a 3 α -HSDH. Molecular genetic analysis of the 27 kDa protein gene revealed that multiple copies were present in the bacterial chromosome [179]. Three copies of this protein have since been cloned and sequenced [26,28,64,179]. Two of the genes (27K-1 and 27K-3) are identical and are transcribed on an approx 1 kb monocistronic message [28,179]. The third copy (27K-2) is about 80% identical to the nucleotide sequence of the others copies and nearly 90% homologous to

FIGURE 8: A New Model for 7 α -Dehydroxylation by *Eu. sp.* VPI 12708 Which Accounts for Allo-Bile Acid Formation.

their deduced amino acid sequences. The 27K-2, gene is transcribed as part of a 6 to 8 kb polycistronic message [178]. The function of the 45 kDa protein, which is also part of the large operon, is still unclear. A cholic acid-inducible NADH:flavin oxidoreductase is also expressed by *Eu. sp. VPI 12708*. This enzyme has previously been partially purified and characterized [108]. The physiological function of this protein is thought to be related to the production of free reduced flavins for the reduction of 3-oxo- $\Delta^{4,6}$ -deoxycholic acid to 3-oxo- Δ^4 -deoxycholic acid. To date, however, it has not been possible to unequivocally assign a catalytic activity to any of the cholic acid-induced proteins. Bacterial dehydroxylation of 7 β -hydroxy bile acids has also been reported [52,175]. However, the reaction mechanism for this biotransformation *in vivo* or *in vitro* has not been studied.

Physiological Significance of Bile Acid Biotransformations: The microbial modifications of bile acids have a direct impact upon their physicochemical properties. This, in turn, may alter the physiological effects exerted by these molecules. These changes have important implications for the host animal. For example, microbial modifications of bile acids are important in the regulation of human serum cholesterol levels. In general, the bacterial reactions described above (deconjugation, oxidation/reduction of hydroxy groups, and dehydroxylation) reduce the polarity and solubility of the bile acids. As a result, these products do not emulsify lipids as well [22,80], and are not themselves absorbed from the intestinal tract as efficiently as their parent compounds [23]. Hydrophobic bile acids have also been demonstrated to be potent regulators of both cholesterol and bile acid biosynthesis in the liver [76,77]. The combined action of reduced cholesterol and

lipid absorption, depression of HMG-CoA reductase activity, and the loss of bile acids from the enterohepatic circulation all act to reduce serum cholesterol levels. In addition, the more hydrophobic bile acids (especially the secondary bile acids, deoxycholic acid and lithocholic acid) are more toxic than their precursors [152]. The production of these toxic products may be partially responsible for the increased intestinal epithelial cell turnover rate and depressed growth rate seen in conventional animals as compared to germ-free animals. The secondary bile acids have also been postulated to be involved in the promotion of colon cancer [25,128].

The stability and composition of the intestinal microflora is also affected by bile acids biotransformations. Free bile acids, but not conjugated bile acids have been shown to inhibit both Gram-positive and Gram-negative bacteria [57]. Furthermore, the bile acid hydrophobicity was directly related to toxicity to bacteria. Oxidized bile acids, such as 7-oxo-cholic acid, has also been shown to be potentially bacteriocidal [169]. The production of secondary bile acids, then, may be involved in determining the composition of the autochthonous intestinal flora. Moreover, the presence of these compounds may be an important mechanism for the exclusion of pathogens from the intestinal tract.

The importance of these biotransformations to the bacteria which perform them are not precisely clear. It has been shown that the bile acid modifications performed by the intestinal anaerobes are a nutrient in nature [72]. Some bacteria capable of deconjugation, though, could conceivably utilize the liberated amino acids as a carbon and energy source. The primary function of these reactions is probably to achieve a selective advantage in the competitive environment of the intestinal

lumen. The oxidation and/or epimerization of bile acid hydroxy moieties may also ameliorate their relative toxicity to the bacterial flora. The pathway proposed for the 7α -dehydroxylation of bile acids may be physiologically significant for the bacteria carrying out this biotransformation. The two step oxidation, followed by a three step reduction, results in the net loss of one reducing equivalent. Therefore, the 3-oxo- $\Delta^{4,6}$ -deoxycholic acid during 7α -dehydroxylation may be thought of as a potential electron acceptor for these bacteria. The 7α -dehydroxylation of bile acids may, then, provide an alternative to proton reduction *via* NAD-ferredoxin oxidoreductase and hydrogenase, under unfavorable conditions, as described for other anaerobic bacteria [33,93].

STATEMENT OF PROBLEM AND OBJECTIVES

Eubacterium sp. VPI 12708 is an anaerobic intestinal bacterium which is capable of both oxidizing 7α -hydroxy bile acids to their corresponding 7-oxo-forms, and 7-dehydroxylating either 7α - or 7β -bile acids to give rise to secondary bile acids. The products of these reactions differ from the parent compounds both with respect to physicochemical properties and their physiological effects. However, the mechanism for these reactions as well as the identity and properties of the enzymes catalyzing them are poorly understood. A pathway for 7α -dehydroxylation of bile acids by *Eu.* sp VPI 12708 involving a two step oxidation, followed by dehydration, and a three step reduction has previously been proposed [27]. Such a scheme evokes the presence of at least four or five catalytic activities. Previous studies have also identified four cholate-inducible proteins formed by *Eu.* sp VPI 12708 (23 kDa, 27 kDa, 45 kDa, and 72 kDa) [174]. Additionally, a cholate-inducible NADH-dependent flavin oxidoreductase has been detected in cell free extracts and has been partially purified [108]. However, despite much effort, it has not been possible to assign catalytic functions to the cholate-inducible polypeptides.

The objectives of this study were to:

- 1) Purify the constitutive 7α -HSDH to electrophoretic homogeneity and characterize its physical and kinetic properties. The nature of the

interaction between the 7α -HSDH and the cholate-inducible dehydroxylation system was also to be examined.

- 2) Clone the gene for the 7α -HSDH into *E. coli* and determine if the gene product can be expressed in this organism.
- 3) Determine the nucleotide and derived amino acid sequence for the 7α -HSDH. Homology to other enzymes was evaluated using computer generated searches of protein data bases.
- 4) Purify the cholate-inducible NADH:FOR to electrophoretic homogeneity and characterize its physical and kinetic properties.

EXPERIMENTAL PROCEDURES

MATERIALS

Bile Acids: Cholate, Glycocholate, Glycodeoxycholate, Glycochenodeoxycholate, Glycoursodeoxycholate, Taurocholate, Taurodeoxycholate, Taurochenodeoxycholate, Tauroursodeoxycholate, 3-Deoxycholate, Tauro-3-Deoxycholate, 12-oxo-chenodeoxycholate were purchased from Calbiochem (San Diego, CA). 7 β -methyl-cholate and 7 β -methyl-chenodeoxycholate were generous gifts from E. H. Mosbach. All other bile acids were purchased from Steraloids (Wilton, NH).

Radiochemicals: Radiolabelled nucleotides, γ -³²P-ATP, α -³²P-CTP, and α -³⁵S-dATP were obtained from New England Nuclear (Boston MA).

Enzymes: Bacteriophage T4 polynucleotide kinase and ligase were purchased from Bethesda Research Laboratories (Gaithersburg, MD). Bovine pancreatic DNase was obtained from Sigma Chemical Company (St. Louis, MO). AMV reverse transcriptase, Sequenase and the ³⁵S-sequencing kits were obtained from United States Biochemical Corp. (Cleveland, OH). The restriction endonucleases used in this study were purchased from either BRL, Pharmacia (Piscataway, NJ), or International Biotechnologies Incorporated (New Haven, CT).

Chemicals and Other Supplies: The following materials were obtained from the

indicated sources. DTT, phenyl sepharose CL-4B, sepharose CL-6B, reactive red 120-agarose, acriflavine agarose, NAD-agarose attached either at C-8 or the ribose hydroxyls, reactive blue 4 agarose, reactive blue 72 agarose, reactive brown 10 agarose, reactive green 5 agarose, reactive green 19 agarose, reactive yellow 3 agarose, reactive yellow 86 agarose, native molecular mass standards, NAD⁺, NADH, NADP⁺, NADPH, FAD, EDTA, EGTA, iodoacetate, iodoacetamide, NEM, PMS, and NBT were purchased from Sigma. Acriflavine, Rotenone, and N-bromosuccinamide, were from J. T. Baker (Phillipsburg, NJ). Centiprep and centricon sample concentration cartridges, and Cibacron Blue A were purchased from Amicon (Danvers, MA). DE52 anion exchange resin was bought from Whatman (Clifton, NJ). SDS, glycine, high and low molecular weight, and pre-stained SDS-PAGE size standards, goat anti-rabbit antibodies conjugated to horseradish peroxidase, 4-chloro-1-naphthol, and nitrocellulose membranes were obtained from Biorad (Richmond, CA). XOMAT RP X-ray film, and pyronin Y, were from Kodak (Rochester, NY) All other chemicals were of the highest grade commercially available.

Bacterial Strains and Bacteriophage: *Eubacterium* sp. VPI 12708, an original intestinal isolate, was obtained from the culture collection of Dr. Phillip Hylemon. The culture was maintained both on chopped meat media under anaerobic conditions at 20°C and as 33% (v/v) glycerol stocks of broth cultures at -70°C. *Escherichia coli* strains DH5 α , and 1090r⁻ were obtained from BRL (Gaithersburg, MD) and Stratagene (La Jolla, CA), respectively, and maintained on LB plates containing appropriate antibiotics at 4°C. Bacteriophage λ gt11 and was also purchased from

Stratagene. Recombinant phage stocks were stored as clarified cell lysates in the presence of a small amount of chloroform at 4°C.

METHODS

Bacterial Culture Conditions: *Eubacterium* sp. VPI 12708 was cultured as previously described [176] except that the growth medium was modified by replacing Brain Heart Infusion broth with Tryptic Soy broth (30 g/l). One liter starter cultures grown to late log phase (16 hr) were diluted with 7 liters of fresh media in 8 liter carboys. Bacterial growth was monitored using a Klett-Summerson photoelectric colorimeter with a red (number 66) filter. If cultures were to be induced, 0.1 mM sodium cholate was added when the culture turbidity reached 30, 60, 90, and 120 Klett units. Cells were harvested by centrifugation (6,000 x g, 4°C, 30 min) when the turbidity reached 175 to 180 Klett units. Sixteen liters normally yielded 55 g of wet cell pellets. The cells were stored at -20°C for up to 10 days before use with no ill effects.

Enzyme Assay Conditions: The 7 α -HSDH and NADH:FOR assays were measured spectrophotometrically under aerobic conditions at 20°C by monitoring NAD(P)H production or utilization at 340 nm using either a Shimadzu UV160U or a Beckman model 35 recording spectrophotometer. Assays contained, in a final volume of 1 ml, the following:

7 α -HSDH (direction of bile acid oxidation): Sodium phosphate buffer (pH 8.5), 100 mM; NADP⁺, 0.1 mM; cholic acid, 0.1 mM, and an appropriate amount of enzyme.

7 α -HSDH (direction of bile acid reduction): Sodium phosphate buffer (pH 6.0), 100 mM; NADPH, 0.1 mM; 7-oxo-cholic acid, 0.1 mM, and an appropriate amount of enzyme.

Escherichia coli 7 α -HSDH assay: The NAD(H)-dependent 7 α -HSDH activity of *E. coli* was assayed as previously described [143]. The assays contained sodium phosphate buffer (pH 8.0), 100 mM; NAD⁺, 1.7 mM, cholic acid, 1.0 mM and an appropriate amount of enzyme.

NADH:FOR: Sodium phosphate buffer (pH 6.8), 100 mM; NADH, 0.15 mM; FAD, 0.15 mM; and an appropriate amount of enzyme.

Activities were based upon a molar extinction coefficient of $6.22 \times 10^3 \text{ M}^{-1} \cdot \text{cm}^{-1}$ for NAD(P)H.

Preparation of Cell Free Extract: Frozen cell pellets were resuspended in 20 ml of solution A (25 mM sodium phosphate (pH 6.8), 5% (v/v) glycerol, and 1 mM DTT) and disrupted with two passages through a French pressure cell (10,000 psi) at 4°C. Bovine pancreatic DNase I (approx 1 mg) was added between the two passages. Unbroken cells and cell debris were removed by centrifugation (105,000 $\times g$, 4°C, 120 min). The resulting supernatant was collected and dialyzed using cellulose dialysis tubing (12,000 to 14,000 MW cut off; American Scientific Products, McGraw Park, IL) against 4 liters of solution A for 16 hr.

Purification of the 7 α -HSDH: Unless otherwise noted, all purification steps were performed aerobically at 4°C. Protein concentrations were determined using either the dye-binding assay of Bradford [20], or approximated using the spectrophotometric method of Kalb and Bernlohr [94]. Total protein elution profiles for each

chromatographic separation were obtained by measuring the absorbance at 280 nm for each collected fraction. The 7 α -HSDH activity was measured in the direction of bile acid oxidation.

Step 1: DEAE-Cellulose Chromatography: DE-52 (40 g) was equilibrated with solution A giving a column of 2.5 x 20 cm. Dialyzed cell free extract was loaded onto the column at a flow rate of 1.2 ml/min. The column was then washed with 50 ml of solution A, Bound proteins were eluted with a 400 ml linear, increasing NaCl gradient (0 to 500 mM in solution A). Fractions were collected at 4 min intervals.

Step 2: Phenyl Sepharose Chromatography: Pooled DE-52 fractions were placed in a 250 ml beaker with a sufficient amount of solid ammonium sulfate to bring the solution to 30% saturation. This solution was stirred for 45 min at 4°C while the pH was maintained at 6.8 with the addition of 1 N ammonium hydroxide. The proteins were then loaded onto a phenyl sepharose column (1.5 x 20 cm) which was previously equilibrated with solution A containing ammonium sulfate at 30% saturation. The column was then washed with 50 ml of the equilibration buffer. Bound proteins were eluted with a 150 ml linear, decreasing gradient of ammonium sulfate (30% to 0% saturation) at a flow rate of 1 ml/min. Fractions were collected at 5 min intervals.

Step 3: Reactive Red-A Affinity Chromatography: Pooled phenyl sepharose fractions were placed in a 50 ml beaker and brought to pH 8.5 with the addition of 0.1 N NaOH. The proteins were then directly loaded onto

a reactive red 120 agarose column (1 x 3 cm) previously equilibrated with solution B (25 mM sodium phosphate (pH 8.5), 5% (v/v) glycerol, 1 mM DTT) at 20°C. Unbound proteins were removed by washing the column with 5 bed volumes of solution B. Loosely associated proteins were eluted with 5 bed volumes of solution B containing 250 mM NaCl. Specific elution of the 7 α -HSDH was effected using 2 bed volumes of solution B containing 250 mM NaCl and 10 mM NADP⁺. The flow rate for loading and all washes was 1.5 ml/min, with fractions collected at 1 min intervals.

Step 4: DEAE-HPLC Chromatography: Pooled reactive red fractions were concentrated to approx 5 ml using a centrprep 10 cartridge (Amicon; Danvers, MD). Salt and NADP⁺ were removed with 3, 10 ml washes of solution C (25 mM sodium phosphate (pH 7.5), 5% (v/v) glycerol, and 1 mM DTT), re-concentrating as above between washes. The equilibrated protein sample was applied to a pre-equilibrated Spherogel DEAE-3SW HPLC column (Beckman; Fullerton, CA), at a flow rate of 0.4 ml/min. The flow rate was increased to 0.85 ml/min when sample application was completed. Bound proteins were eluted with the following NaCl gradient in solution C; 0 to 100 mM NaCl in 10 min, 100 to 300 mM NaCl in 80 min, and 300 to 500 mM NaCl in 10 min. Fractions were collected at 1 min intervals. The protein elution profile was continuously monitored at 280 nm using a Beckman 164 variable wavelength detector.

Purification of the NADH:FOR: Unless otherwise noted all purification steps were performed aerobically at 4°C. The methods for protein determination and enzymatic assay of NADH:FOR are described above.

Step 1: DEAE-Cellulose Chromatography: A Whatman De-52 column was prepared and run exactly as described above.

Step 2: Reactive Red A Affinity Chromatography: Pooled DE-52 fractions were concentrated and desalted using a Centriprep 10 cartridge and described previously. The sample's pH was then brought to 8.5 and the proteins were loaded and eluted from the reactive red agarose column as above. The eluted 7 α -HSDH was saved for further purification and characterization studies.

Step 3: Cibacron Blue A Affinity Chromatography: The loading eluate (unbound proteins) from the reactive red agarose was collected and the pH adjusted to 7.0 by the addition of 0.1 N HCl. This solution was then loaded onto a Cibacron blue A (Amicon, Danvers, MD) column (1.5 x 10 cm) which was equilibrated with solution D (25 mM sodium phosphate buffer (pH 7.0), 5% (v/v) glycerol, and 1 mM DTT). Due to relatively poor binding of the NADH:FOR to this resin, multiple applications of the protein samples were necessary to achieve an acceptable recovery. This was accomplished by collecting the column eluate and re-applying it to the column an additional five times. After six total applications 75 to 80% of the originally detectable activity had been sequestered by the column. The column was then washed with

15 bed volumes of solution D to remove any unbound protein. Bound proteins were eluted with solution D containing 1 M KCl. All flow rates were about 1.0 ml/min and fractions were collected at 4 min intervals.

Step 4: DEAE-HPLC Chromatography: The pooled Cibacron blue A fractions were concentrated and desalted with solution D using a Centriprep 10 cartridge as described above. The equilibrated proteins were then loaded onto a Beckman Spherogel DEAE-3SW column and eluted as described above, except that the column was equilibrated with solution D (pH 7.0) instead of solution C (pH 7.5).

Step 5: Phenyl-HPLC Chromatography: Pooled DEAE-HPLC fractions were placed in a 250 ml beaker at 4°C and 20% (w/v) solid ammonium sulfate was added. The pH of the solution was maintained at 7.0 by the addition of 1 N ammonium hydroxide. The protein sample was then loaded at a flow rate of 0.4 ml/min onto a Spherogel Phenyl-5PW column (Beckman, Fullerton, CA) which had been equilibrated with solution D containing 20% (w/v) ammonium sulfate. After sample application was complete, the flow rate was increased to 1.0 ml/min. Bound proteins were eluted with a 40 min linear, decreasing ammonium sulfate gradient (20% (w/v) to 0%). The column was then washed for additional 10 min with solution D (no ammonium sulfate) to assure complete elution of most proteins. The NADH:FOR was then eluted by injecting 1.0 ml of solution D containing 10% (v/v)

ethanol over the column at a flow rate of 1.0 ml/min. Fractions were collected at 1.0 min intervals.

Electrophoresis Conditions: Slab gel sodium dodecyl sulfate polyacrylamide gel electrophoresis was performed at 20°C at a constant current of 1.5 mA/cm as described by Laemmli [105], except that 5% acrylamide stacking and 12% acrylamide separating gels were used. Gels were run until the bromphenol blue tracking dye reached the bottom of the separating gel (approx 3.5 hr). Proteins were visualized by staining with Coomassie R-250 in ethanol:acetic acid:water (25:7:68) for 2 hr. The gels were destained with the same solvent system without the Coomassie dye.

Native gel electrophoresis was performed in 7% acrylamide slab gels at 4°C using the buffers of Laemmli [105] except that SDS was omitted from all solutions. The tracking dye solution was also modified by the deletion of 2-mercaptoethanol. Protein samples were not boiled prior to loading onto the gel. Gels were run, and proteins were stained as described above. Activity stains for the 7 α -HSDH and NADH:FOR were derived from that for other oxidoreductases [153]. The 7 α -HSDH activity stained contained: 100 mM sodium phosphate buffer (pH 8.5), 1 mM cholic acid, 1 mM NADP⁺, 0.3 mg/ml NBT, and 0.02 mg/ml PMS. The NADPH generated by the 7 α -HSDH reduces the PMS, which in turn reduces the NBT dye to form a dark blue precipitate. The NADH:FOR activity stain contained: 100 mM sodium phosphate buffer (pH 6.8), 0.15 mM NADH, 0.15 mM FAD, and 0.3 mg/ml NBT. Note that there is no PMS in this activity stain (since NADH is used, the presence of PMS would turn the entire gel blue). In this case the NADH:FOR uses the NADH to reduce FAD which in turn may reduce the NBT dye directly to form a

dark blue precipitate.

Native Molecular Mass Determinations: A sepharose CL-6B gel filtration column (2.5 x 75 cm) was equilibrated with solution A containing 100 mM NaCl at a flow rate of 0.5 ml/min. The column void volume (V_o) was determined, as judged by the elution of blue dextran 2000, to be 153 ml. The column was calibrated using apoferritin (443 kDa), β amylase (200 kDa), alcohol dehydrogenase (150 kDa), albumin (66 kDa), carbonic anhydrase (29 kDa), and cytochrome C (12.4 kDa). A standard curve was obtained by plotting the log of molecular mass vs. relative elution volumes (V_e / V_o) as previously described [7,173]. Purified 7 α -HSDH and NADH:FOR were chromatographed as above, and their native molecular mass estimated from the standard curve.

Characterization of Substrates and Inhibitors: Bile acid substrates and cofactors for the 7 α -HSDH were screened at 1 mM final concentrations in the direction of bile acid oxidation or reduction as appropriate. Reactions were performed in triplicate and quantitated spectrophotometrically as described above.

Putative enzyme inhibitors were added to purified proteins in the assay buffer and allowed to incubate for 10 min at 20°C. Reactions were initiated with the addition of substrate. Percent inhibition of control activity was calculated from the average of three independent determinations.

Determination of Apparent Kinetic Constants: Kinetic constants were derived for the purified proteins using initial velocity saturation kinetics. While maintaining one substrate concentration at a constant value, the other substrate concentration was varied. A series of saturation curves at different constant substrate concentrations

were obtained in this manner. Primary plots of these data were generated using the method of Hanes [66]. Secondary plots using the apparent K_m , and V_{max} values derived from the primary plots ($[NADP^+]/V_{max}$ vs. $[NADP^+]$ and $[NADP^+]\cdot K_m/V_{max}$ vs. $[NADP^+]$) were made as described [29]. Unweighted first order linear regressions were used to calculate all plotted values. To compare the apparent kinetic constants for various substrates (bile acids or flavin compounds) the pyridine nucleotide cofactor concentration was maintained in great excess ($100 \times K_m$) while the bile acid or flavin concentrations were varied. At least five points, each the mean of three independent determinations, were used for each plot.

Product inhibition patterns were obtained for the 7α -HSDH by determining substrate saturation kinetics as above, in the presence of different constant concentrations of each end product. The primary plots were generated using the method of Hanes [66], and the inhibition patterns were evaluated (eg. competitive, non-competitive, or un-competitive).

Amino Terminal Amino Acid Sequence Determination: The purified proteins (approx 1 nmol) were extensively dialyzed against HPLC-grade water (Altech, Deerfield, IL) and concentrated to 200 μ l using a 2 ml centricon-10 concentrator (Amicon, Danvers, MA). The N-terminal amino acid sequences were determined by Dr. Bryan White in the Department of Animal Sciences, University of Illinois, Urbana-Champaign using an Applied Biosystems gas phase amino acid sequenator.

Generation of Polyclonal Antibodies: White, New Zealand male rabbits (2 kg) were obtained from Blue and Gray Rabbitry and housed in MCV animal resources facilities. A 20 ml sample of pre-immune blood was drawn from the ear, and the

serum was collected and saved at -20°C . The animals were initially challenged by injecting $100\ \mu\text{g}$ of purified protein, in Freund's Complete adjuvant, *i.m.* into the thigh. The antibody titer was boosted with two subsequent injections of $100\ \mu\text{g}$ of protein in Freund's Incomplete adjuvant at 3 week intervals. Immune serum was collected 1 week after the second boost. After it was ascertained that the antibody titer was sufficiently high, the animals were sacrificed by exsanguination, the immune serum collected, and stored at -20°C for further use.

Western Blot Analysis: Protein samples were loaded and run on 12% SDS-PAGE slab gels as described above, except that 0.01 % (w/v) pyronin Y was added to each sample to act as a lane marker. Prestained molecular mass markers were used for size determinations. The proteins were electrophoretically transferred to a nylon membrane. The rabbit polyclonal antisera were utilized as the primary antibody, while goat anti-rabbit antiserum conjugated to horse radish peroxidase was used as the secondary antibody. Bound anti-rabbit antibodies were visualized using 4-chloro-1-naphthol in the presence of 0.15% hydrogen peroxide.

Immunoinhibition Studies: The purified proteins were placed in assay buffer in the presence of different volumes pre-immune or immune sera. The mixtures were allowed to incubate for 15 min at 20°C . Enzymatic reactions were initiated with the addition of substrate, and quantitated spectrophotometrically as described above. Controls reactions with no additions were also performed. No 7α -HSDH or NADH:FOR activity was detected in the rabbit sera used. Ochterlony plates were prepared as previously described [136]. The center wells contained $100\ \mu\text{l}$ of serum while the test wells contained 4 mg of cholic acid-induced or uninduced cell-free

extract or 20 μg of purified NADH:FOR.

Generation of Restriction Maps: Total chromosomal DNA from *Eu. sp.* VPI 12708 was purified as previously described [122]. The DNA (10 μg) was treated with restriction endonucleases according to the manufacturer's specifications. The digested DNA was then separated by electrophoresis on 0.8% (w/v) agarose gels in TAE buffer [11]. Synthetic oligonucleotides, synthesized by the Molecular Biology Core Facility, were radiolabelled using ^{32}P -ATP and T4-polynucleotide kinase. The DNA was then either transferred to a nylon membrane by the method of Southern [162], and probed with the labelled oligonucleotide, or probed *in situ* after drying the gel [11]. The size of the hybridizing fragments was estimated from their migration relative to that of 1 kb ladder markers. Double digests using various restriction enzymes were used to order the fragments and to generate a rough, chromosomal restriction map.

Cloning of the 7 α -HSDH: Chromosomal DNA from *Eu. sp.* VPI 12708 was digested to completion with *EcoRI* and size fractionated on a 0.7% agarose gel. Fragments from 5 to 7 kb were excised from the gel and purified using a Qiagen kit (Dusseldorf, FRG) as described by the manufacturer. The purified fragments were then ligated to pre-digested $\lambda\text{gt}11$ DNA. Recombinant bacteriophage DNA was then packaged using GigaPack Gold kit as described by the manufacturer. The phage were plated on *E. coli* strain Y1090r⁻ and screened with a synthetic oligonucleotide probe. Several putative positive clones were plaque purified and one of these $\lambda\text{gt}11$ 1+ was characterized further. This clone possessed a 6 kb *EcoRI* insert from *Eu. sp.* VPI 12708. The *EcoRI* insert could not be efficiently excised from $\lambda\text{gt}11$ 1+. Therefore,

a 3.8 kb *KpnI-PstI* fragment was excised from this clone and purified as described above. This fragment, which contains approx 2.9 kb of *Eu. sp. VPI 12708* DNA and 0.9 kb of λ gt11 DNA, was ligated to pUC19 previously digested with *EcoRI* and *PstI*. The resulting clone, termed pBH51, contained the entire open reading frame for the 7 α -HSDH along with the putative transcriptional promotor and terminator regions.

Sequencing the 7 α -HSDH Gene: Qiagen purified plasmid DNA from pBH51 was used as a template for dideoxy-termination reactions using the method of Sanger [149]. The sequencing reactions were performed using Sequenase, essentially as described by the manufacturer. The synthetic oligonucleotide probe, 32-2, was used as the initial sequencing primer. After termination and denaturation of the reactions, the samples were run on 8% acrylamide sequencing gels in the presence of urea (45 cm x 0.25 mm to 0.5 mm wedge gels). The gels were then dried and exposed to XOMAT type RP film (-70°C for 24 to 72 hr). Beginning from this sequence, the entire gene encoding the 7 α -HSDH along with the 5' and 3' non-coding regions was then determined by walking upstream and downstream using new synthetic oligonucleotides, complementary to the known sequence, as primers. All sequences were read manually, and the sequence for each position was determined for both DNA strands.

Northern Blot Analysis: The 0.9 kb *BglII* fragment, which comprises approx. 90% of the 7 α -HSDH coding region was excised from pBH51, purified using a Qiagen column, and nick translated using a Nick Translation System from BRL (Gaithersburg, MD) and [α -³²P]-dCTP. Total RNA was isolated from *E. coli* and uninduced and cholate-induced cultures of *Eu. sp VPI 12708* as previously described

[102]. The RNA samples were subjected to electrophoresis on a 1% agarose in the presence of formaldehyde [11]. After capillary transfer of the RNA to a nylon membrane, the samples were probed with the labelled restriction fragment as described elsewhere [11]. Hybridized probe was detected by autoradiography using Kodak XOMAT type RP film.

Primer Extension Analysis: Total RNA was isolated from *E. coli* and *Eu. sp.* VPI 12708 as described above. A synthetic oligonucleotide primer, the reverse complement to the first 30 nucleotides of the 7 α -HSDH open reading frame was 5' end labelled with ³²P using T4 kinase, and annealed to the mRNA. The primer was then extended using AMV reverse transcriptase as described previously. The primer extension products were run on sequencing gels, with sequence reactions acting as a sizing ladder, as described above.

Protein and DNA Sequence Analysis: Protein and DNA sequence analysis was performed using the University of Wisconsin Genetics Computer Group programs (UWGCG) [35] installed on the VAX cluster at the MCV computer resources center. Computer assisted searches of the NBRF and Swiss Protein data banks for sequence to the derived amino acid sequences for the purified protein (and also the entire translated open reading frame for the 7 α -HSDH) were performed with FASTA using the wordsearch algorithm of Wilbur and Lipman [140]. Alignments of 7 α -HSDH with other polyol/dehydrogenases were accomplished using the GAPS program, using the algorithm of Needleman and Wunsch [132], with a gap width of 3.0 and a gap weight of 0.1. A growing consensus sequence was generated by comparing the 7 α -HSDH sequence with the 27-1 sequence. The resulting gapped consensus sequence was

compared to the 27-2 sequence, and a new gapped consensus was generated. This process was repeated, sequentially, for the sequences of a 20 β -HSDH, 17 β -HSDH, 15-hydroxyprostaglandin dehydrogenase, the two glucose dehydrogenases, ribitol dehydrogenase, and *Drosophila* alcohol dehydrogenase. The resulting, maximally gapped, consensus sequence was used to align each of the original sequences individually. The alignment metrics were noted, as they indicate the quality of the match between the 7 α -HSDH and the other sequences. The gapped alcohol/polyol sequences were then displayed using **LINEUP**. The consensus sequence for all ten aligned sequences was calculated using **PRETTY**. The **COMPARE** program, using the method of Maizel and Lenk [19], was also used to search for conserved areas between the proteins (using a window of 21 and a stringency of 12). This data was displayed using the **DOT PLOT** program. The secondary structure of the 3', putative terminator region was calculated using the **FOLD** program which uses the method of Zuker [182]. The calculated structure was then displayed using **SQUIGGLES**.

RESULTS

Purification of the 7 α -HSDH: Sixteen liters of *Eubacterium* sp. VPI 12708 yielded greater than 500 units of 7 α -HSDH activity, with a specific activity of 0.31 units/mg protein. Purification to apparent electrophoretic homogeneity was achieved using four chromatographic steps, and is summarized in Table 1. An overall purification of over 1200-fold with greater than a 30% recovery of detectable units was routinely obtained. The 7 α -HSDH eluted as a single symmetrical peak from all purification steps (Figures 9-12). The key steps in the purification were phenyl-sepharose (Figure 10) and reactive red agarose (Figure 11) chromatography. The phenyl-sepharose column gave a purification factor of 5.5-fold with a recovery of 86%. The best step, however, was reactive red agarose which produced a 65-fold purification with a 64% recovery of loaded units. In later purification attempts, it was found to be possible to omit the phenyl sepharose step with no apparent effect to final enzyme purity or specific activity. The overall yield, however, increased to 40 to 45%.

Aliquots from each step of the purification scheme were subjected to SDS-PAGE as a means of assessing the purity of the enzyme preparation. After DEAE-HPLC, the 7 α -HSDH appeared as a single band on Coomassie stained gels (Figure 13). A subunit molecular mass of 31 kDa was estimated, based upon the migration of several molecular mass standards. Additionally, gel filtration of the purified 7 α -

TABLE 1: Purification of the 7 α -HSDH.

The purification was performed using 55 g of cells (wet pellet weight). Details of the purification procedure are given in the Methods section. All enzymatic activities were determined in the direction of cholate oxidation.

Purification Step	Volume	Protein	Activity	Activity	Specific Purification	Yield
	<i>ml</i>	<i>mg</i>	<i>Units^a</i>	<i>Units/mg</i>	<i>Fold</i>	<i>Percent</i>
Cell Free Extract	55.0	1820.	561.0	0.31	1.0	100
DE-52	94.0	518.	384.5	0.74	2.4	69
Phenyl Sepharose	15.5	82.0	332.2	4.1	13	59
Reactive Red 120	9.0	0.80	212.1	265	854	38
DEAE-HPLC (pH 7.5)	9.5	0.45	176.7	393	1267	32

^a One unit of activity is defined as 1 μ mol of NADPH produced/min/ml.

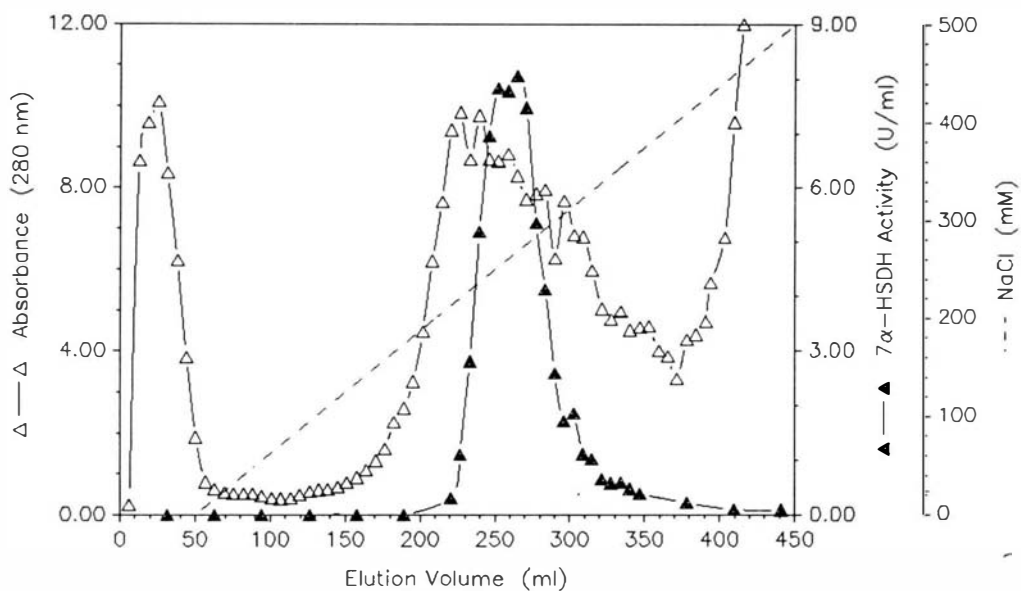


FIGURE 9: 7α-HSDH DEAE-Cellulose Elution Profile. Cell free extract (1.8 g) was loaded onto a pre-equilibrated DE-52 column. Bound proteins were eluted with an increasing NaCl gradient at a flow rate of 1 ml/min.

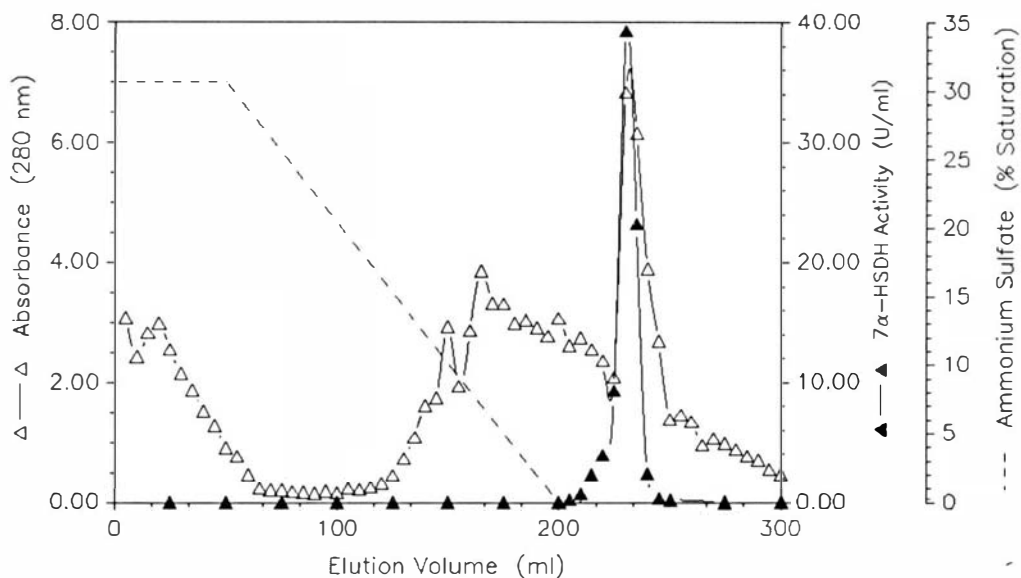


FIGURE 10: 7 α -HSDH Phenyl Sepharose Elution Profile. Following addition of solid ammonium sulfate, the pooled DE-52 fractions were loaded onto the column, previously equilibrated with solution A containing ammonium sulfate at 30% saturation. Proteins were eluted with a decreasing ammonium sulfate gradient.

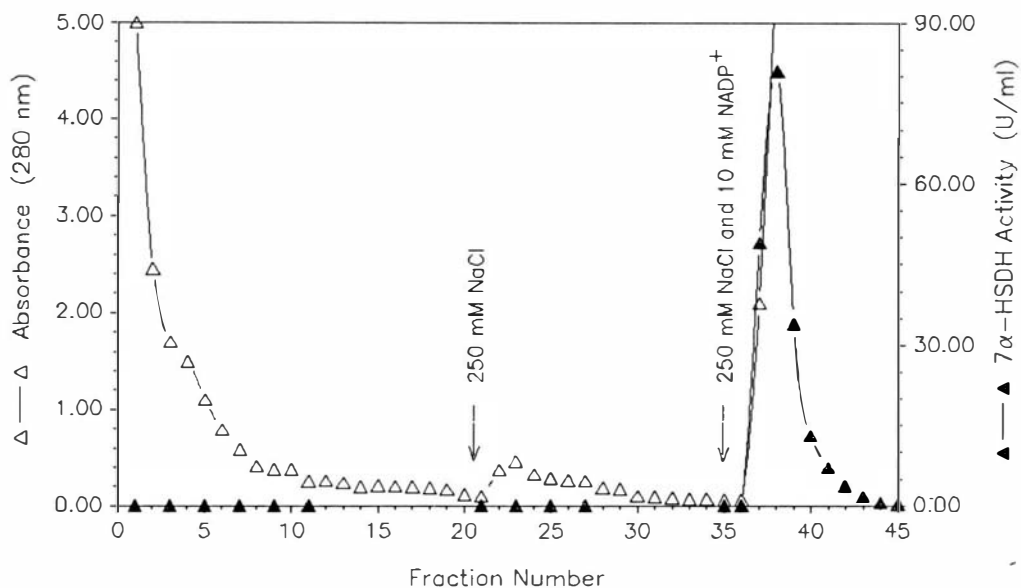


FIGURE 11: 7α-HSDH Reactive Red A Agarose Elution Profile. Pooled and equilibrated phenyl sepharose fractions were applied to a reactive red 120-agarose column which had been equilibrated with solution B. Specific elution of the 7α-HSDH was achieved using 250 mM NaCl and 10 mM NADP⁺.

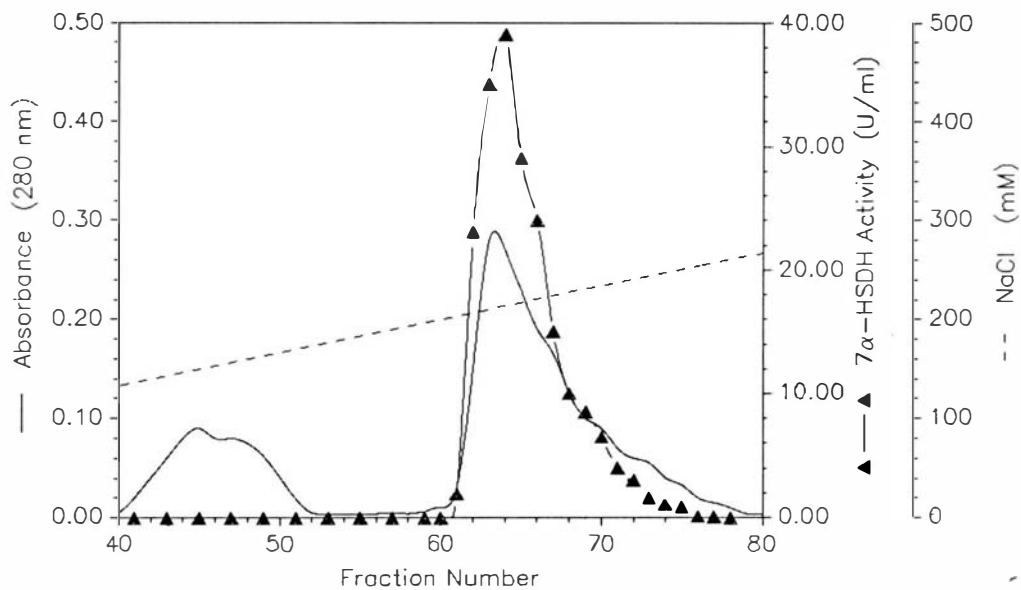
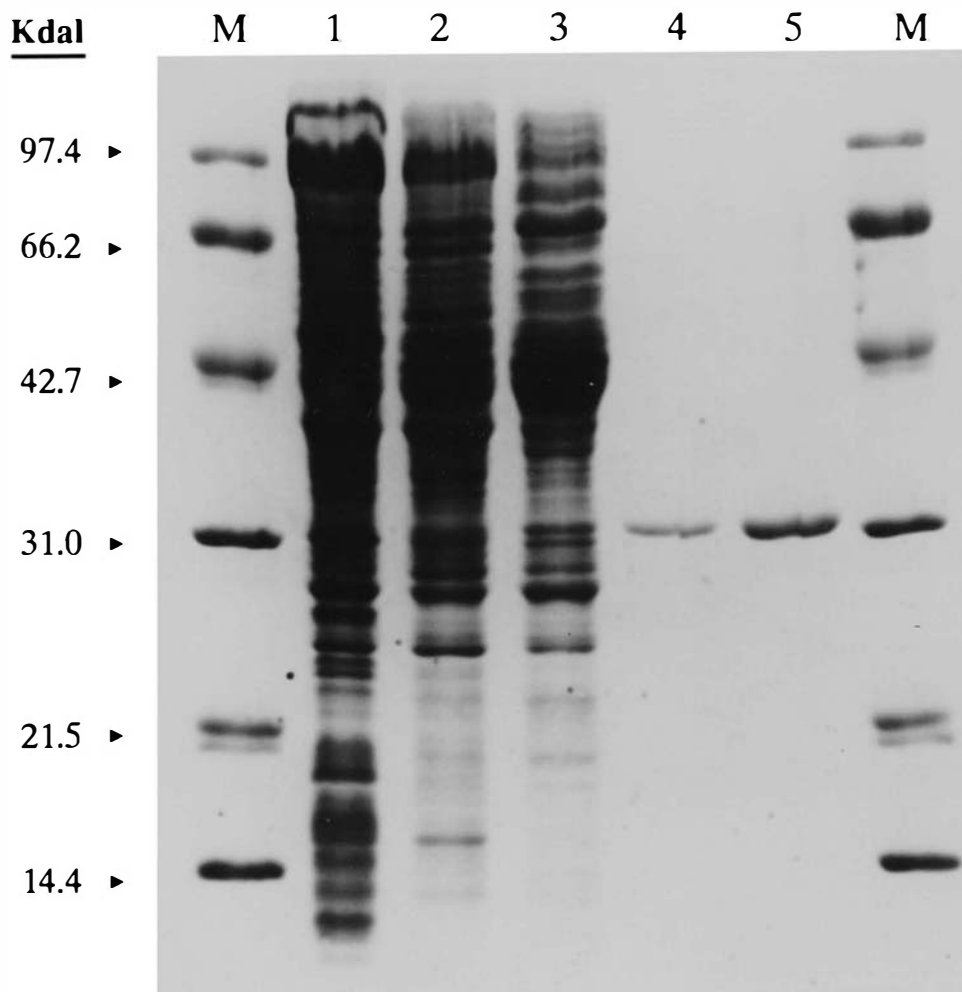


FIGURE 12: 7α -HSDH DEAE-HPLC Elution Profile. Pooled red 120-agarose fractions were equilibrated with solution C and applied to a DEAE-3SW column. Bound proteins were eluted with an increasing NaCl gradient. The total protein elution profile was continuously monitored at 280 nm using a variable wavelength detector.

FIGURE 13: SDS-PAGE of Protein Aliquots from the Purification of the 7 α -HSDH. Aliquots of the 7 α -HSDH at each stage of purification were subjected to electrophoresis using a 12% acrylamide slab gel. Lanes contained the following: M: Biorad Low Molecular Weight Markers, 1: Cell Free Extract (50 μ g), 2: Pooled DE-52 Fractions (40 μ g), 2: Pooled Phenyl Sepharose Fractions (35 μ g), 4: Pooled Reactive Red A Fractions (10 μ g), Pooled DEAE-HPLC Fractions (10 μ g). The molecular mass of the size standards are given in the left margin.



HSDH using a calibrated sepharose CL-6B column gave a single symmetrical peak of protein which corresponded to 7α -HSDH activity. The native molecular mass of this enzyme was estimated to be 124 kDa, suggesting that it exists as a tetramer of identical subunits (Figure 14).

The purified protein was also shown to be very stable to long term storage. Stock solutions of 50 $\mu\text{g/ml}$ stored in solution A were frozen at -20°C for over 4 months with no detectable loss of enzymatic activity. Working solutions (1 $\mu\text{g/ml}$) retained greater than 80% activity when stored in solution A at 4°C for up to 1 week.

Bile Acid Substrate and Pyridine Nucleotide Cofactor Specificity of the 7α -HSDH.

Substrate utilization studies revealed that the purified 7α -HSDH was extremely regio- and stereo-specific in the oxidation of the 7α -hydroxy moiety (Table 2). This is demonstrated by the lack of activity with bile acids lacking a 7α -hydroxy group (deoxycholic acid, and hyodeoxycholic acid), or possessing a 7β -hydroxyl group (ursocholic acid, and ursodeoxycholic acid). Moreover, bile acids which contained 7α -hydroxy groups hindered by the presence of a 7β -methyl group also failed to act as substrates for this enzyme. The presence of either a 6α -hydroxy (hyocholic acid) or a 12-oxo (12-oxo-cholic acid) group greatly diminished, but did not totally prohibit enzymatic activity. In contrast, the presence of a 3-oxo moiety (3-oxo-cholic acid) essentially abolished activity. Interestingly, a wide variety of substitutions at C-24 were tolerated by the 7α -HSDH. Both glycine and taurine conjugates of 7α -hydroxy bile acids were utilized as substrates. However, the conjugates were not used with equal effectiveness. Activities measured using glycine or taurine conjugates were approx 68% and 50% that detected using unconjugated bile acids, respectively.

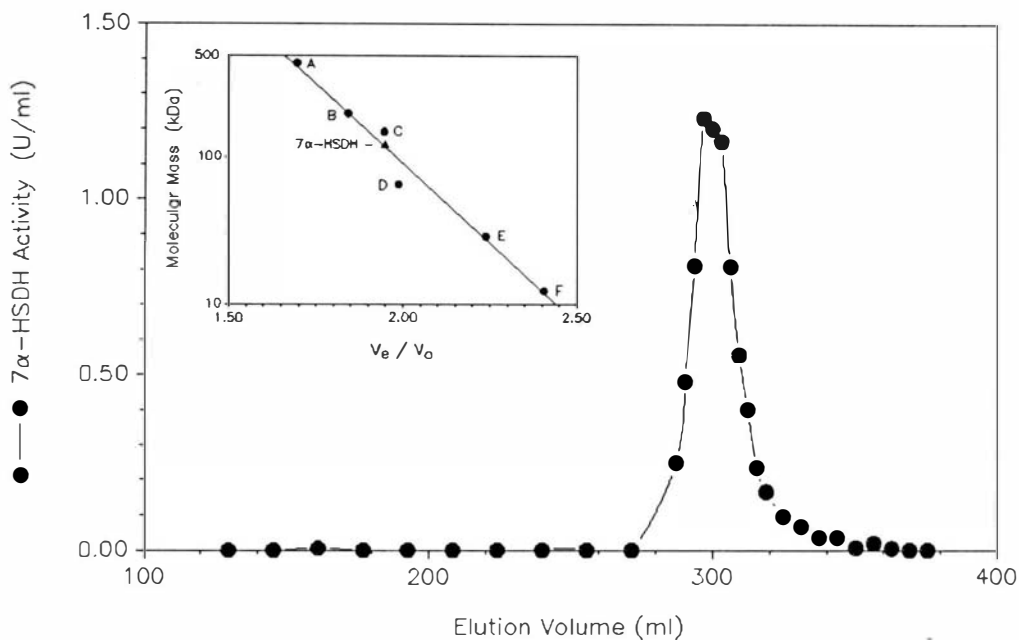


FIGURE 14: Gel Filtration Elution Profile and Native Molecular Mass Estimation of the Purified 7α-HSDH. Purified 7α-HSDH (40 μg) was chromatographed on a sepharose CL-6B column equilibrated with solution A containing 100 mM NaCl, and its relative elution volume was calculated.

Inset: A molecular mass standard curve was generated from the Log_{10} molecular mass vs. the relative elution volumes (V_e/V_o) of several standards. The proteins used were as follows - A: apoferritin, B: β amylase, C: alcohol dehydrogenase, D: albumin, E: carbonic anhydrase, F: cytochrome C. The filled triangle represents the 7α-HSDH.

TABLE 2: Bile Acid Substrate Specificity of the 7 α -HSDH.

Bile Acid Substrate	Positions and Substitutions					Relative Activity *
	3	6	7	12	24	
Cholic Acid	α OH	H	α OH	α OH	COOH	100
3-Deoxycholic Acid	H	H	α OH	α OH	COOH	128
Chenodeoxycholic Acid	α OH	H	α OH	H	COOH	68
3-oxo-Cholic Acid	Oxo	H	α OH	α OH	COOH	< 1
12-oxo-Chenodeoxycholic Acid	α OH	H	α OH	Oxo	COOH	33
Hyochoolic Acid	α OH	α OH	α OH	H	COOH	56
Deoxycholic Acid	α OH	H	H	α OH	COOH	6
Hyodeoxycholic Acid	α OH	α OH	H	H	COOH	2
Ursocholic Acid	α OH	H	β OH	α OH	COOH	5
Ursodeoxycholic Acid	α OH	H	β OH	H	COOH	< 1
7 β Methyl Cholic Acid	α OH	H	α OH/ β Me	α OH	COOH	2
7 β Methyl Chenodeoxycholic Acid	α OH	H	α OH/ β Me	H	COOH	1

TABLE 2 <CONT>

Bile Acid Substrate	Positions and Substitutions					Relative Activity *
	3	6	7	12	24	
Glycocholic Acid	α OH	H	α OH	α OH	CO-Gly	68
Taurocholic Acid	α OH	H	α OH	α OH	CO-Tau	52
Glychenodeoxycholic Acid	α OH	H	α OH	H	CO-Gly	46
Taurochenodeoxycholic Acid	α OH	H	α OH	H	CO-Tau	33
Tauro-3-deoxycholic Acid	H	H	α OH	α OH	CO-Tau	78
Glycodeoxycholic Acid	α OH	H	H	α OH	CO-Gly	8
Taurodeoxycholic Acid	α OH	H	H	α OH	CO-Tau	3
Glycoursodeoxycholic Acid	α OH	H	β OH	H	CO-Gly	< 1
Tauroursodeoxycholic Acid	α OH	H	β OH	H	CO-Tau	3
7-oxo-Cholic Acid **	α OH	H	Oxo	α OH	COOH	60
7-oxo-Chenodeoxycholic Acid **	α OH	H	Oxo	H	COOH	57
7,12-Di-oxo-Cholic Acid **	α OH	H	Oxo	Oxo	COOH	42

* Values were normalized by setting activity assayed with cholate (401 μ mol/min/mg) to 100.

** Reaction performed in the direction of bile acid reduction.

Cholic acid and chenodeoxycholic acid possessing an amide, methyl ester, or hydroxy group at C-24 utilized as substrates (data not shown). 7 α -hydroxycholesterol was not a substrate for this enzyme under the conditions examined. Due to the limited solubility of these steroids in aqueous solutions, these reactions were not quantitated spectrophotometrically. Attempts to solubilize the derivatives using dimethylsulfoxide, ethanol, and methanol all resulted in the inactivation of the 7 α -HSDH activity at greater than 5% (v/v) final concentrations. Therefore, substrate utilization was scored as either positive or negative by 7-oxo product formation, as detected by TLC or GC. The purified enzyme was highly specific for NADP(H), as no activity was detected using NAD(H) under the conditions employed (Table 3).

Apparent Kinetic Constants for the Purified 7 α -HSDH: Initial velocity kinetic studies were performed, using the purified enzyme, for both bile acid substrates and pyridine nucleotide cofactors in the oxidative and reductive directions. Primary and secondary Hanes plots were used both to derive kinetic constant values for NADP(H), cholic acid, and 7-oxo-cholic acid (Figure 7B, and 7C), and to examine the reaction mechanism (Table 4). Apparent kinetic constants were also determined under saturating conditions to compare different substrates (Table 3). The affinity of the 7 α -HSDH for most bile acids was very high; most K_m values ranged from 4 to 20 μ M, the exceptions being hyocholic acid (49 μ M), and 3- and 12-oxo bile acids (854 μ M and 208 μ M, respectively). The V_{max} values generally reflected the relative activities determined in Table 2. The V_{max}/K_m values did not vary substantially for most substrates examined (56.1 ± 7.8). However, the value determined for chenodeoxycholic acid was significantly higher, while those for hyocholic acid, and

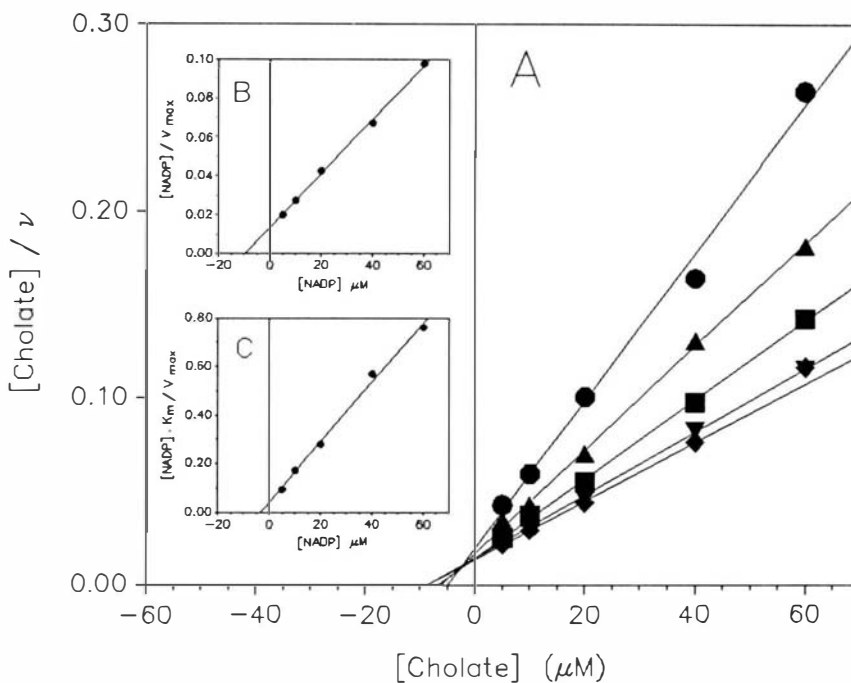


Figure 15: Hanes Plots of 7 α -HSDH Saturation Kinetics. Saturation kinetics were performed as described in the Methods section. An example of typical results is illustrated above.

- A:** Primary plots of cholate saturation kinetics at different constant concentrations of NADP⁺. The concentrations of NADP⁺ used were: (●) 5 μ M, (▲) 10 μ M, (■) 20 μ M, (▼) 40 μ M, (◆) 60 μ M.
- B:** Secondary plot of $[\text{NADP}^+]/V_{\text{max}}$ vs. $[\text{NADP}^+]$. The slope of the line is equal to $1/V_{\text{max}}$, and the x-intercept is $-K_m^{\text{NADP}}$.
- C:** Secondary plot of $[\text{NADP}^+] \cdot K_m/V_{\text{max}}$ vs. $[\text{NADP}^+]$. The slope of this plot is equal to K_m^{cholate} , and the x-intercept is $-K_i^{\text{cholate}} \cdot K_m^{\text{NADP}}/K_m^{\text{cholate}}$.

TABLE 3: Apparent Kinetic Constants for the Purified 7 α -HSDH.

Variable Substrate ^a	K_m	V_{max}	V_{max}/K_m
	μM	$\mu mol/min/mg$	$(\mu mol/min/mg)/\mu M$
Cholic Acid	11.0	601	54.6
Chenodeoxycholic Acid	5.6	468	83.6
3-Deoxycholic Acid	18.7	907	48.5
3-oxo-Cholic Acid	854.0	84	0.1
12-oxo-Cholic Acid	207.7	303	1.5
Hyochoolic Acid	49.4	253	5.1
Glycocholic Acid	8.8	409	46.5
Taurocholic Acid	4.5	272	60.4
Glycochenodeoxycholic Acid	5.5	337	61.3
Taurochenodeoxycholic Acid	4.7	288	61.3
Tauro-3-deoxycholic Acid	7.6	466	61.3
NADP ⁺	9.0	619	68.8
NAD ⁺		-- No Activity --	
7-oxo-Cholic Acid	12.7	674	53.1
7-oxo-Chenodeoxycholic Acid	13.9	621	44.7
7,12-Di-oxo-Cholic Acid	12.2	162	13.3
NADPH	3.0	650	216.7
NADH		-- No Activity --	

^a Bile acid constants were derived with a constant concentration of 100 μM NADP⁺ or NADPH. Pyridine dinucleotide cofactor constants were determined using a constant concentration of 100 μM cholate and 7-oxo-cholic acid in the oxidative and reductive directions, respectively.

the 3- and 12-oxo bile acids were significantly lower than this value. The data also showed that pyridine nucleotides bound tighter when reduced than when oxidized. Substrate inhibition was noted at concentrations above 60 μM in the direction of bile acid reduction, but were less noticeable in the oxidative direction. Primary Hanes plots of substrate saturation, in both the oxidative and reductive directions, resulted in a family of lines intersecting to the left of the ordinate (Figure 7A). Product inhibition studies revealed that NADPH exhibited competitive inhibition with respect to NADP^+ , and *vice versa* (Table 4). All other product inhibition patterns were characteristic of mixed inhibition when plotted using the method of Hanes.

Optimizing the pH for 7 α -HSDH Catalysis: The effect of pH on enzymatic activity in both the direction of bile acid oxidation and reduction was determined over a pH range of 4.0 to 12.0 (Figure 16). The optimal pH range for the reduction of 7-oxo-cholic acid was found to be between 5.7 to 6.5. Oxidation of cholic acid by 7 α -HSDH showed two plateaus of activity at alkaline pH. A lower, broad plateau occurred between pH 7.5 to 9.0, whereas a higher and sharper peak was apparent between pH 10.5 and 11.5. The activity was not affected by the buffer systems employed. However, 100 mM MOPS buffer at pH 8.0 was found to give 70% inhibition of the 7 α -HSDH activity.

Inhibitors of 7 α -HSDH Activity: The effect of various sulfhydryl-reactive and metal ion-chelating compounds on 7 α -HSDH activity was also evaluated (Table 5). The enzyme was found to be very susceptible to inactivation by p-CMB and N-bromo-succinamide. Mercuric, zinc, and cupric chlorides were also strongly inhibitory. Other sulfhydryl inhibitors (NEM, iodoacetate, and iodoacetamide) were less

TABLE 4: Product Inhibition Patterns for the 7 α -HSDH.

Fixed substrates were kept at 20 μ M for all reactions, while the second substrate concentration was varied from 5 to 60 μ M. Products were tested at 25 and 50 μ M and were compared to water controls. All reactions were performed using 20 ng of purified 7 α -HSDH. The inhibition patterns were discerned using Hanes plots.

Variable Substrate	Fixed Substrate	Product	Inhibition Pattern
<i>Oxidative Reactions</i>			
NADP ⁺	Cholic Acid	NADPH	Competitive
NADP ⁺	Cholic Acid	7-oxo-Cholic Acid	Mixed
Cholic Acid	NADP ⁺	NADPH	Mixed
Cholic Acid	NADP ⁺	7-oxo-Cholic Acid	Mixed
<i>Reductive Reactions</i>			
NADPH	7-oxo-Cholic Acid	NADP ⁺	Competitive
NADPH	7-oxo-Cholic Acid	Cholic Acid	Mixed
7-oxo-Cholic Acid	NADPH	NADP ⁺	Mixed
7-oxo-Cholic Acid	NADPH	Cholic Acid	Mixed

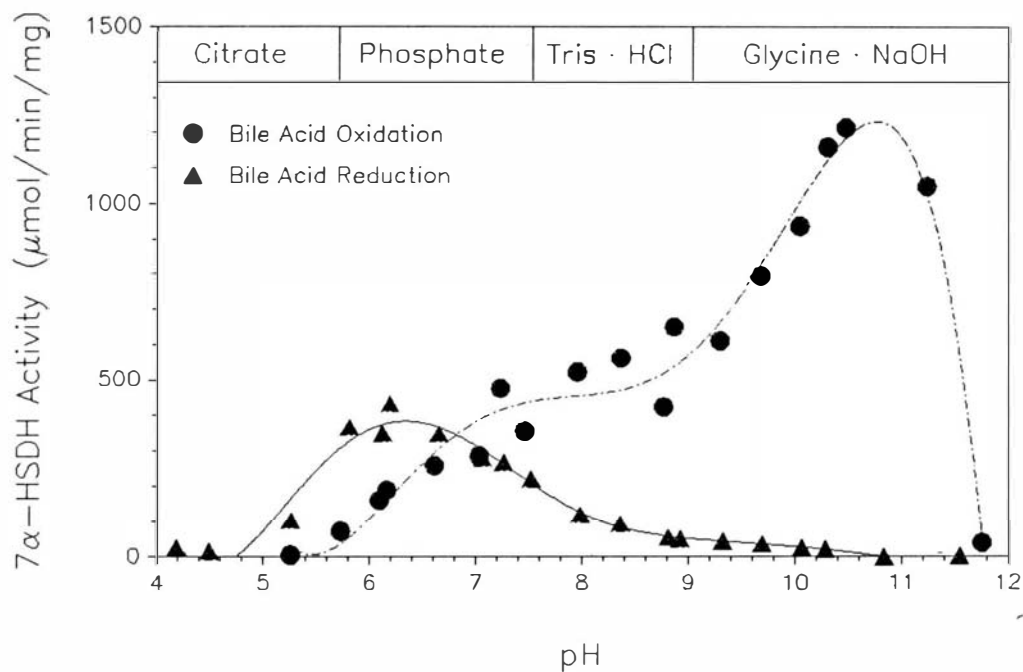


FIGURE 16: Optimization of pH for the Activity of the Purified 7α-HSDH. All assay buffers were used, at a final concentration of 100 mM, over the pH ranges indicated. The pH determinations were made immediately following the completion of the 7α-HSDH activity assays.

TABLE 5: Effect of Sulfhydryl-Reactive and Metal-Chelating Compounds on 7 α -HSDH Activity.

Purified protein (20 ng) was pre-incubated with the indicated amount of a putative inhibitor for 10 min at 20°C in 100 mM Tris · HCl (pH 8.0). All reactions were performed in the direction of cholate oxidation as described in the Methods section.

Inhibitor ^a	Final Concentration (mM)	% Inhibition ^b
p-CMB	0.5	100
HgCl ₂	5.0	100
	2.5	74
ZnCl ₂	5.0	76
	2.5	31
CuCl ₂	5.0	100
	2.5	58
NEM	10.0	88
Iodoacetate	5.0	46
Iodoacetamide	10.0	10
N-Bromosuccinamide	0.2	100

^a NaN₃, KCN, EDTA, and EGTA did not inhibit 7 α -HSDH activity when present at up to 10 mM concentrations.

^b Values are the mean of three independent determinations.

effective. Metal ion chelators (EDTA, and EGTA) had no detectable effect upon 7α -HSDH activity under the conditions employed.

Use of the Purified 7α -HSDH for the Quantitation of Bile Acids: Experiments were undertaken to evaluate the utility of the purified 7α -HSDH as an analytical reagent for the quantitation of free and conjugated bile acids. Spectrophotometric quantitation of NADPH (absorbance at 340 nm) generated by the enzyme was found to correlate very well with bile acid concentrations ranging from 1 to 100 μ M (Figure 17A). Additionally, the increased sensitivity afforded by spectrofluoremetry allowed detection of NADPH produced from free and conjugated bile acid final concentrations ranging from 10 nM to 1 μ M (Figure 17B).

N-Terminal Amino Acid Sequence Analysis of the 7α -HSDH: The first 22 N-terminal amino acid residues were determined using a gas phase protein sequencer. The amino acid sequence displayed a significant homology to several short, non-zinc alcohol/polyol dehydrogenases and a putative, cholate-inducible HSDH from *Eu. sp* VPI 12708 [26] (Figure 18). The best match, however, was obtained with the N-terminal amino acid sequence of a 7α -HSDH from *Clostridium absoum* (Dr. James Coleman, personal communication). These proteins exhibited 63.6% identity, with conservative changes in amino acid sequence representing another 9%, over the first 22 residues. The 27-2 sequence, which is thought to be a 3α -HSDH, also showed a strong homology (55% identity and 36% similarity) to the N-terminal sequence.

Cloning the Gene Encoding the 7α -HSDH: Two synthetic oligonucleotides (31-1 and 31-2) were created which are complementary to the codons corresponding to a portion of the 7α -HSDH N-terminal amino acid sequence (Figure 19A). Using an

FIGURE 17: Quantitation of Free and Conjugated Bile Acids Using the 7 α -HSDH. The concentrations of glycocholic acid (\square) and chenodeoxycholic acid (\triangle) were determined spectrophotometrically (A) and spectrofluorometrically (B) as described in the Methods section. All determinations were performed in triplicate and the average results \pm standard deviation are plotted. Points were fitted using unweighted, first-order linear regressions ($r > 0.995$).

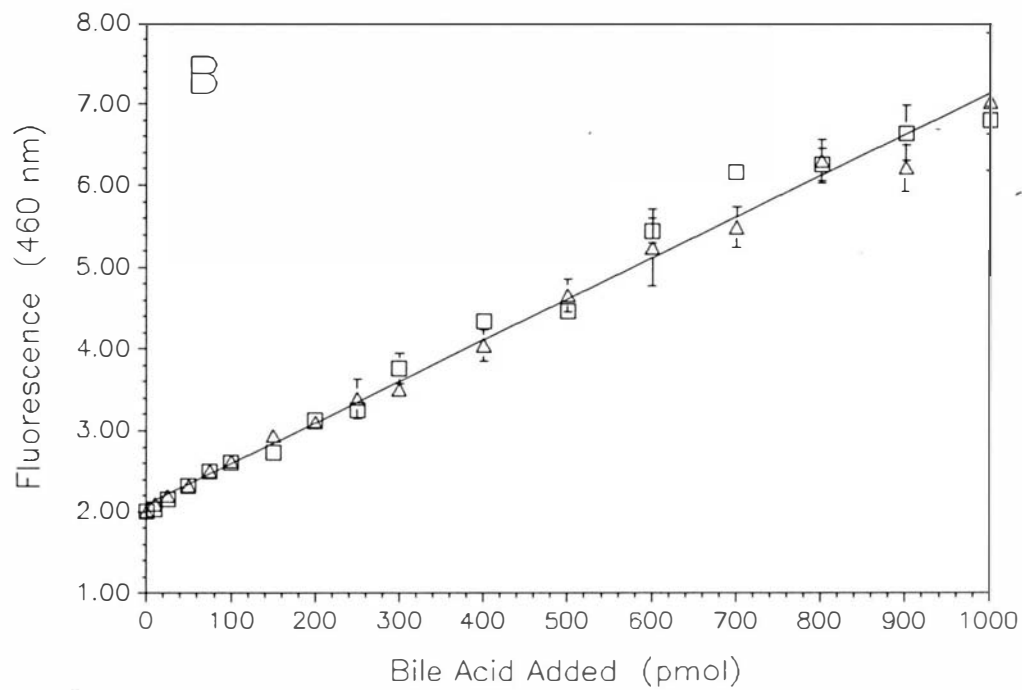
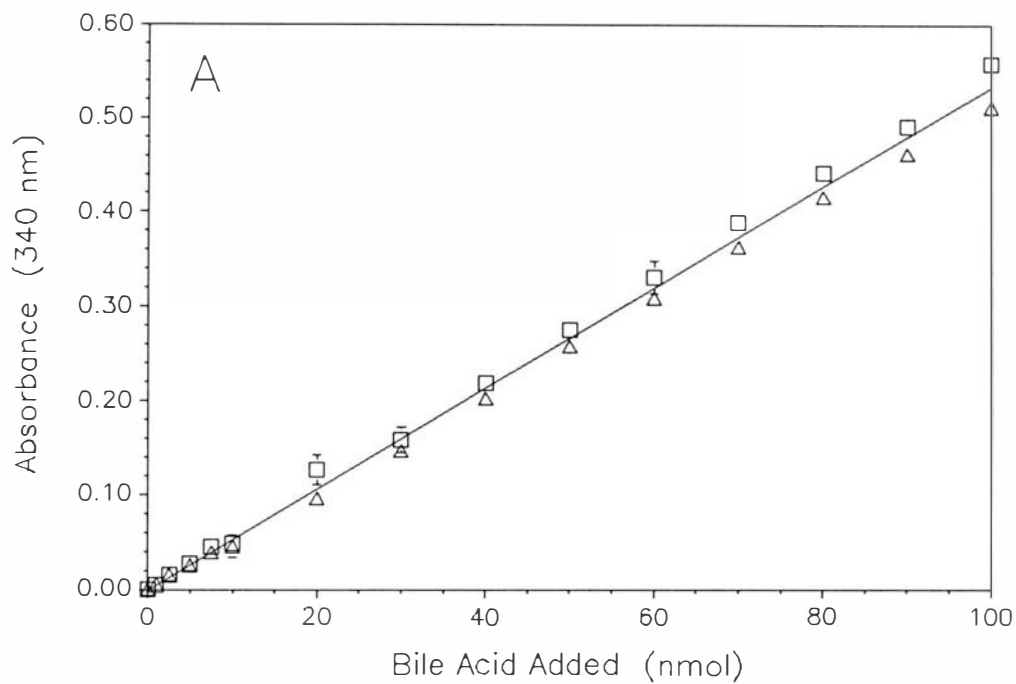


FIGURE 18: N-Terminal Amino Acid Sequence of the Purified 7 α -HSDH and Homology to Other Alcohol/Polyol Dehydrogenases. The first 22 N-terminal amino acid residues of purified 7 α -HSDH are illustrated. The sequence is aligned with several alcohol/polyol dehydrogenases which belong to a family of short non-zinc enzymes. The full names and origins of the enzymes listed are given in the Table of Abbreviations. The βA denotes a β -pleated sheet structure which is part of the pyridine nucleotide binding domain.

β A

<i>DmADH</i>	1	Ser Phe Thr	Leu Thr	Asn Lys	Asn	Val Ile	Phe Val	Ala Gly	Leu Gly	Gly Ile	Gly Leu	Asp Thr	Ser Lys	Glu Leu	Leu Lys
<i>BmGDH-B</i>	2	Tyr Lys Asp	Leu Glu	Gly Lys	Val Val	Val Ile	Thr Gly	Ser Ser	Thr	Gly Leu	Gly Lys	Ser Met	Ala Ile	Arg Phe	Ala Thr
<i>KaRDH</i>	9	Asn Thr Ser	Leu Ser	Gly Lys	Val Ala	Ala Ile	Thr Gly	Ala Ala	Ser	Gly Ile	Gly Leu	Gly Cys	Ala Arg	Thr Leu	Leu Gly
<i>Eu27K-1</i>	1	Met Lys Leu	Val Gln	Asp Lys	Ile Thr	Ile Ile	Thr Gly	Gly Thr	Arg Gly	Ile Gly	Phe Ala	Ala Ala	Lys Leu	Phe Ile	Glu
<i>Ca7α-HSDH</i>	1	--- Asn Lys	Leu Glu	Asn Lys	Val Ala	Leu Val	Thr Ser	Ala Thr	Arg Gly	Ile Gly	Leu Ala	Asp Ala	Ile Lys		
<i>Eu7α-HSDH</i>	1	Met Arg	Leu Lys	Asp Lys	Val Ile	Leu Val	Thr Ala	Ser Thr	Arg Gly	Ile Gly	Leu Ala	Ile Ala			

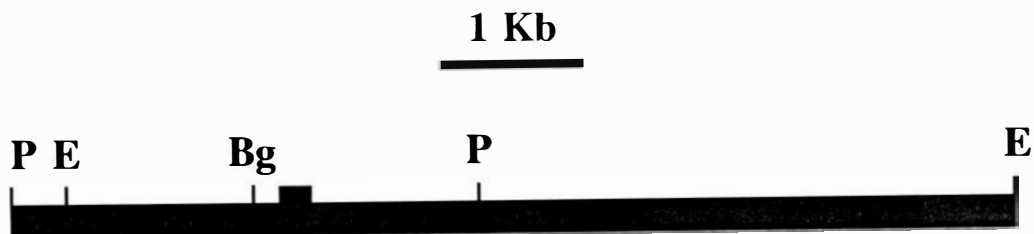
FIGURE 19: Synthetic Oligonucleotide Probes and Chromosomal Restriction Map for the 7 α -HSDH.

The two oligonucleotide probes, 31-1 and 31-2, synthesized for Southern analysis are illustrated in Panel A. The amino acid sequence that these sequences correspond to is shown above the probes.

The chromosomal restriction map for the 7 α -HSDH gene, as deduced from Southern analysis, is shown in Panel B. The restriction sites are abbreviated as follows: P - *Pst*I, E - *Eco*RI, Bg - *Bgl*II. The region where the probe is thought to anneal is shown as a thicker bar.

A

	NH ₂	Met	Arg	Leu	Lys	Asp	Lys	Val	
31-1	5'	ATG	AGA	T ^T G C ^T G	AA ^A G	GAT	AA ^A G	GT	3'
31-2	5'	ATG	AGA	T ^T G C ^T G	AA ^A G	GAC	AA ^A G	GT	3'

B

end-labelled oligonucleotide probe, (31-2), a chromosomal restriction map for the 7 α -HSDH gene was generated from Southern blot analysis (Figure 19B). Based upon these results a 6 kb *EcoRI* fragment was chosen to be cloned into the bacteriophage vector λ gt11. A 3.8 kb *KpnI-PstI* fragment was subsequently subcloned into pUC19 giving rise to the recombinant plasmid pBH51. The sequence of over 1300 bp was determined from double-stranded DNA sequencing, using the dideoxy chain termination method as described in the Methods section. The sequence obtained contained one open reading frame of 789 bp (extending from residue 231 to 1031) which encoded a 266 amino acid polypeptide (Figure 20). The subunit molecular mass of this polypeptide was calculated to be 28 kDa, in approximate agreement with the size determined from SDS-PAGE. The amino acid sequenced translated from this open reading frame agreed exactly with the 22 residues derived from N-terminal sequence analysis of the purified 7 α -HSDH. Several regions homologous to the canonical *E. coli* promoter sequence were located 5' to the open reading frame. Possible -35 hexanucleotides begin at residues 57, 106, and 120, whereas the -10 regions begin at 32, 129, and 143. Each of these areas matches the consensus sequence for *E. coli* promoters in at least 4 of the six positions and have near optimal spacing. A reasonable ribosome binding domain was also located 5' to the open reading frame (positions 218 to 224). Downstream from the 7 α -HSDH gene, five regions possessing diad symmetry were detected. Using the FOLD and SQUIGGLES programs (UWGCG), a complex secondary structure involving all five inverted repeats was predicted (Figure 21). The Gibbs free energy for this 128 nucleotide structure was calculated to be -50.4 kCal.

FIGURE 20: Determination of the 7 α -HSDH Gene Sequence: Approximately 1300 base pairs of the cloned 3.8 kb *KpnI-PstI* restriction fragment were sequenced. The numbering of the nucleotides begins arbitrarily at the first base sequenced. The sequence containing the putative ribosome binding region is shown in bold case letters. The deduced amino acid sequence for the 7 α -HSDH is shown below the sequence in italic case letters. Amino acids corresponding to the residues determined by direct amino acid sequencing are shown as bold and underlined. The five sequences containing diad symmetry in the 3' untranslated region are underscored with arrows. The transcriptional start site, as determined by primer extension analysis is denoted by a star and is labelled + 1.

GCA	CGG	GCT	GAC	GAG	ATG	AAT	GCG	GCA	GGC	GGC	AAT
<i>Ala</i>	<i>Arg</i>	<i>Ala</i>	<i>Asp</i>	<i>Glu</i>	<i>Met</i>	<i>Asn</i>	<i>Ala</i>	<i>Ala</i>	<i>Gly</i>	<i>Gly</i>	<i>Asn</i>
	400										
	●										
GTA	AAG	TAT	GTT	TAC	AAT	GAT	GCG	ACA	AAA	GAA	GAG
<i>Val</i>	<i>Lys</i>	<i>Tyr</i>	<i>Val</i>	<i>Tyr</i>	<i>Asn</i>	<i>Asp</i>	<i>Ala</i>	<i>Thr</i>	<i>Lys</i>	<i>Glu</i>	<i>Glu</i>
						450					
						●					
ACA	TAC	GTG	ACG	ATG	ATT	GAG	GAA	ATC	ATC	GAG	CAA
<i>Thr</i>	<i>Tyr</i>	<i>Val</i>	<i>Thr</i>	<i>Met</i>	<i>Ile</i>	<i>Glu</i>	<i>Glu</i>	<i>Ile</i>	<i>Ile</i>	<i>Glu</i>	<i>Gln</i>
											500
											●
GAA	GGG	CGC	ATA	GAC	GTG	CTT	GTA	AAT	AAT	TTC	GGC
<i>Glu</i>	<i>Gly</i>	<i>Arg</i>	<i>Ile</i>	<i>Asp</i>	<i>Val</i>	<i>Leu</i>	<i>Val</i>	<i>Asn</i>	<i>Asn</i>	<i>Phe</i>	<i>Gly</i>
TCA	TCA	AAT	CCC	AAG	AAA	GAT	CTT	GGA	ATT	GCC	AAT
<i>Ser</i>	<i>Ser</i>	<i>Asn</i>	<i>Phe</i>	<i>Lys</i>	<i>Lys</i>	<i>Asp</i>	<i>Leu</i>	<i>Gly</i>	<i>Ile</i>	<i>Ala</i>	<i>Asn</i>
			550								
			●								
ACA	GAC	CCG	GAG	GTA	TTC	ATC	AAG	ACG	GTA	AAT	ATC
<i>Thr</i>	<i>Asp</i>	<i>Phe</i>	<i>Glu</i>	<i>Val</i>	<i>Phe</i>	<i>Ile</i>	<i>Lys</i>	<i>Thr</i>	<i>Val</i>	<i>Asn</i>	<i>Ile</i>
								600			
								●			
AAC	CTA	AAG	AGC	GTA	TTT	ATC	GCA	AGC	CAG	ACG	GCT
<i>Asn</i>	<i>Leu</i>	<i>Lys</i>	<i>Ser</i>	<i>Val</i>	<i>Phe</i>	<i>Ile</i>	<i>Ala</i>	<i>Ser</i>	<i>Gln</i>	<i>Thr</i>	<i>Ala</i>
GTT	AAG	TAT	ATG	GCG	GAA	AAT	GGA	GGT	GGA	AGC	ATC
<i>Val</i>	<i>Lys</i>	<i>Tyr</i>	<i>Met</i>	<i>Ala</i>	<i>Glu</i>	<i>Asn</i>	<i>Gly</i>	<i>Gly</i>	<i>Gly</i>	<i>Ser</i>	<i>Ile</i>
											650
											●
ATC	AAT	ATC	TCA	TCC	GTA	GGA	GGC	CTG	ATA	CCA	GAT
<i>Ile</i>	<i>Asn</i>	<i>Ile</i>	<i>Ser</i>	<i>Ser</i>	<i>Val</i>	<i>Gly</i>	<i>Gly</i>	<i>Leu</i>	<i>Ile</i>	<i>Pro</i>	<i>Asp</i>

700
●

ATC	TCT	CAG	ATT	GCC	TAT	GGA	ACC	AGC	AAA	GCG	GCA
<i>Ile</i>	<i>Ser</i>	<i>Gln</i>	<i>Ile</i>	<i>Ala</i>	<i>Tyr</i>	<i>Gly</i>	<i>Thr</i>	<i>Ser</i>	<i>Lys</i>	<i>Ala</i>	<i>Ala</i>

750
●

ATC	AAC	TAT	CTG	ACG	AAA	CTG	ATA	GCC	GTA	CAC	GAG
<i>Ile</i>	<i>Asn</i>	<i>Tyr</i>	<i>Leu</i>	<i>Thr</i>	<i>Lys</i>	<i>Leu</i>	<i>Ile</i>	<i>Ala</i>	<i>Val</i>	<i>His</i>	<i>Glu</i>

800
●

GCA	AGG	CAT	AAC	ATC	AGA	TGC	AAT	GCG	GTA	CTT	CCA
<i>Ala</i>	<i>Arg</i>	<i>His</i>	<i>Asn</i>	<i>Ile</i>	<i>Arg</i>	<i>Cys</i>	<i>Asn</i>	<i>Ala</i>	<i>Val</i>	<i>Leu</i>	<i>Pro</i>

850
●

GGA	ATG	ACG	GCA	ACA	GAT	GCG	GTG	CAG	GAT	AAT	CTG
<i>Gly</i>	<i>Met</i>	<i>Thr</i>	<i>Ala</i>	<i>Thr</i>	<i>Asp</i>	<i>Ala</i>	<i>Val</i>	<i>Gln</i>	<i>Asp</i>	<i>Asn</i>	<i>Leu</i>

850
●

ACG	GAT	GAC	TTC	CGA	AAC	TTC	TTC	TTG	AAG	CAT	ACG
<i>Thr</i>	<i>Asp</i>	<i>Asp</i>	<i>Phe</i>	<i>Arg</i>	<i>Asn</i>	<i>Phe</i>	<i>Phe</i>	<i>Leu</i>	<i>Lys</i>	<i>His</i>	<i>Thr</i>

900
●

CCA	ATT	CAG	CGT	ATG	GGG	CTC	CCG	GAA	GAG	ATC	GCG
<i>Pro</i>	<i>Ile</i>	<i>Gln</i>	<i>Arg</i>	<i>Met</i>	<i>Gly</i>	<i>Leu</i>	<i>Pro</i>	<i>Glu</i>	<i>Glu</i>	<i>Ile</i>	<i>Ala</i>

900
●

GCA	GCC	GTA	GTA	TAC	TTC	GCA	AGC	GAT	GAT	GCC	GCA
<i>Ala</i>	<i>Ala</i>	<i>Val</i>	<i>Val</i>	<i>Tyr</i>	<i>Phe</i>	<i>Ala</i>	<i>Ser</i>	<i>Asp</i>	<i>Asp</i>	<i>Ala</i>	<i>Ala</i>

950
●

TAT	ACC	ACA	GGA	CAG	ATT	CTT	ACC	GTA	TCT	GGC	GGT
<i>Tyr</i>	<i>Thr</i>	<i>Thr</i>	<i>Gly</i>	<i>Gln</i>	<i>Ile</i>	<i>Leu</i>	<i>Thr</i>	<i>Val</i>	<i>Ser</i>	<i>Gly</i>	<i>Gly</i>

1000
●

TTC	GGA	CTG	GCA	ACG	CCG	ATA	TTT	GGA	GAT	CTG	TCT
<i>Phe</i>	<i>Gly</i>	<i>Leu</i>	<i>Ala</i>	<i>Thr</i>	<i>Pro</i>	<i>Ile</i>	<i>Phe</i>	<i>Gly</i>	<i>Asp</i>	<i>Leu</i>	<i>Ser</i>

GAA CGC TCA GAT GCC CGC GGG TAG AAT TTC ATG GGT
Glu Arg Ser Asp Ala Arg Gly **STP**

1050

TAA CTT AAT CAA AAG CAG AAT CAG GAA AAG AGA CAG

1100

CCG GGA GCG GCT GTC TCT TTT ATC TAT AGT GCG CCT
 ▶ ←

1150

AGC GGC GCA CGT TTC TAA CTT TAT AGA AAA GTT CTC
 ← ▶

CTT TCG GAG AAC TTG GGG ACT AAA ATA GCC CGC TCA
 ▶ ← ▶

1200

AAA GCG GGC ATA GTG AAT CAG ACG GTT TGG ATT AAA
 ← ▶

1250

AGA TGT AAA AGC CCT CTT CAC CAA AAT CGT CAT CAT
 ●

CAA GGT TAT CAA ATT CAT GTA AGA AAT AAT CCA TAT

1300

CCA GAA GTT C
 ●

FIGURE 21: Calculated Secondary Structure for the Putative Terminator Region. The secondary structure of the region 3' to the 7 α -HSDH open reading frame was predicted using SQUIGGLES (UWGCG). The sequence from position 1068 to 1197, inclusively, is illustrated. The hydrogen bonding for each base pair is shown as two or three lines. The orientation relative to the 7 α -HSDH gene is given at the respective termini.

Expression of the 7 α -HSDH in *Eubacterium* sp. VPI 12708 and *Escherichia coli*: The expression of the 7 α -HSDH in *Eu.* sp VPI 12708 and recombinant *E. coli* clones was examined at the level of transcription, translation, and enzymatic activity. The enzymatic activity appeared to be constitutively expressed in *Eu.* sp VPI 12708 since the specific activity was not affected by the addition of cholic acid to the growth medium (Table 6). Both λ gt11 1+, containing the 6 kb *EcoRI* fragment, and pBH51 transformants, containing the 3.8 kb *KpnI-PstI* fragment, over-expressed the NADP-dependent 7 α -HSDH activity. The specific activities of these clones was 25- to 30-fold higher than that of *Eu.* sp VPI 12708 cell free extracts. A small amount of NAD-dependent activity was also detected in the *E. coli* preparations and may indicate the presence of an NAD-dependent 7 α -HSDH produced by this organism. The NADP-dependent 7 α -HSDH produced by a pBH51 transformant was purified to homogeneity using the purification protocol described in the Methods section. Aliquots from each purification step were subjected to SDS-PAGE and are shown in Figure 22A. It was possible to purify as much as 2.5 mg of pure 7 α -HSDH from a 1 liter culture of *E. coli*. The specific activity of this purified preparation was comparable to that obtained from *Eu.* sp VPI 12708 (Table 6). Furthermore, the enzyme from the pBH51 transformant exhibited similar kinetics with the bile acid substrates; cholic acid, glycochenodeoxycholic acid, and 12-oxo-cholic acid (data not shown). Additional evidence for the identity between these 7 α -HSDH preparations came from electrophoretic analysis of the purified proteins from *Eu.* sp VPI 12708 and a pBH51 transformant. SDS-PAGE analysis of both preparations revealed a protein having a molecular mass of 31 kDa (Figure 22A). In the pBH51 trans-

TABLE 6: Activity of the 7 α -HSDH in *Eu. sp.* VPI 12708 and Recombinant Constructions in *E. coli* Strains.

Material assayed ^a	Activity (units/mg protein) ^b	
	NADP ⁺	NAD ⁺
<i>Eu. sp.</i> VPI 12708:		
Uninduced cells	0.30	NA ^c
Cholate-induced cells	0.30	NA
Lambda gt11 phage lysates:		
wild type	NA	0.03
recombinant (1+)	7.01	0.30
<i>E. coli</i> transformants:		
pUC19	NA	0.32
pBH51	8.93	0.70
Purified 7 α -hydroxysteroid dehydrogenase from:		
<i>Eu. sp.</i> VPI 12708	374.0	0.16
pBH51 transformant	332.0	0.24

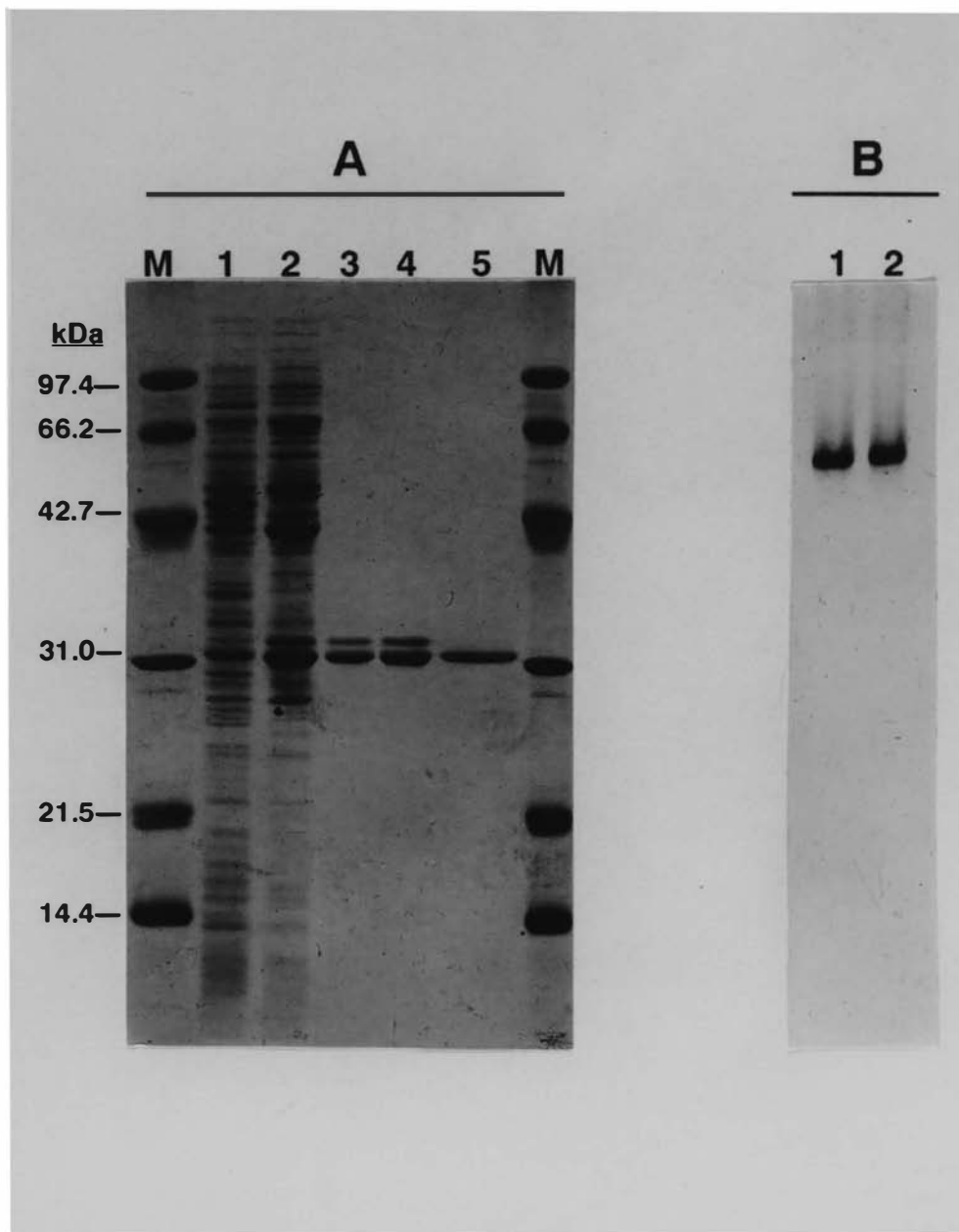
^a CFE of *Eu. sp.* VPI 12708 and *E. coli* were made as described in the methods section. Phage lysates were obtained by centrifugation of 6 h cultures of *E. coli* Y1090r⁻ infected with λ gt11 phage.

^b All 7 α -HSDH reactions were performed as described in the Methods section.

^c No activity detected.

FIGURE 22: SDS- and Native-PAGE of 7 α -HSDH Expressed in *Eu. sp* VPI 12708 and *E. coli*. The purity of the 7 α -HSDH from *Eu. sp* VPI 12708 and *E. coli* was assessed on 12% SDS (A) and 7 to 30% exponential gradient native (B) gels. The lanes in panel A contained the following: M - molecular mass markers, 1 - pBH51 transformant cell-free extract (25 μ g), 2- pooled DE-52 fractions (20 μ g), 3 - pooled Red A fractions (2.5 μ g), 4 - pooled DEAE-HPLC fractions (2.5 μ g), 5 - purified 7 α -HSDH from *Eu. sp* VPI 12708 (1.8 μ g). The proteins were visualized using Coomassie brilliant blue. The molecular mass of the marker proteins is shown, in kDa, to the left of the gel.

In panel B the lanes each contained 0.5 μ g of 7 α -HSDH purified from 1 - a pBH51 transformant, and 2 *Eu. sp* VPI 12708. The proteins were visualized using the activity stain described in the Methods section.



formant, however, a second band of approx 32 kDa was also observed. After subjecting the purified proteins to native gel electrophoresis, the 7α -HSDH band was visualized using an activity stain. The enzyme produced by both organisms appeared as a single band of estimated to be 95 kDa by its relative migration (Figure 22B). When native gels were stained for protein, using Coomassie, the only band detected corresponded to 7α -HSDH activity (data not shown).

Rabbit polyclonal antiserum raised against the 31 kDa protein purified from *Eu. sp* VPI 12708 was used to examine the expression of the 7α -HSDH. The specificity of this antiserum for the 7α -HSDH was shown by immunoinhibition (Figure 23). Approx. 50% inhibition of enzymatic activity was observed after incubation of purified 7α -HSDH in the presence of 10 μ l of immune serum, while less than 10% inhibition was detected with 150 μ l of preimmune serum. Western analysis also confirmed that the 7α -HSDH protein is constitutively expressed in *Eu. sp* VPI 12708, since bands of equal intensity were detected in uninduced and cholate-induced CFE (Figure 24). A 31 kDa band was also detected in CFE from *E. coli* harboring pBH51, but not pUC19. The purified proteins from both *E. coli* and *Eu. sp* VPI 12708 were recognized by the polyclonal antiserum. In addition, the 32 kDa band present in the purified 7α -HSDH preparation from *E. coli* was also immunoreactive.

Northern blot analysis of the 7α -HSDH also demonstrated that the transcription of this gene was constitutive in *Eu. sp* VPI 12708 (Figure 25). The transcript detected from both *Eu. sp* VPI 12708 and *E. coli* was approx 1 kb, suggesting that the 7α -HSDH is contained on a monocistronic message. The amount of 7α -HSDH message detected in a pBH51 transformant was about 30-fold greater than that of

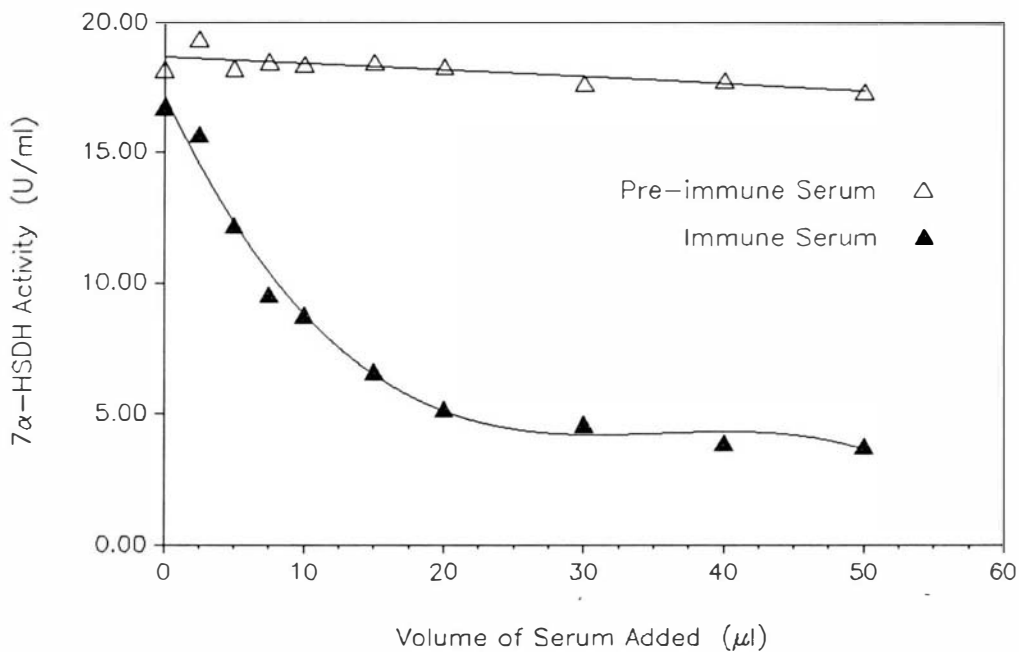


FIGURE 23: Immunoinhibition of Purified 7α-HSDH Enzymatic Activity by Rabbit Polyclonal Antisera. Various volumes of rabbit serum were added to 50 ng of 7α-HSDH purified from *Eu. sp.* VPI 12708 and allowed to incubate for 15 min at 20°C. Enzymatic reactions were then initiated by the addition of substrate, and were quantitated spectrophotometrically as described in the Methods section.

FIGURE 24: Western Analysis of 7 α -HSDH Expression in *Eu. sp* VPI 12708 and *E. coli*. The protein samples were run on a 12% acrylamide gel and Western blotted on a nitrocellulose membrane as described in the Methods section. The lanes each contained the following: M - Prestained molecular mass markers, 1 - Cholic acid-Induced *Eu. sp.* VPI 12708 CFE (15 μ g), 2 - Uninduced *Eu. sp.* VPI 12708 CFE (15 μ g) 3 - Purified 7 α -HSDH from *Eu. sp.* VPI 12708 (0.3 μ g), 4 - *E. coli* strain DH5 α pUC19 transformant CFE (0.2 μ g), 5 - *E. coli* strain DH5 α pBH51 transformant CFE (0.2 μ g), 6 - Purified 7 α -HSDH from *E. coli* strain DH5 α pBH51 transformant. The size of the prestained molecular mass markers is given, in kDa, to the left of the blot.

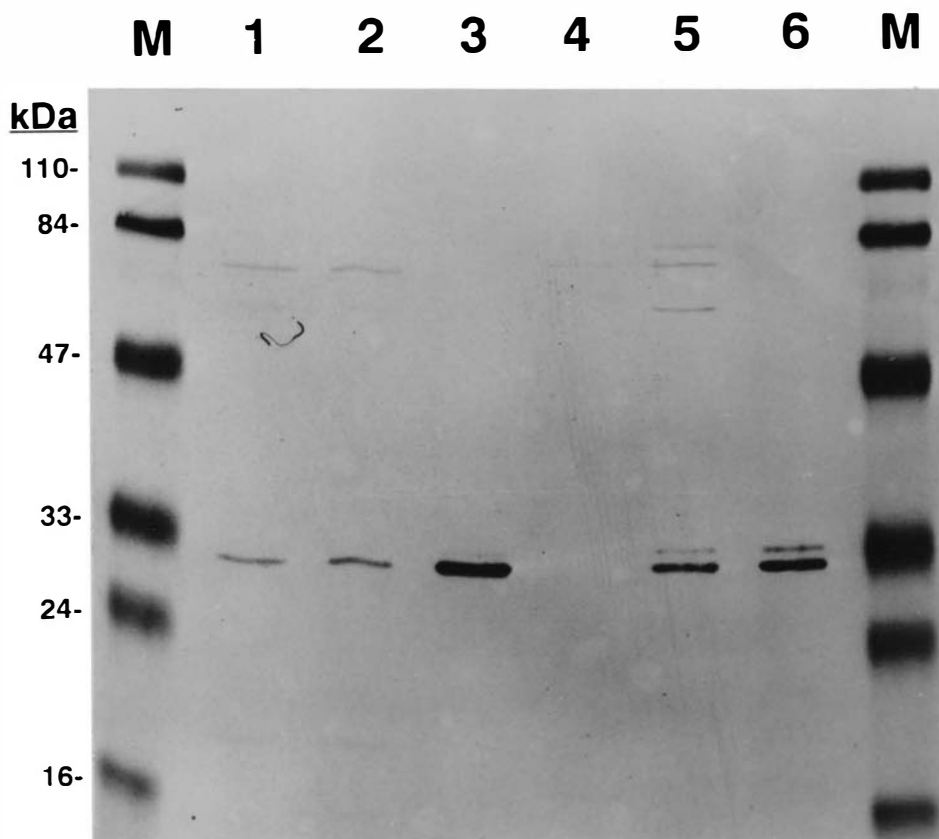
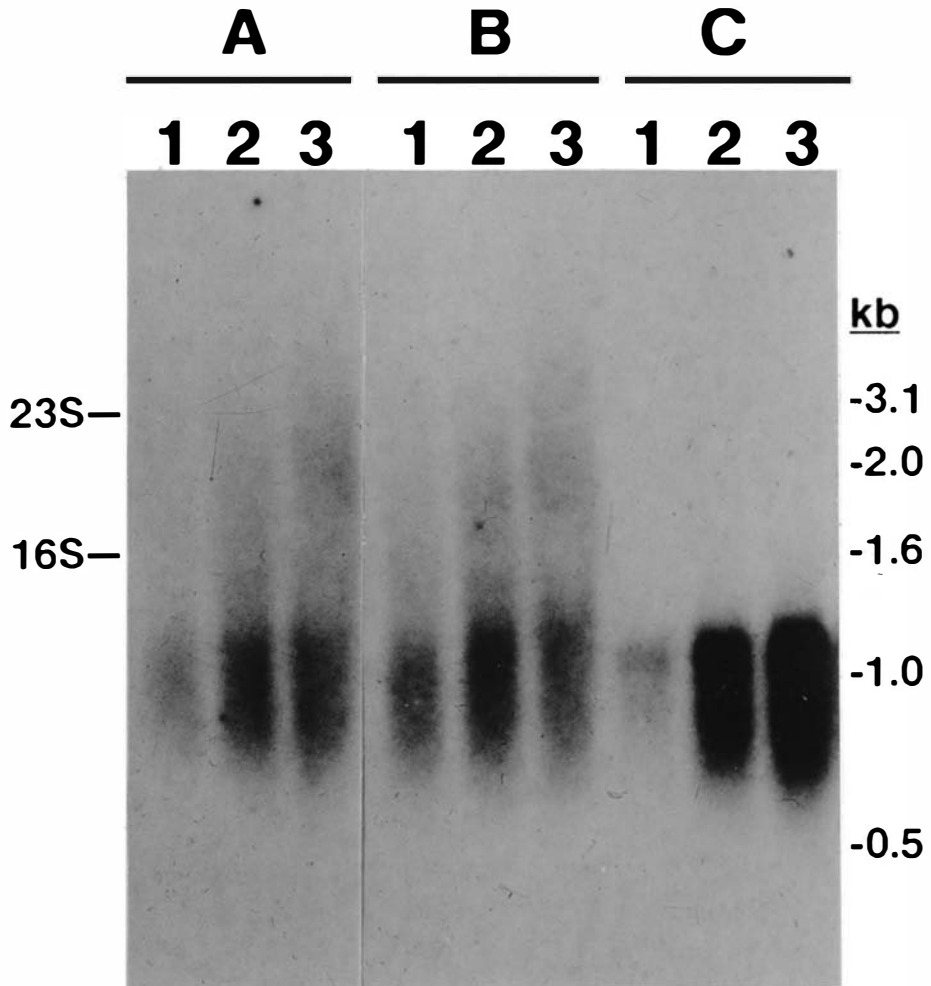


FIGURE 25: Northern Analysis of 7 α -HSDH Transcription in *Eu. sp* VPI 12708 and *E. coli*. Samples of total RNA from either uninduced (A) or cholic acid-induced (B) cultures of *Eu. sp.* VPI 12708 and an *E. coli* pBH51 transformant were run on a 1% agarose gel in the presence of formaldehyde as described in the Methods section. Lanes 1, 2, and 3 in both sections A and B contained 2.5, 5.0, and 10.0 μ g of RNA, respectively. Lanes 1, 2, and 3 in section C contained 0.1, 0.25, and 0.5 μ g of RNA. The migration distances for the 16S and 23S ribosomal RNA's are shown to the left of the autoradiogram, while the positions of the 1 Kb ladder markers are given on the right.



Eu. sp. VPI 12708 RNA preparations. These results are in agreement with the relative levels of enzymatic activity detected in CFE from these organisms.

The transcriptional start site for the 7α -HSDH message generated in both *E. coli* and *Eu. sp.* VPI 12708 was determined by primer extension analysis (Figure 26). A major band, corresponding to A-153, was found using 7α -HSDH mRNA isolated from *Eu. sp.* VPI 12708. A similar start site was found using mRNA from a pBH51 transformant, however, two additional bands (A-150 and C-147) were also detected. *E. coli* harboring only pUC19 did not produce any signal, demonstrating that these represent 7α -HSDH related transcripts.

Sequence Homology Between the 7α -HSDH and Several Other Alcohol/Polyol

Dehydrogenases: The entire 7α -HSDH amino acid sequence, as deduced from the nucleotide sequence, was compared against proteins in the NBRF and Swiss protein data bases using FASTA (UWGCG). Several members of the short-chain, non-zinc alcohol/polyol dehydrogenase superfamily exhibited significant homology to this protein. Nine proteins, including two 27 kDa cholate-inducible polypeptides from *Eu. sp.* VPI 12708, were selected to be compared to the 7α -HSDH and a consensus sequence was created using GAPS (UWGCG) (Figure 27). Extensive homology was detected in the amino terminal half of the proteins. This region has previously been demonstrated to contain the pyridine nucleotide binding domain [90-92]. However, substantial homology was also noted in the carboxy terminal region as well. The relative identity between these 10 proteins is illustrated as a histogram in Figure 28. When displayed in this manner, five regions of strong identity between these proteins was noted (centered at positions 17, 92, 125, 135, and 173). The GAPS program

FIGURE 26: Primer Extension Analysis of the 7 α -HSDH Start of Transcription.

The primer extension and dideoxy reactions were performed as described in the Methods section, and run on a 8% acrylamide sequencing gel. Lanes A, G, C, and T contained the corresponding sequencing reactions. The nucleotide sequence from positions 138 to 168 is shown to the right of the autoradiogram. Lanes 1, 2, and 3 are the primer extension reactions performed with RNA from *E. coli* DH5 α pUC19 transformant, *E. coli* DH5 α pBH51 transformant, and *Eu. sp.* VPI 12708, respectively. The start site for transcription A-153 is denoted by an arrow and is illustrated in bold-faced type. A possible -10 region for the 7 α -HSDH promoter is labelled P (-10).

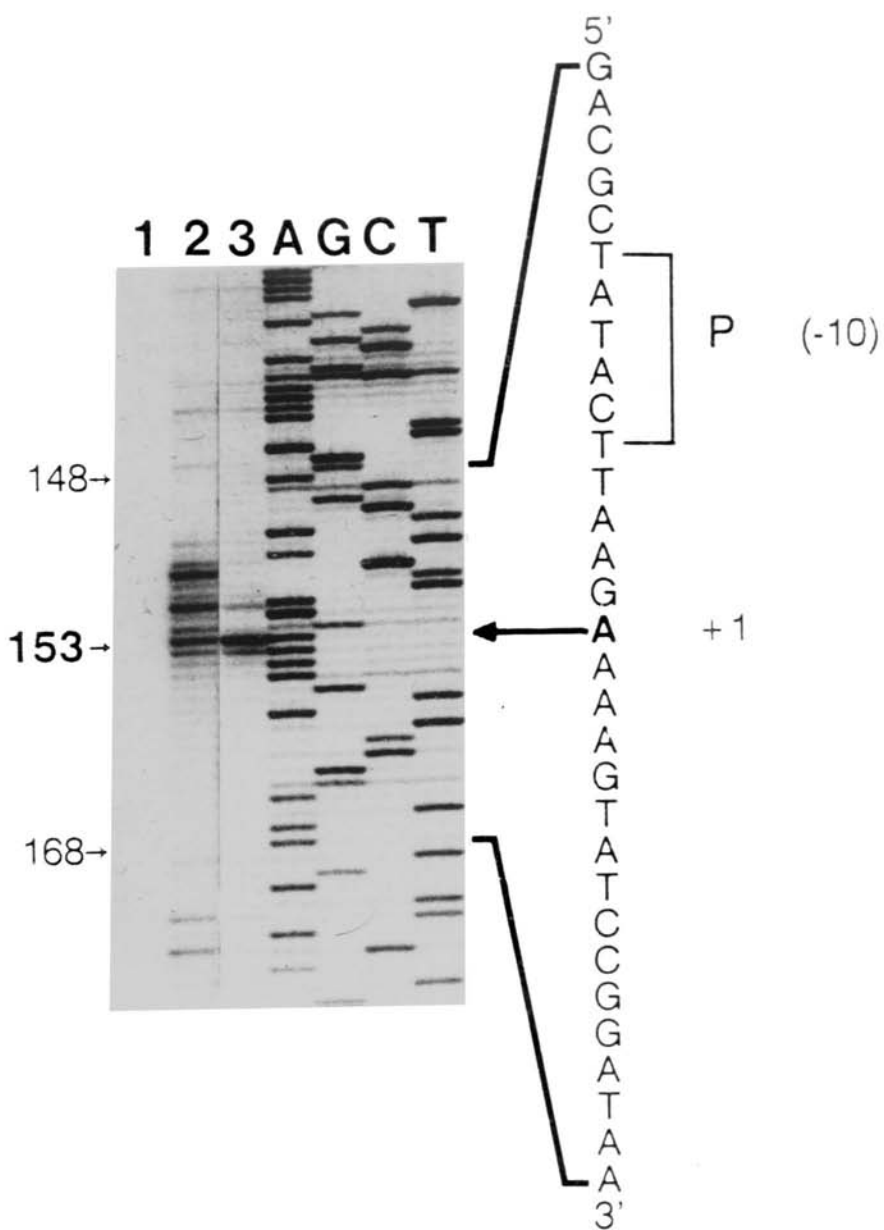


FIGURE 27: Alignment of the Derived Amino Acid Sequence for the 7 α -HSDH With Nine Other Alcohol/Polyol Dehydrogenases Using GAPS/LINEUP/PRETTY (UWGCG): The entire derived amino acid sequence for the 7 α -HSDH was compared against the sequences of several alcohol/polyol dehydrogenases using the UWGCG programs as described in the Methods section. A consensus for all 10 sequences compare was obtained and is displayed on the top line of each grouping. Positions in each of the sequences which match the consensus sequence are shown in bold type. Positions which are conserved among all of the sequences are shown as in capital letters in the consensus sequence and have an asterisk above them. The names, and origins of all of the sequences are given in the Table of Abbreviations.

* *

CONSENSUS	1	mtll·kvv·itgg·rGiGla·akr··egakvvkvyllfge·ee·eea·aalkelnpaggv1·vq
<u>Eu7α</u> -HSDH	1	mrl-kdkvilvtastrgig1AiAqacakega---kvym---garnlerakarademnaaggnvkvy
<u>Eu27K-1</u>	1	mklvqdkitiiitggtrgigfaaaklfienaga---kvsifgetqeevdtalaqlkelypeeevlgfa-
<u>Eu27K-2</u>	1	mlnvqdkvtiitggtrgigfaaakifidnga---kvsifgetqeevdtalaqlkelypeeevlgfa-
<u>Sh20β</u> -HSDH	1	mdlsgktviiitggarglg---aeaarqavaagarvvl---advldeegaatarelgdaa---ryqh
<u>Hs17β</u> -HSDH	1	----artvvlitgcssgig1hlavrlasdpqsqsfkvyatlrldktqgrlweaaralacppgsletlq
<u>Hs15</u> -HPGDH	1	-mhvngkvalvtgaaqgigrafaealllkg---kvalvdwnleagvqckaaldeqfepqktl-fiq
<u>BmGDH-A</u>	2	ytdlkdkvvitggstglgramavrfgqeeakvvinyy-----nneeealdakkeveeaggqaiivq
<u>BmGDH-B</u>	2	ykdllegkvvitgsstglgksmairfatekakvvvnyr----skedeanslveeeikkvgeaiavk
<u>KaRDH</u>	9	ntslsgkvaaitgaasgiglecartllgaga---kvvlidregeklnlkvlaelge-nafalqvdlmq
<u>DmADH</u>	3	ftltnknvifv-aglggig1dtskellkrdlknlvildrienpaaiaelka----inpkvtvtfypy

* *

CONSENSUS	68	·dvtdeedv·alvqtvigefgr1Dvlinnagi··pnpshelgls·v·eev·kv·diNltgvfngsr
<u>Eu7α</u> -HSDH	61	ndatkeetyvtmieeieeegridvlnn--fgssnpkkdlgiantdpevfiktvnlnksvfiasq
<u>Eu27K-1</u>	64	pdltsrдавmaavgtvaqkygrldvminnagit-----mnsvfrsvseedfknimdinvgvfngaw
<u>Eu27K-2</u>	64	pdltsrдавmaavggvaqkygrldvminnagitsnn-----vfrsvseeefkhimdinvtgvfngaw
<u>Sh20β</u> -HSDH	59	ldvtieedwqrvvayareefgsvdglvnnagist-----gmfletesverfrkvvdinltgvfigmk
<u>Hs17β</u> -HSDH	64	ldvrdsksvaarervt--egrvdvlvcnaglgllgplealg-----edavasvldvvnvgtvrmlq
<u>Hs15</u> -HPGDH	63	cdvadqqqlrdtfrkvvdhfg1rdilvnnagv---nnekn-----wektlqinlvsvigsty
<u>BmGDH-A</u>	64	gdvtkeedvnlvqtaikefgtldvminnagvenpvpshelsldn-----wnkvidtnltgaf1gsr
<u>BmGDH-B</u>	65	gdvtvesdvinlvqsaikefgkldvminnagmenpvsshems1sd-----wnkvidtnltgaf1gsr
<u>KaRDH</u>	73	adqvdn-----llqgilq1tgrldifhanagayigpp-----vaegdpdvdrvlgl1ninaafrcvr
<u>DmADH</u>	65	dvtvpiaettk1lktifaqlktvdvlin-----gagilddhqiertiavnytglvnttt

CONSENSUS	269	epeeiaav·flasd·asgit·ttyttg·l·v·····sgg·····fa···mg·ypsf·a·rg··
<u>Eu7α</u> -HSDH	218	lpeeiaavvyfasddaa-----yttgqiltv-----sgg---fglatpifgdlersdarg-
<u>Eu27K-1</u>	217	-peeianvylflasdlasgitattisvdgayrp-----
<u>Eu27K-2</u>	217	epeeianvylflasdlasgitattvsvdgayrp-----
<u>Sh20β</u> -HSDH	214	epgeiagavkllsdtss-----yvtgaelav-----dggwttgptvkyvmgq-----
<u>Hs17β</u> -HSDH	234	npeevae--vftalrapkptlryftterflplrmlrddpsgsnyvtamhrevfgdvpakaeaga-
<u>Hs15</u> -HPGDH	242	pplianglitlieddalngaimkitt-----skgihfqdydttpfqaktq-----
<u>BmGDH-A</u>	221	-peeavaavaaflassqas-----yvtgitl-----fadggmtkypsfqagrg-
<u>BmGDH-B</u>	224	-peelaavaawlasseas-----yvtgitl-----fadggmtkypsfqagrg-
<u>KaRDH</u>	207	mdealadgsl-mqpievaesvlfmvtrsknvtvrdivilpnsvdl-----
<u>DmADH</u>	252	wdsgi-----

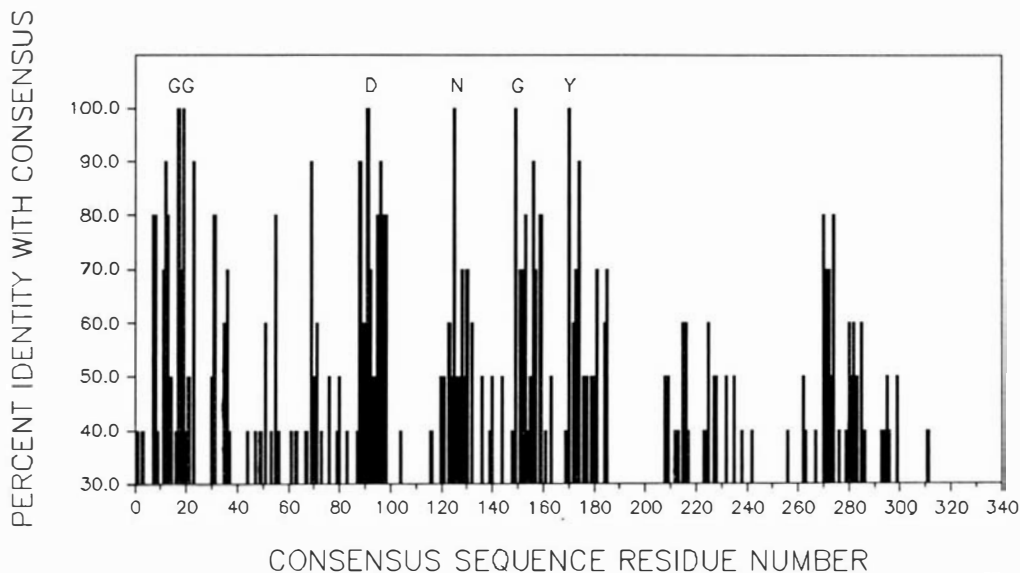


FIGURE 28: Relative Identity Between Several Alcohol/Polyol Dehydrogenases. The percentage of the protein sequences from Figure 21 which agreed with the consensus sequence, as generated by PRETTY, is illustrated for every position of the consensus as a histogram. The six perfectly conserved residues are labelled with single letter abbreviations.

identified six residues which were absolutely conserved in all of the dehydrogenases examined; these amino acids are labelled in Figure 28. Moreover, eight additional amino acids positions were identical in 90% of the sequences, with another eleven residues showing 80% conservation. Since these dehydrogenases are comprised of, on the average, approx 260 amino acids, it appears that about 10% of the amino acid residues are conserved greater than 80% within this superfamily.

During alignment of the different sequences to the 7α -HSDH, the GAPS program calculated several parameters which are useful measures of the relative relatedness of these proteins. These alignment metrics are shown in Table 7. The sequence with the best overall match to the 7α -HSDH sequence was *BmGDH-A*. The sequences for *Eu27K-2* and *Hs17 β -HSDH* also received high quality scores. The *Sh20 β -HSDH* and *Eu27K-2* exhibited the most identity and similarity to the 7α -HSDH sequence, respectively. The poorest matches were generated from the *KaRDH* and *DmADH* sequences. The GAPS algorithm was not designed for multiple sequence alignments. In addition, the program is capable of ignoring areas of good homology in order to optimize the alignment elsewhere in the sequence. This problem is only compounded by the multiple alignments necessary to achieve an overall consensus sequence. Therefore, all nine secondary alcohol dehydrogenases were compared to the 7α -HSDH using ALIGN and DOTPLOT (Figure 29). Although no consensus sequence or numerical quality scores are generated, this format allows one to visually obtain a qualitative assessment of the alignment for each of the alcohol/polyol dehydrogenase sequences. With these programs, stretches of conserved sequence are illustrated as diagonal lines. These data confirm that *BmGDH-A* and *Eu27K-2* give

TABLE 7: Alignment Metrics for the Alcohol/Polyol Dehydrogenases as Compared to the Derived 7 α -HSDH Sequence Using GAPS (UWGCG).

Sequence ^A	Quality ^B	Ratio ^C	Identity ^D	Similarity ^E
<i>Eu27K-1</i>	126.7	0.509	30.222	53.778
<i>Eu27K-2</i>	132.6	0.533	33.628	57.522
<i>Hs17β-HSDH</i>	140.2	0.527	26.693	51.793
<i>Hs15-HPGDH</i>	126.6	0.476	32.198	55.365
<i>Sh20β-HSDH</i>	132.3	0.521	36.555	56.723
<i>DmADH</i>	105.3	0.411	23.786	45.631
<i>KaRDH</i>	107.5	0.432	27.700	53.991
<i>BmGDH-A</i>	140.5	0.538	32.922	55.967
<i>BmGDH-B</i>	129.6	0.493	28.689	54.918

^A Full sequence names and origins are given in the Table of Abbreviations.

^B Quality is the value optimized by GAPS. The magnitude of the score reflects the number of positions having identity or similarity minus the number of gaps inserted to achieve the match.

^C Ratio is the Quality normalized for the length of the sequence.

^D Identity is the percentage of exact matches between the two sequences.

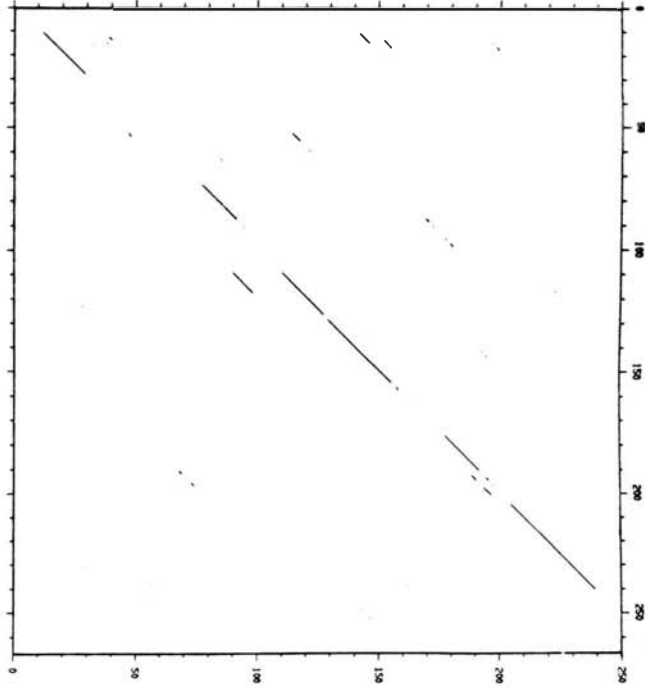
^E Similarity is the percentage of residues representing conservative replacement between the two sequences.

FIGURE 29: Alignment of the Deduced Amino Acid Sequence for the 7 α -HSDH With Several Other Alcohol/Polyol Dehydrogenases Using COMPARE/DOTPLOT (UWGCG). Each of the nine other alcohol/polyol dehydrogenases were aligned with the 7 α -HSDH sequence using the COMPARE program as described in the Methods section. The results as plotted by DOTPLOT are shown in panels A-I. In all panels, the 7 α -HSDH sequence is plotted on the y-axis. The sequences plotted on the x-axis for each panel were the following:

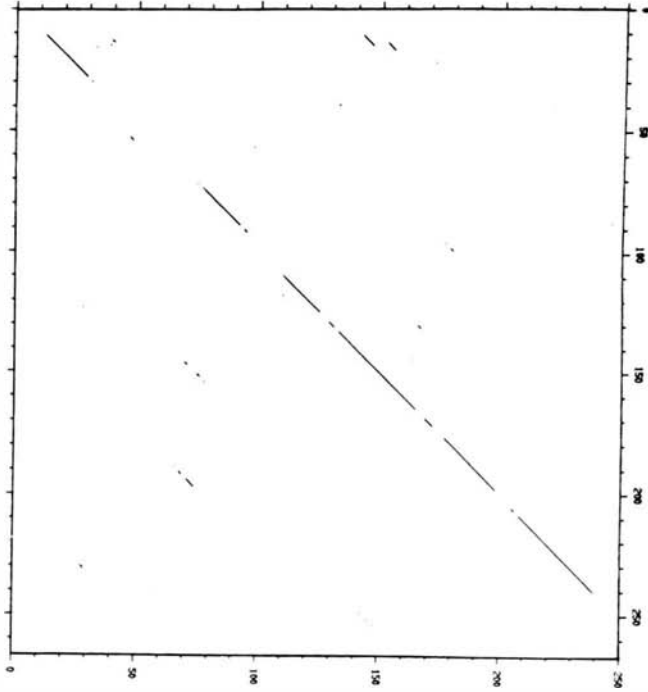
A: *Eu27K-1*, B: *Eu27K-2*, C: *BmGDH-A*, D: *BmGDH-B*, E: *KaRDH*,
F: *DmADH*, G: *Sh20 β -HSDH*, H: *Hs15-HPGDH*, I: *Hs17 β -HSDH*

The full names, and origins are given in the Table of Abbreviations.

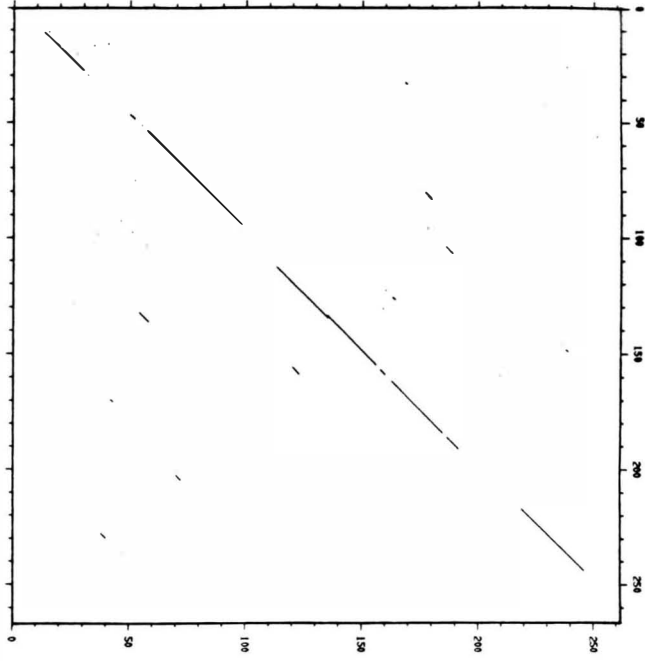
A



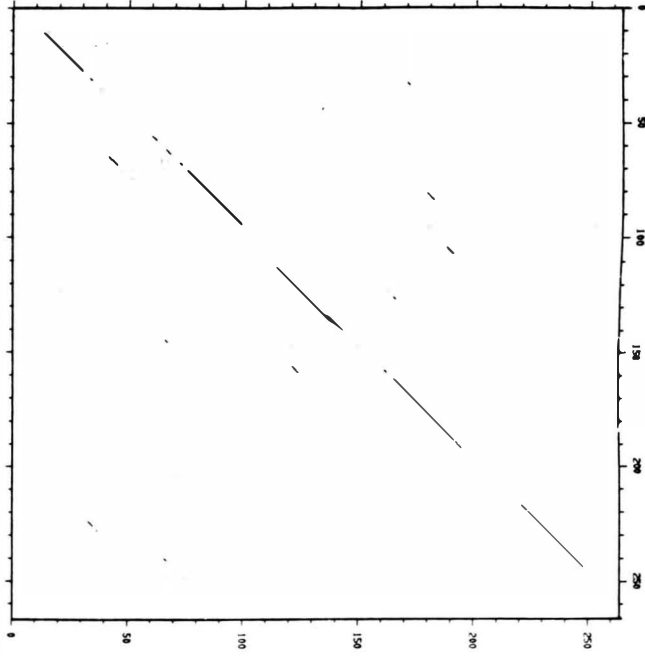
B

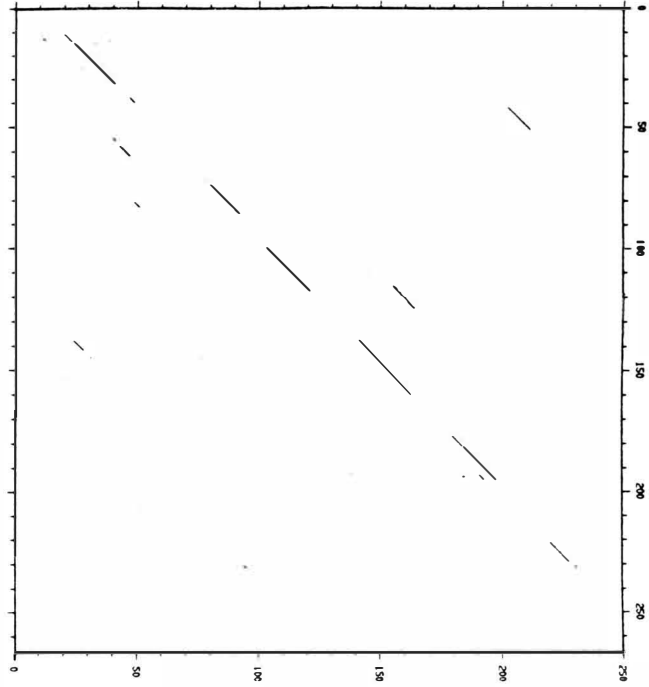
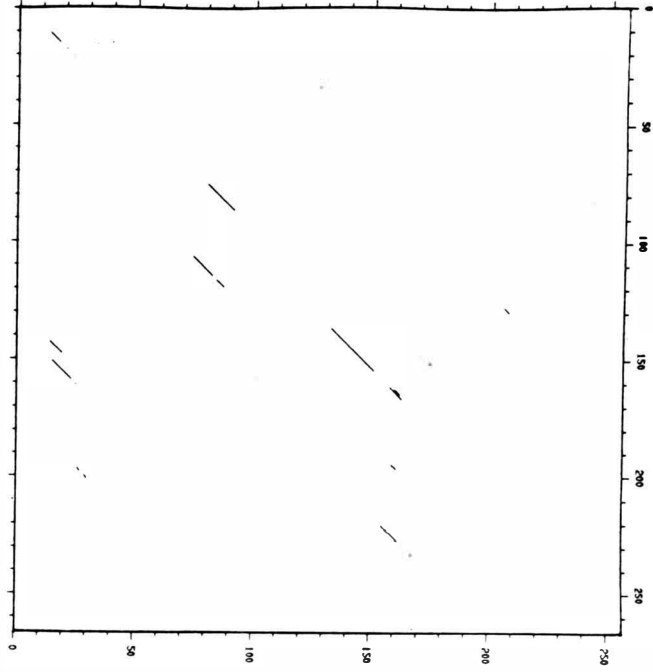


C

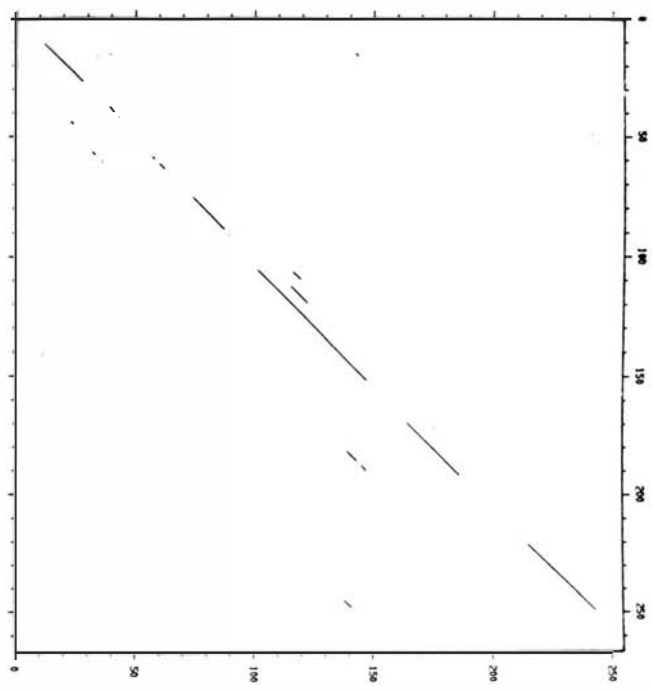


D

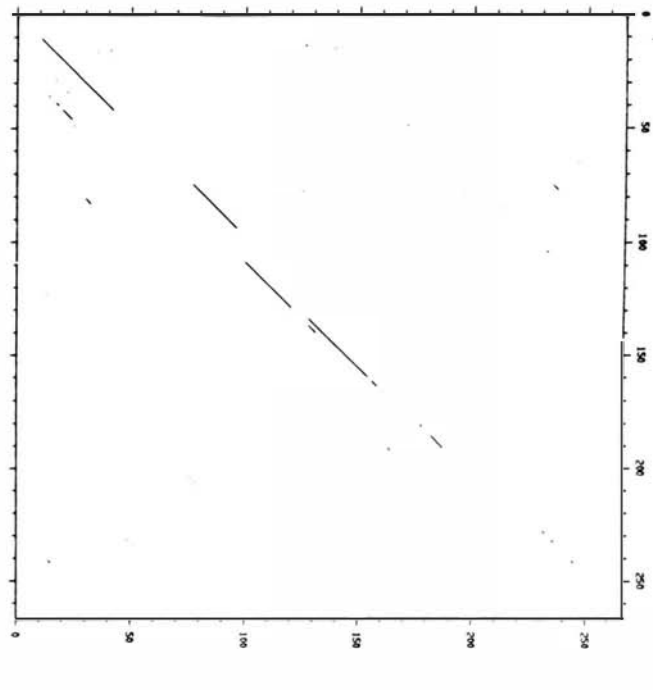


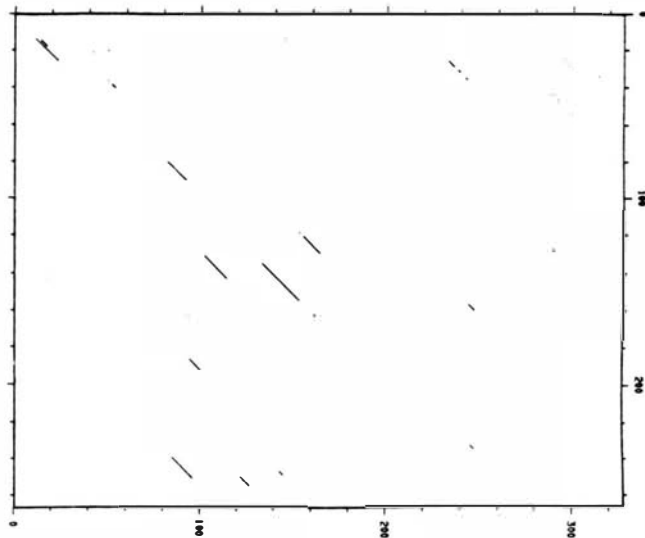
E**F**

G



H



I

the best alignments while *Dm*ADH gives a poor alignment with the 7 α -HSDH sequence. The homology to the glucose dehydrogenases and 27 kDa proteins can be seen to extend throughout the entire length of the proteins. The *Ka*RDH exhibited a better and *Hs*17 β -HSDH showed a poorer alignment than would have been predicted from the GAPS alignment metrics table. All nine sequences appear to be homologous to the 7 α -HSDH between positions 0 to 50 and 100 to 150. These regions are probably part of the pyridine nucleotide binding domain. The region(s) involved in bile acid binding, however, could not be deduced from these data.

Purification of the NADH:FOR: The cholate-inducible NADH:FOR was also purified from *Eubacterium* sp. VPI 12708. Cell free extracts from 16 liters of cells exposed to cholic acid contained over 300 units of NADH:FOR activity, with a specific activity of 0.13. This enzyme was purified to apparent electrophoretic homogeneity using a five step protocol as outlined in Table 8. The most effective steps were Cibacron Blue A and phenyl-HPLC chromatography which gave 6- and 7.6-fold purifications and 41% and 34% recoveries, respectively. A final purification of 372-fold with a 10% overall recovery was ultimately achieved. The enzyme eluted as a single symmetrical peak from DE-52 (Figure 30). Two peaks of activity could be detected using this resin if the pH of the column was above 7.0. Although Red A chromatography did not result in significant purification of the NADH:FOR, it was a necessary step to eliminate 7 α -HSDH activity, which otherwise contaminated the NADH:FOR preparations. Since Cibacron blue A bound the NADH:FOR inefficiently, multiple loadings were necessary to achieve acceptable recoveries. Approximately 20 to 25% of the detectable activity remained unbound even after 10

TABLE 8: Purification of the NADH:FOR.

The purification was performed using 55 g of cells (wet pellet weight), from 16 l of tryptic soy broth. Details of the purification procedure are given in the Methods section.

Purification Step	Volume	Protein	Activity	Sp. Act.	Purification	Yield
	(ml)	(mg)	(Units)¹	(U/mg)	(Fold)	(%)
Cell Free Extract	62.0	2580	329.2	0.13	1.0	100
DE-52	35.0	1190	308.9	0.26	2.0	94
Reactive Red 120	37.0	1060	307.5	0.29	2.2	93
Cibacron Blue A	30.0	72.8	126.0	1.73	13.3	38
DEAE-HPLC (pH 7.0)	19.0	15.2	96.9	6.38	49.1	29
Phenyl-HPLC (pH 7.0)	4.0	0.67	32.4	48.36	372.0	10

¹ One unit of activity is defined as the flavin-dependent oxidation of 1 μ mol NADH/min.

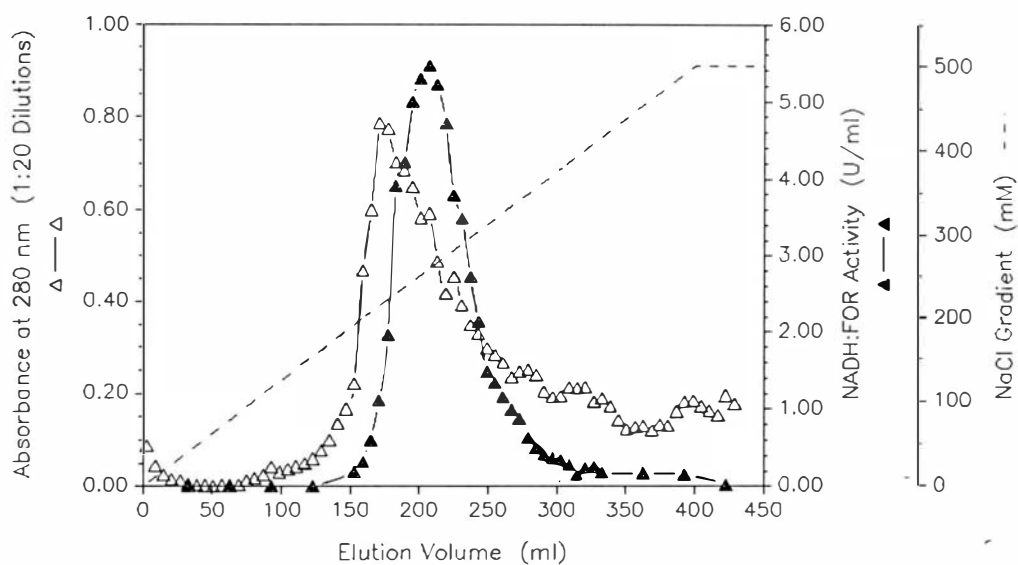


FIGURE 30: DEAE-Cellulose Elution Profile for the NADH:FOR. Cell free extract (2.6 g) was loaded onto a pre-equilibrated DE-52 column. Bound proteins were eluted with an increasing NaCl gradient at a flow rate of 1.0 ml/min.

passages over the column. The bound NADH:FOR could only be eluted using 1 M KCl (Figure 31). Solutions containing up to 2 M NaCl and 20 mM NAD(H) resulted in enzyme recoveries of less than 5%. A variety of other affinity matrices (including NAD-agarose, acriflavine agarose, and reactive blue 4, blue 72, brown 10, green 5, green 19, yellow 3, and yellow 86 agarose) were found not to bind the NADH:FOR activity. The elution profile of the NADH:FOR from DEAE-HPLC was complex, as three peaks of activity were detected (Figure 32). The predominant form eluted at 35 ml, while smaller peaks of activity were detected at 50 and 65 ml (for the sake of discussion these peaks shall be referred to as forms I, II and III, respectively). For the protocol shown in Table 8, the form I fractions were pooled and used for further purification. The flavin oxidoreductase exhibited substantial hydrophobic character on phenyl-HPLC. The bound protein was only partially eluted from this hydrophobic interaction column by a decreasing ammonium sulfate gradient (Figure 33). The specific elution of most of the loaded NADH:FOR activity was achieved by injecting 10% ethanol over the column. The enzyme preparation after phenyl-HPLC was judged to be >95% homogeneous by SDS-PAGE (Figure 34). The purified enzyme contained a single protein subunit of 72 kDa. Gel filtration chromatography, using Sepharose CL-6B, gave a native molecular mass of 210 kDa (Figure 35). These data suggest that the NADH:FOR exists either as a dimer or trimer of identical subunits. The purified enzyme was somewhat stable to storage at either 4°C or -20°C in the presence of 10% glycerol and 1 mM DTT (50% loss of activity in 2 to 3 weeks). Since the presence of multiple peaks of NADH:FOR activity during elution from DEAE-HPLC was unexpected, further experiments were performed to discern the

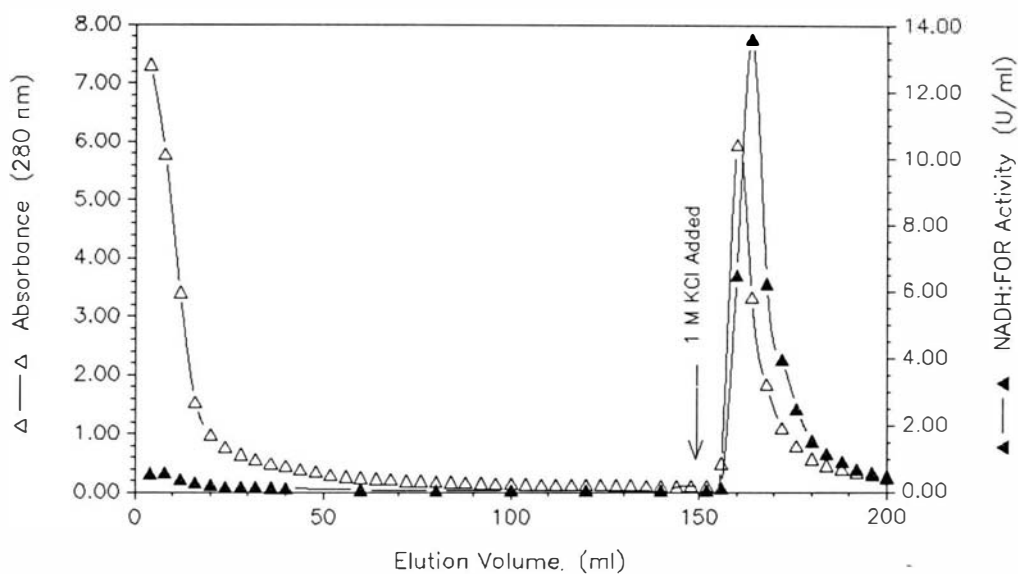


FIGURE 31: Cibacron Blue A Elution Profile for the NADH:FOR. The column eluate from Reactive Red chromatography was adjusted to pH 7.0 and passed over a pre-equilibrated Cibacron Blue A column six times. Unbound proteins were washed off with 15 column volumes of buffer. The bound proteins were then eluted with 1 M KCl.

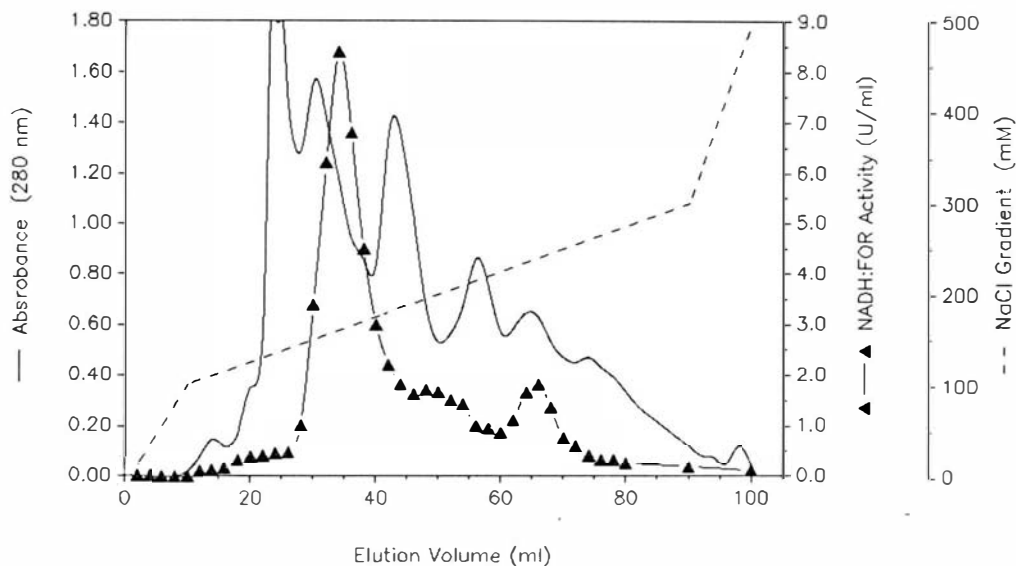


FIGURE 32: DEAE-HPLC Elution Profile for the NADH:FOR. Pooled and desalted fractions from Cibacron Blue A were loaded onto a DEAE-3SW HPLC column at a flow rate of 0.4 ml/min. Bound proteins were eluted with an increasing NaCl gradient at a flow rate of 0.85 ml/min. The protein elution profile was monitored at 280 nm using an online variable wavelength detector.

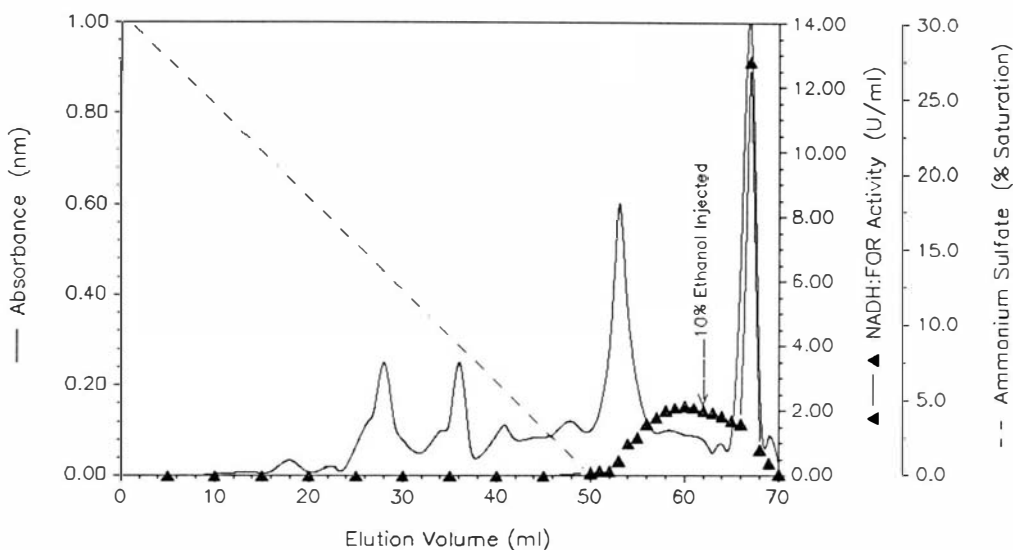
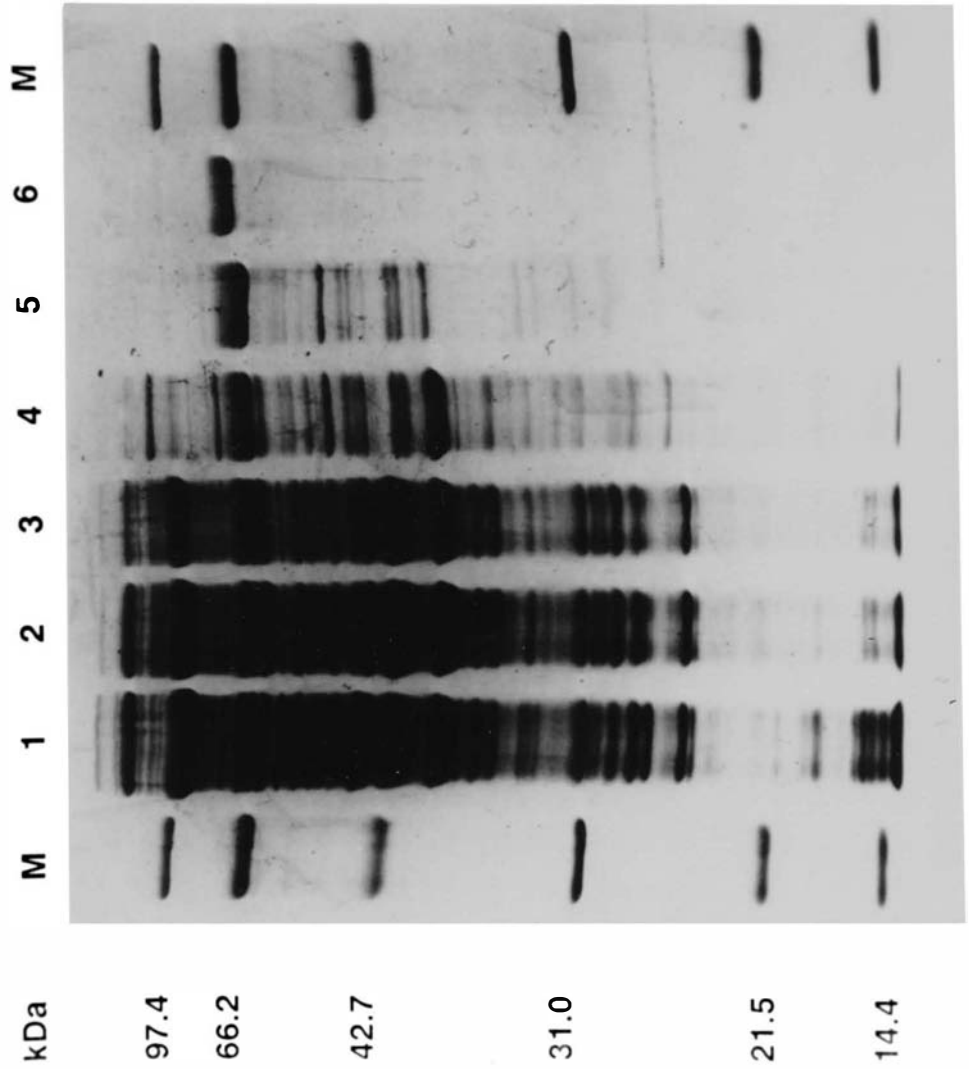


FIGURE 33: Phenyl-HPLC Elution Profile for the NADH:FOR (Form I). Pooled DEAE-HPLC fractions from peak I were brought to 20% (w/v) ammonium sulfate by the addition of the solid salt. The proteins were then loaded onto a phenyl-5PW HPLC column which had been equilibrated with buffer containing 20% ammonium sulfate. Loosely bound proteins were eluted with a decreasing ammonium sulfate gradient. The NADH:FOR was specifically released by injecting 20% ethanol onto the column. The protein elution profile was followed at 280 nm, using a variable wavelength detector.

FIGURE 34: SDS-PAGE of the NADH:FOR. Aliquots from each step of the purification were subjected to electrophoresis using a 12% acrylamide slab gel. The lanes contained the following: M - Low molecular weight mass markers, 1 - CFE (50 μg), 2 - Pooled DE-52 fractions (40 μg), 3 - Pooled Red A flow through (40 μg), 4 - Pooled Cibacron Blue A fractions (35 μg), 5 - Pooled DEAE-HPLC (Peak I) fractions (15 μg), 6 - Pooled Phenyl-HPLC fractions (10 μg). The molecular mass of the marker proteins is shown, in kDa, to the left of the gel.



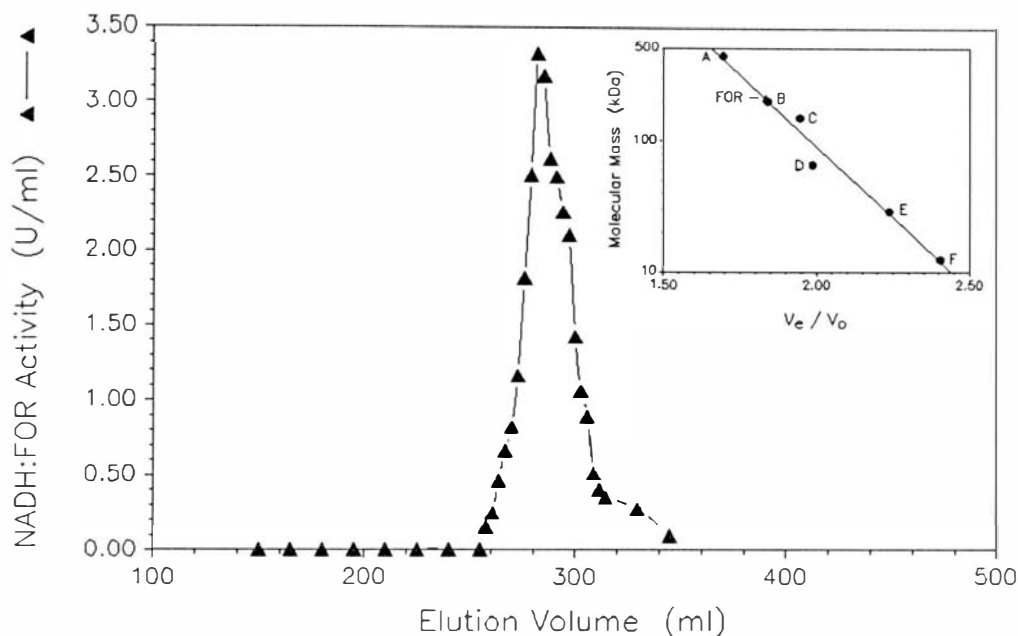


FIGURE 35: Gel Filtration Elution Profile and Native Molecular Mass Determination for the Purified NADH:FOR. Purified NADH:FOR (40 μ g) was chromatographed on a sepharose CL-6B column equilibrated with solution A containing 100 mM NaCl, and its relative elution volume was calculated.

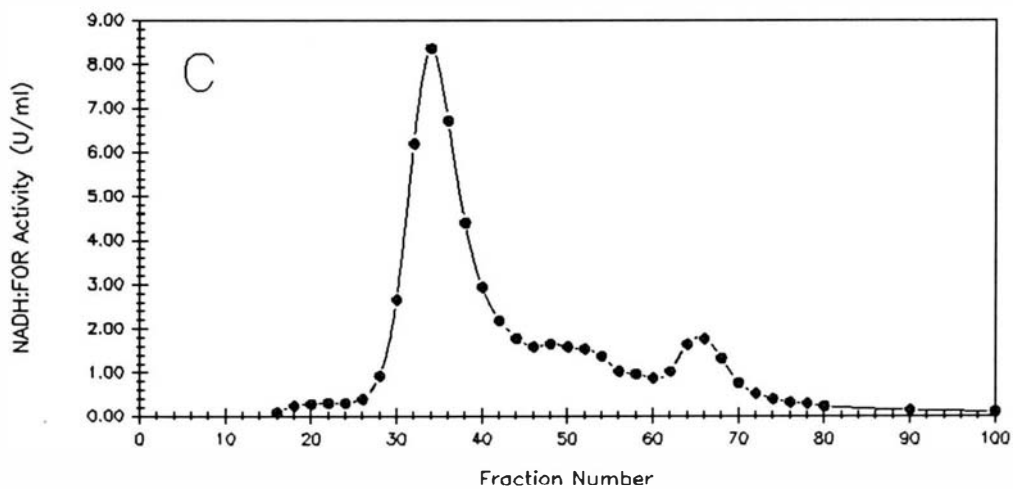
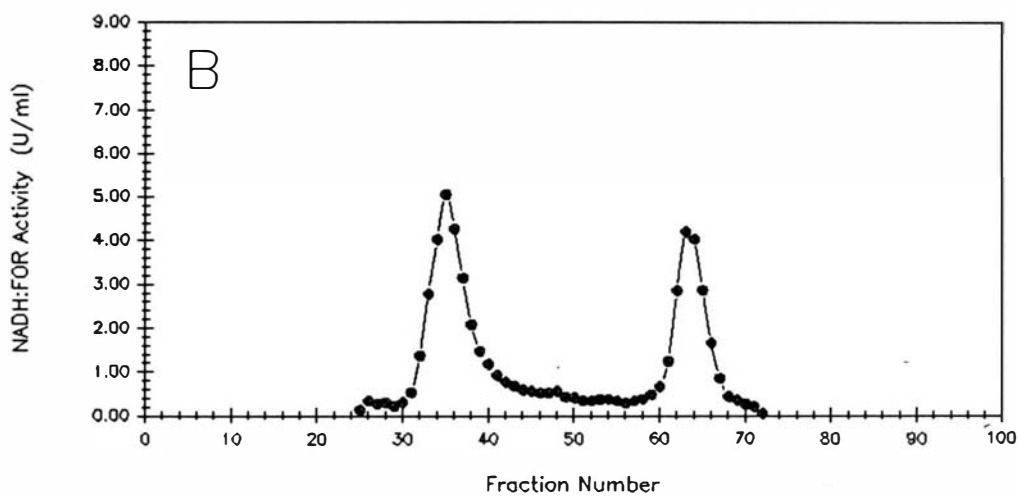
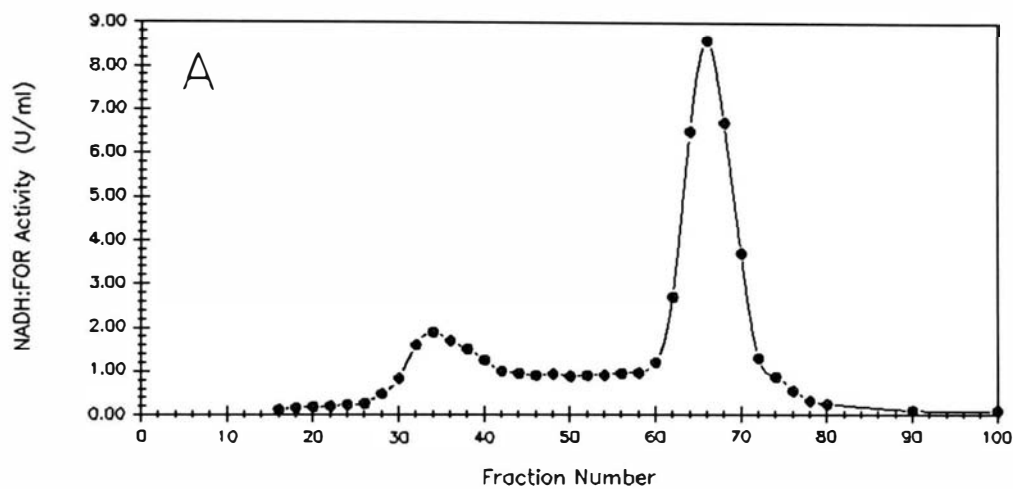
Inset: A molecular mass standard curve was generated from the \log_{10} molecular mass vs. the relative elution volumes (V_e/V_o) of several standards. The proteins used were as follows - A: apoferritin, B: β amylase, C: alcohol dehydrogenase, D: albumin, E: carbonic anhydrase, F: cytochrome C. The filled triangle represents the NADH:FOR.

reason for this behavior. Aliquots of the NADH:FOR preparation from various points in the purification protocol were found to give remarkably different elution profiles on DEAE-HPLC (Figure 36). In the least purified enzyme preparations, the predominant form (>80%) was form III. The relative proportion of form III detected was found to decrease, with the concomitant increase of form I, as the enzyme was subjected to further purification. After performing both red A and cibacron blue A chromatography, form I represented approx 75 to 80% of the NADH:FOR activity. Form II, although detected, was only present as a minor peak under the conditions examined. The material from the form III peak shown in Figure 32, was pooled and subjected to phenyl-HPLC (Figure 37). Although some of the NADH:FOR activity exhibited an elution profile similar to form I, a new, less hydrophobic peak was also detected. The fractions of this new peak also contained a 72 kDa protein (data not shown), but were noticeably yellow-brown as compared to the colorless fractions obtained from form I. The absorbance spectra of the purified proteins from both form I and form III were compared between 300 and 500 nm (Figure 38). Form III, but not form I, was found to have two absorbance peaks at 340 and 475 nm, indicative a bound flavin. Due to the lack of material, the identity of the flavin was not determined. Attempts to add FAD to form I, aerobically, did not alter the activity elution profile to that of form III. Furthermore, alteration of the buffer pH alone was not sufficient to change the elution profile of form III from the pooled DE-52 fractions. Thus, the interaction of the NADH:FOR with these column resins is required for this effect.

Expression of the NADH:FOR in *Eu. sp.* VPI 12708: The expression of the NADH:

FIGURE 36: Effect of the Purification Protocol Upon the DEAE-HPLC Elution Profile of the NADH:FOR. Protein samples were chromatographed, using DEAE-HPLC, at several points in the NADH:FOR purification protocol. Approximately the same amount of NADH:FOR activity was loaded in each panel. After separation, the fractions were assayed for NADH:FOR activity. The proteins analyzed were obtained at the following points:

- A: Proteins from pooled DE-52 fractions.
- B: Proteins after DE-52 and Cibacron Blue A chromatography.
- C: Proteins after DE-52, Reactive Red A, and Cibacron Blue A chromatography.



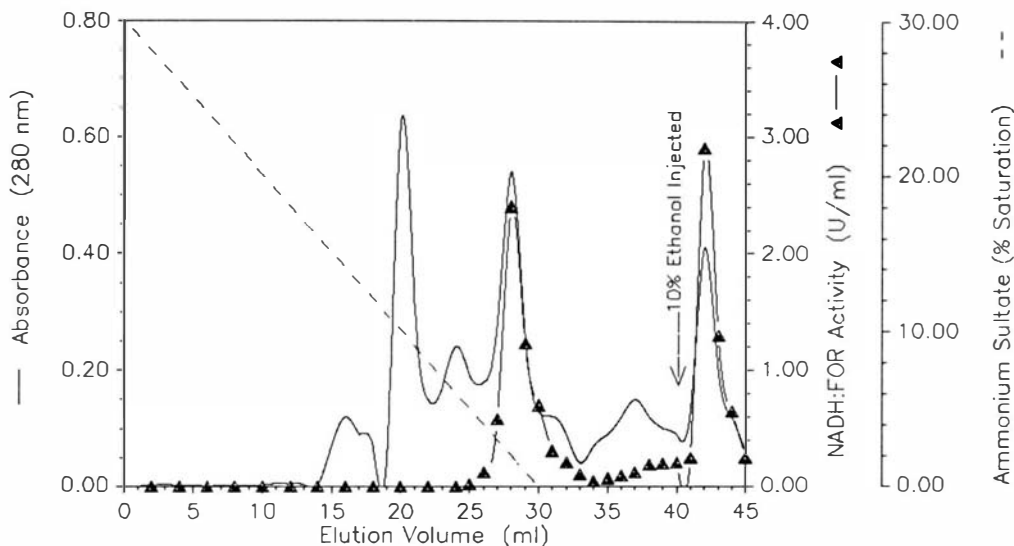
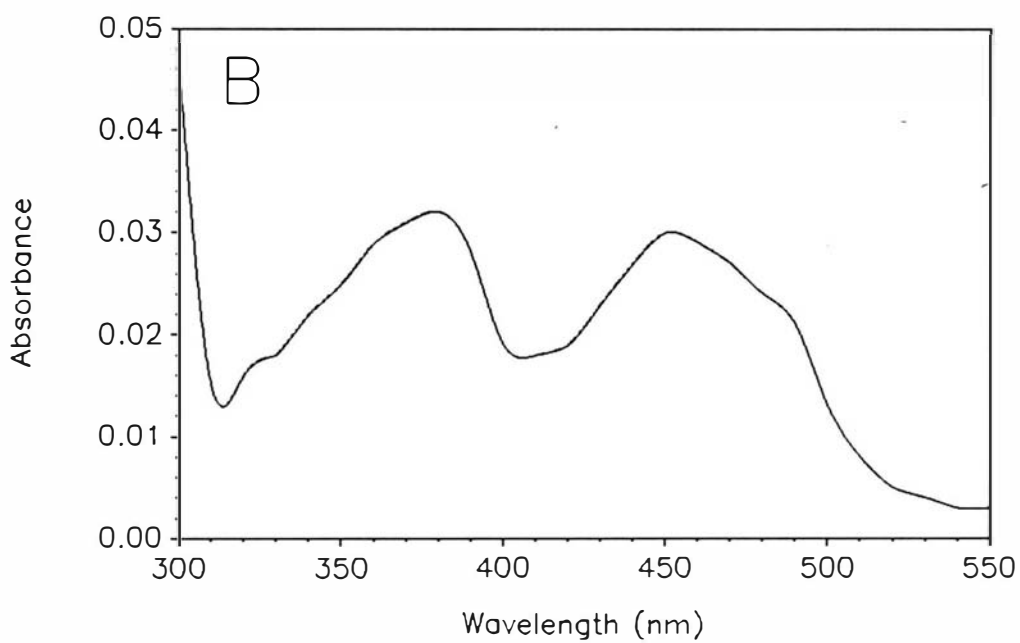
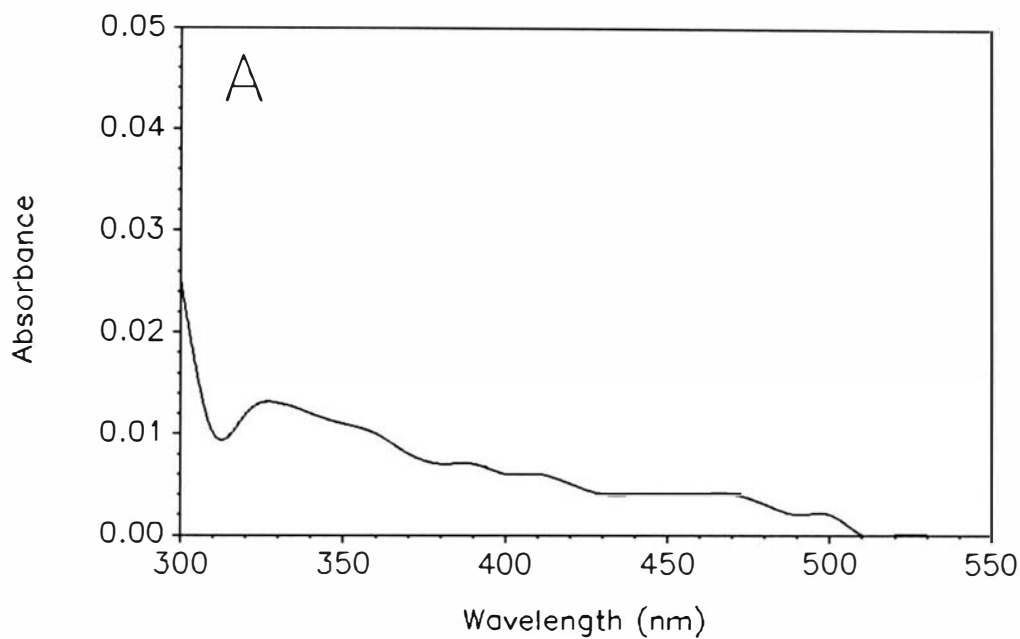


FIGURE 37: Phenyl-HPLC Elution Profile of the NADH:FOR (Form III). Pooled DEAE-HPLC fractions from peak III were brought to 20% (w/v) ammonium sulfate by the addition of the solid salt. The proteins were then loaded onto a phenyl-5PW HPLC column which had been equilibrated with buffer containing 20% ammonium sulfate. Loosely bound proteins were eluted with a decreasing ammonium sulfate gradient. Some NADH:FOR was released by injecting 20% ethanol onto the column. The protein elution profile was followed at 280 nm, using a variable wavelength detector.

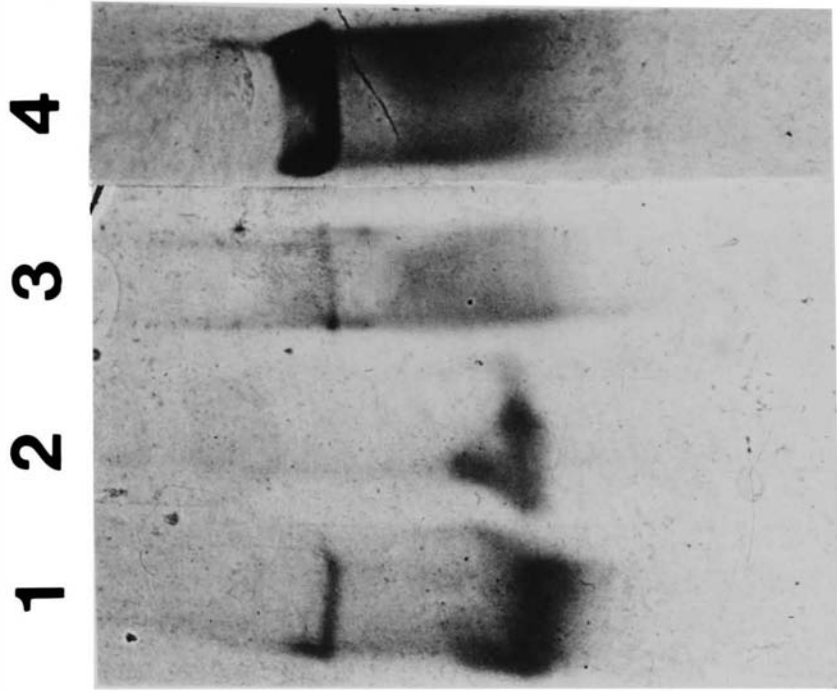
FIGURE 38: Absorbance Spectra of Purified NADH:FOR Forms I and III. The absorbance spectra of purified NADH:FOR forms I and III (400 μg each) were determined on a Shimadzu UV160U recording spectrophotometer, using a quartz cell with a 1 cm path length at 20°C.



FOR in *Eu. sp.* VPI 12708 was confirmed to be cholate-inducible by native gel electrophoresis, Ochterlony plates, and Western analysis. Activity stains of native gels showed the presence of a cholic acid-inducible NADH:oxidoreductase band with a calculated molecular mass of 120 kDa (Figure 39). The migration of this band corresponded to the purified enzyme. A constitutively expressed band of lower molecular mass was also detected in uninduced cell-free extracts. Analysis of cell-free extract and purified NADH:FOR using Ochterlony plates showed that the rabbit polyclonal antiserum raised against the NADH:FOR reacted with a cholic acid-inducible protein (Figure 40A). Furthermore, Western analysis revealed that a 72 kDa protein was specifically recognized by these antibodies (Figure 40B). Both form I and form III were observed to react with the immune serum. The specificity of the rabbit antiserum for the NADH:FOR was confirmed by immunoinhibition (Figure 41). About 50% inhibition of the catalytic activity of the purified NADH:FOR was achieved after incubating the enzyme with 150 μ l of immune serum. No inhibition was detected using preimmune serum.

Effect of Various Compounds Upon NADH:FOR Activity: The purified enzyme was found to be very sensitive to the presence of several sulfhydryl inhibitors. Near complete inhibition of catalytic activity was achieved after incubating the NADH:FOR with either CuCl_2 , HgCl_2 , NEM, or pCMS at 1 mM final concentrations (Table 9). The enzyme was also inhibited by 1 mM ZnCl_2 (approx 73%). Similar concentrations of iodoacetate and iodoacetamide, however, failed to substantially inhibit catalytic activity. The metal ion chelators EDTA and o-phenanthroline, but not EGTA and NaN_3 , were also found to reduce NADH:FOR activity. In addition,

FIGURE 39: Native Gel Electrophoresis of the NADH:FOR. Protein aliquots were run on an 8% acrylamide slab gel using the buffer system of Laemmli, except that SDS was excluded. The NADH:FOR was visualized with the activity stain described in the Methods section. The arrows denote the location of the cholic acid-inducible NADH:FOR (FOR) and a constitutive activity (CON). The lanes contained the following: 1 - Cholic Acid-Induced CFE (50 μ g), 2 - Uninduced CFE (50 μ g), 3 - Purified Form I (10 μ g), 4 - Purified Form III (10 μ g).



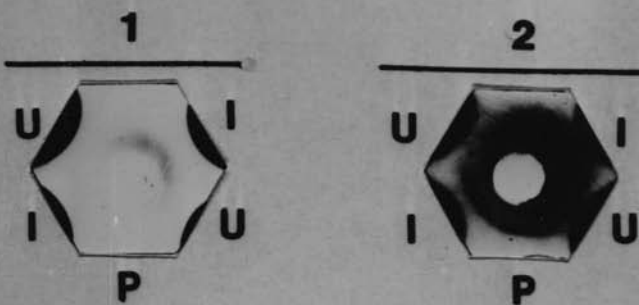
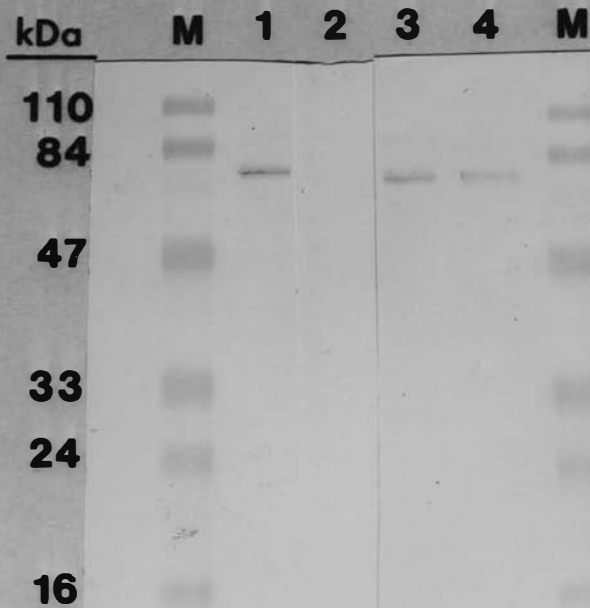
FOR



CON

FIGURE 40: Western Analysis of NADH:FOR Expression in *Eu. sp.* VPI 12708. The expression of the NADH:FOR protein was analyzed using both Ochterlony plates (A) and Western blots (B). In Panel A, the center wells contained 100 μ l of either preimmune (1) or immune (2) serum. The other wells contained the following: I - Cholic Acid-Induced CFE (2 mg), UI - Uninduced CFE (2mg), P - Purified FOR (Form I) (50 μ g). The plate were allowed to incubate at 37°C for 48 hours.

Western blot analysis was performed from samples run on a 12% acrylamide SDS-slab gel and electrophoretically transferred to a nylon membrane. The lanes contained the following: M - Prestained Molecular Mass Markers, 1 - Cholic Acid-Induced CFE (10 μ g), 2 - Uninduced CFE (10 μ g), 3 - Purified NADH:FOR Form I (1 μ g), 4 - Purified NADH:FOR Form III (1 μ g). The molecular mass of the marker proteins is given, in kDa, to the left of the blot.

A**B**

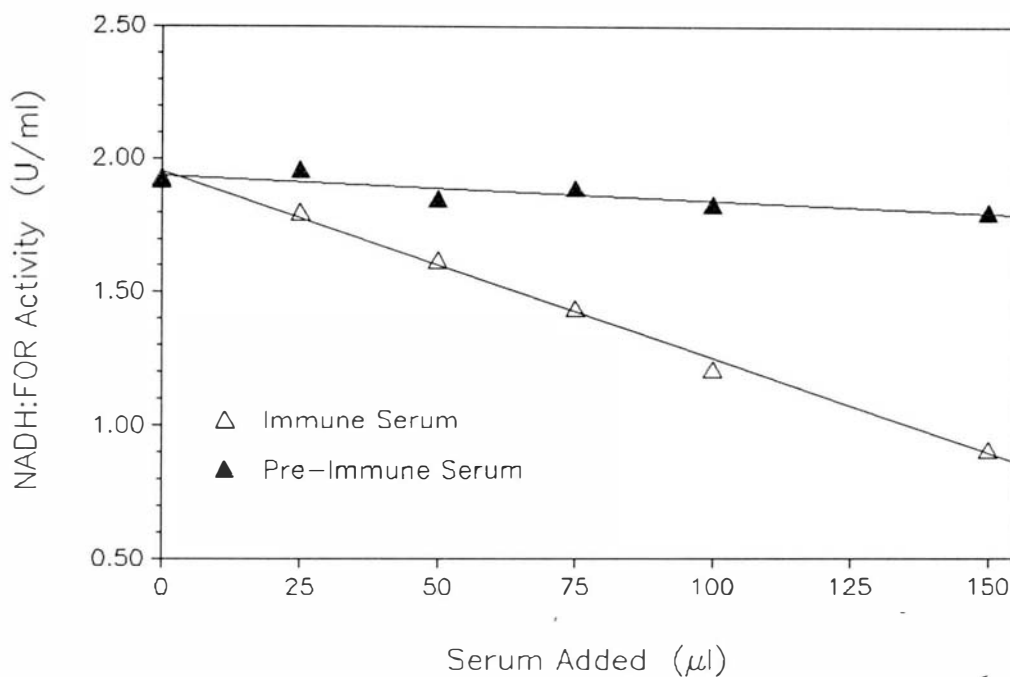


FIGURE 41: Immunoinhibition of NADH:FOR Catalytic Activity by Rabbit Polyclonal Antisera. Various volumes of rabbit serum were added to 50 ng of NADH:FOR purified from *Eu. sp. VPI 12708* and allowed to incubate for 15 min at 20°C. Enzymatic reactions were then initiated by the addition of substrate, and were quantitated spectrophotometrically as described in the Methods section.

TABLE 9: The Effect of Several Different Compounds Upon NADH:FOR Activity.

Purified protein (10 ng) was pre-incubated with the indicated amount of a putative inhibitor for 10 min at 20°C in 100 mM sodium phosphate (pH 6.8). All reactions were initiated by the addition of substrate and were performed as described in the Methods section.

Compound^A	Concentration (mM)^B	Percent Control^C
EDTA	5.0	52
EGTA	5.0	101
o-Phenanthroline	2.0	58
NaN ₃	10.0	99
ZnCl ₂	1.0	27
CuCl ₂	1.0	1
HgCl ₂	1.0	3
NEM	1.0	4
Iodoacetate	1.0	91
Iodoacetamide	1.0	112
PCMS	0.2	5
Acriflavine	0.2 mg/ml	13
N-Bromosuccinamide	0.2	8

^A Full names for abbreviated compounds are given in the List of Abbreviations. Acriflavine is a mixture of 3,6-diamino-10-methylacridinium chloride and 3,6-diaminoacridine.

^B All concentrations except that for acriflavine (mg/ml) are listed in millimols/liter.

^C The activities are expressed as percent of dH₂O control reactions (2 U/ml). The reactions were performed as described in the Methods section. All compound were tested in triplicate and the mean values used.

acriflavine (a flavin analog) and N-bromosuccinamide were both strongly inhibitory at the concentrations tested.

N-Terminal Amino Acid Sequence Analysis of the NADH:FOR: The N-terminal amino acid sequence for the purified NADH:FOR was determined and is shown in Figure 42A. The first 25 residues of this protein were found to exhibit significant homology to an enoate reductase from *Clostridium kluyveri* [104] (36% identity and 44% similarity) when compared using FASTA. However not all aligned residues represent conservative replacements, due to the nature of the algorithm employed by this program. The alignment of the unknown residues (Xxx) in both sequences is illustrated to indicate the possibility that these proteins may both possess similar residues at these positions which are difficult to sequence by Edman degradation. The homology exhibited between these proteins may be indicative of a similarity in reactions performed. The general reaction mechanism for enoate reductase is illustrated in Figure 42B, along with a possible function for the NADH:FOR in 7 α -dehydroxylation.

Two anti-sense oligonucleotide probes were created to probe for the NADH:FOR gene (Figure 43A). A restriction map for the NADH:FOR gene was deduced by *in situ* hybridization of an end-labelled probe (FOR-2) to *Eu. sp. VPI 12708* chromosomal DNA after digesting with several restriction endonucleases and is illustrated in Figure 43B. The entire NADH:FOR coding region should be contained both upon the 8.9 kb *PstI* and the 5.9 Kb *KpnI* fragments. Due to the ambiguities inherent to chromosomal restriction mapping, it is not yet clear if the NADH:FOR gene is part of the polycistronic message previously described [178].

FIGURE 42: Similarities Between the N-Terminal Amino Acid Sequences and Proposed Reaction Mechanisms for the NADH:FOR and Enoate Reductase. The first 25 N-terminal amino acid residues for the NADH:FOR are shown in panel A. Of these, the identity of two could not be determined and are denoted by Xxx. Also, the identity of residue 8 was ambiguous, being either leucine or alanine. The sequence is aligned with that of enoate reductase. The reaction mechanism for enoate reductase, and a possible function for the NADH:FOR in 7α -dehydroxylation of bile acids is illustrated in panel B.

A

<i>Eu</i> NADH:FOR	1	Met Asp	Met Lys His Ser Arg	Leu Ala	Phe Ser	Pro	Leu Glu Ile Gly Ser Leu Thr
<i>Ck2</i> -ENR	1		Met Lys Asn Lys Ser	Leu Phe Glu	Val		Ile Lys Ile Gly Lys Val Glu
<i>Eu</i> NADH:FOR	19	Leu Xxx Asn	Phe	Val Xxx Met			
<i>Ck2</i> -ENR	17	Val Xxx Xxx	Lys	Ile Xxx Met			

B

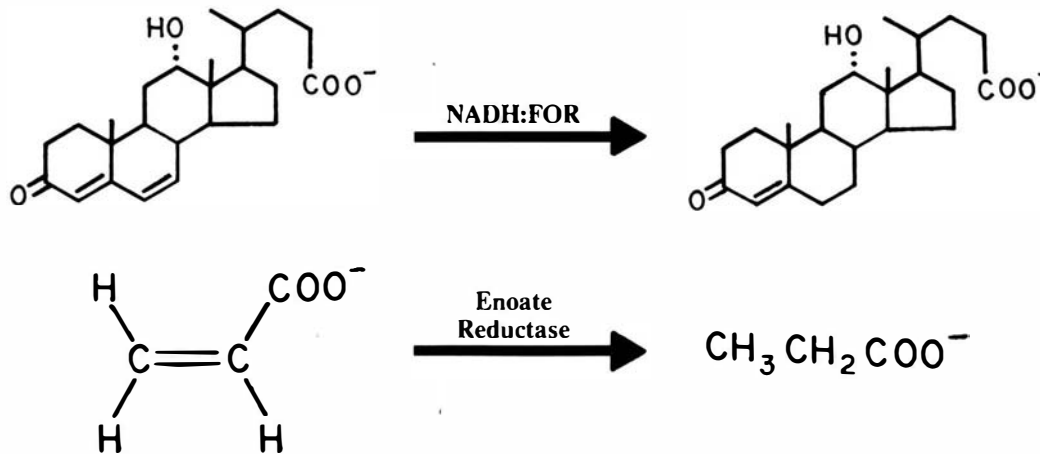
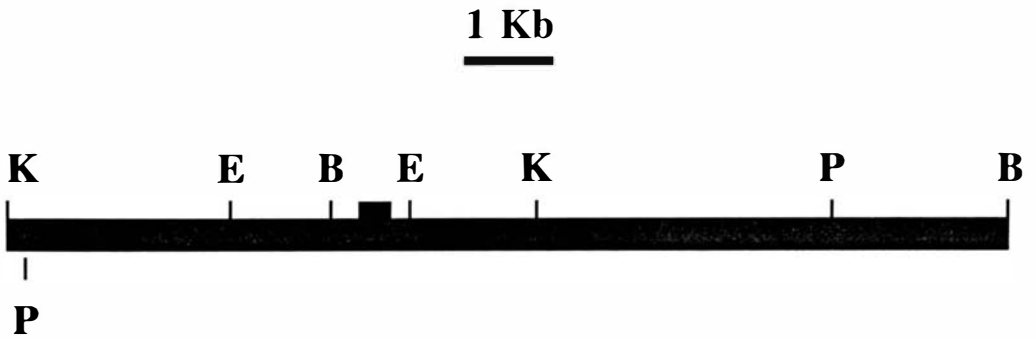


FIGURE 43: Synthetic Oligonucleotide Probes and Chromosomal Restriction Map for the NADH:FOR. The two oligonucleotide probes (FOR-1, and FOR-2) synthesized for the NADH:FOR are shown in panel A. The amino acid sequence to which these probes correspond is shown above them. Note that these probes are for the reverse complement strand (negative strand). The chromosomal restriction map generated by *in situ* hybridization is illustrated in panel B. The restriction enzymes used are abbreviated as follows: E - *EcoRI*, B - *BamHI*, K - *KpnI*, and P - *PstI*. The area where the probe is thought to anneal is illustrated as a thicker bar.

A

	NH ₂	Met	Asp	Met	Lys	His	Ser	Arg
FOR-1	5'	TCT	GCT	$\begin{matrix} G \\ A \end{matrix} \text{TG}$	$\begin{matrix} T \\ C \end{matrix} \text{TT}$	CAT	$\begin{matrix} G \\ A \end{matrix} \text{TC}$	CAT 3'
FOR-2	5'	TCT	$\begin{matrix} T \\ A \\ C \\ G \end{matrix} \text{GA}$	$\begin{matrix} G \\ A \end{matrix} \text{TG}$	$\begin{matrix} T \\ C \end{matrix} \text{TT}$	CAT	$\begin{matrix} G \\ A \end{matrix} \text{TC}$	CAT 3'

B

DISCUSSION

Purification and Characterization of the 7 α -HSDH: The 7 α -HSDH from *Eubacterium* sp. VPI 127908 has been purified to electrophoretic homogeneity. Although bile acid HSDH's with different regio- and stereo-specificities have been purified, this was the first report of the successful purification of a 7 α -HSDH. Recently, however, two additional 7 α -HSDH's have been purified from *Escherichia coli* [143] and *Clostridium absonum* (Dr. James Coleman, personal communication). The purification scheme adopted yielded 450 μ g of pure protein with a final specific activity of over 390 μ mol/min/mg. Affinity chromatography using reactive red 120-agarose was the most effective fractionation technique employed. Immobilized triazine dye-ligand chromatography has been a valuable step in the purification of a variety of pyridine nucleotide-linked enzymes [31] and has been successfully used in the purification of several NADP-dependent hydroxysteroid dehydrogenases (for examples see [3,4,6, 67,110]). However, bound hydroxysteroid dehydrogenases have previously been eluted from affinity columns using either linear or step gradients of NaCl at high concentrations (up to 3 M). In contrast, we were only able to effect the specific release of 7 α -HSDH in the presence of both NaCl (250 mM) and cofactor (NADP⁺, 10 mM). Attempts to elute the activity with either NaCl or cofactor alone were

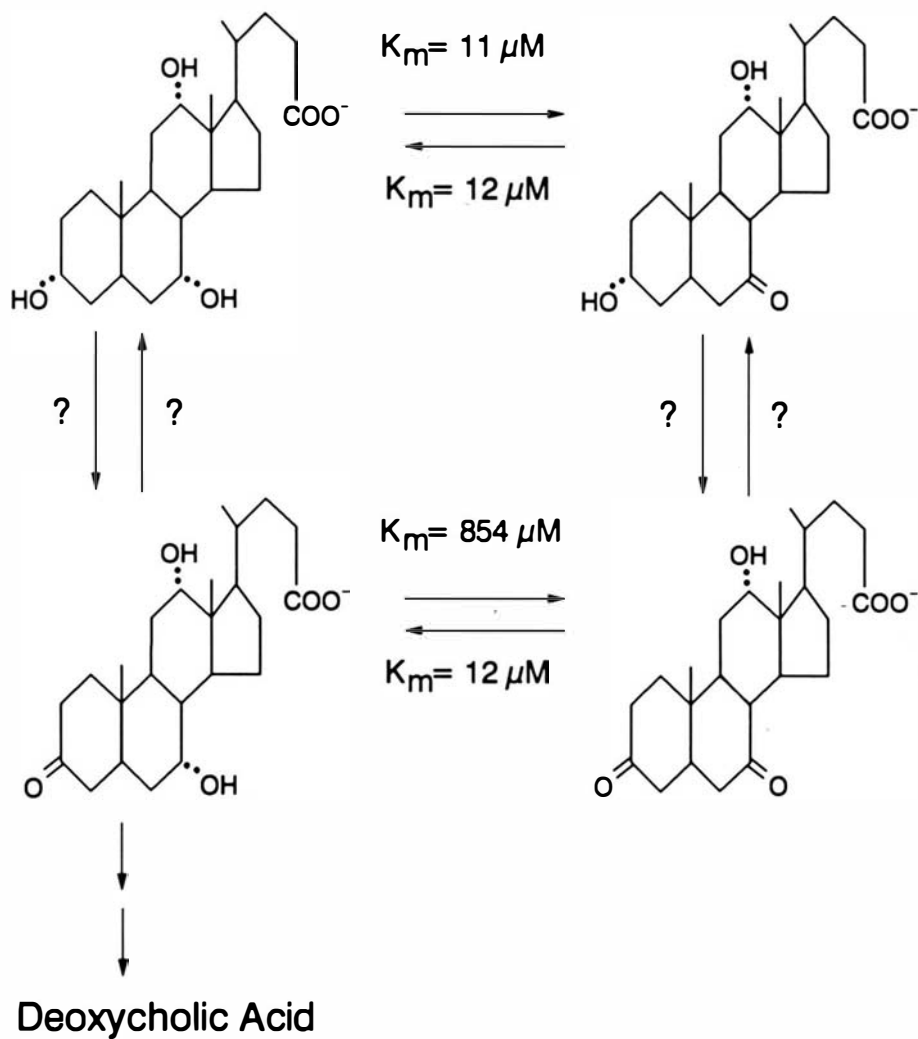
unsuccessful, suggesting that both specific (cofactor-dependent) and non-specific (hydrophobic and/or electrostatic) interactions may play a role in the binding of 7 α -HSDH to this resin.

Bile acid hydroxysteroid dehydrogenases constitute a heterogeneous class of oxidoreductases. The various enzymes which have been examined, either as purified proteins or in partially purified preparations, vary widely with respect to molecular mass, substrate and cofactor specificity, and affinity for substrates as judged by apparent K_m . The 7 α -HSDH purified in this study was similar, in certain respects, to several previously characterized enzymes. The reported molecular mass of bile acid hydroxysteroid dehydrogenases ranges from 45 to 320 kDa, but the majority fall between 60 and 130 kDa. The native molecular mass, as determined by both gel filtration and native gel electrophoresis, is comparable to values reported for NADP-dependent 7 α -HSDH from rat liver microsomes [6], and *Bacteroides fragilis* [86], as well as several other NADP(H)- [44,46,67], and NAD(H)-dependent [47] hydroxysteroid dehydrogenases. The subunit mass of the 7 α -HSDH was estimated by SDS-PAGE to be 31 kDa, suggesting that this enzyme may exist as a tetramer of identical, catalytic subunits. Subunit identity is further supported by the N-terminal amino acid sequence data (Figure 13). The existence of the 7 α -HSDH as a tetramer is somewhat unique, in that most hydroxysteroid dehydrogenases reported to date are present as dimers, although tetrameric [156] and monomeric [67,123] hydroxysteroid dehydrogenases have also been described. The pH optima for bile acid hydroxysteroid dehydrogenases is uniformly alkaline in the direction of bile acid oxidation, with values ranging from 8.5 to 11.0 [85]. The purified 7 α -HSDH agrees

well with this pattern, in that a sharp pH optimum for bile acid oxidation was observed between pH 9.5 and 10.5. A second, less alkaline, pH optimum was observed between pH 7.5 and 8.5 (Figure 16). Similar patterns are apparent in previously published pH optima profiles [44,45,78,123], but their possible significance was not discussed. The physiological significance of extremely alkaline conditions (> pH 9) for most organisms is questionable. It was found that although the apparent V_{\max} was 2- to 3-fold greater at pH 10.5 than at pH 8.5, the apparent K_m increased correspondingly (ie. substrate affinity decreased). Thus V_{\max}/K_m , a measure of enzyme specificity, remained relatively constant between the pH conditions examined. Because pH 8.5 is a more physiological pH, and enzyme function was not discernibly impaired, all characterization of the enzyme in the oxidative direction was performed at this pH. The pH optimum for bile acid reduction was between pH 5.5 and 6.5, in agreement with values obtained for other hydroxysteroid dehydrogenases [85]. The substrate range exhibited by the purified enzyme was similar to that described for other, partially purified 7α -HSDH's [86,113,116,154] in that both free and conjugated bile acids are utilized, albeit to varying degrees. The lack of activity with 7-dehydroxy, 7β -hydroxy, and 7α -hydroxy 7β -methyl bile acids underscores the stereospecificity of this enzyme for an unhindered 7α -hydroxy moiety. The markedly decreased activity observed with hyocholate as well as 3-oxo and 12-oxo-chenodeoxycholate was surprising. The presence of the 6α -hydroxy group might interfere with proper orientation in the substrate binding pocket, due either to steric hinderance or an alteration in bile acid hydrophobicity. It would be of interest to examine the effect of a 6β -hydroxy group as well (α -muricholate and β -muricholate).

This adduct would be in an axial position, projecting into the predominantly hydrophobic domain of the bile acid. Unfortunately, these bile acids were not commercially available at the time of this investigation. The effect of the oxo group on activity was observed in both the direction of bile acid oxidation and reduction. However, this was primarily upon the apparent K_m in the former case, and the V_{max} in the latter (Table 3). These results suggest a possible mechanism for the interaction of the 7α -HSDH with the cholate-inducible 7-dehydroxylation pathway, as illustrated in Figure 44. Since both compete for the same bile acid substrates, the K_m for the initial step in dehydroxylation (3α -HSDH) will most likely be very low ($< 10 \mu\text{M}$) so as to compete with the 7α -HSDH for substrate. The presence of three copies of the 27 kDa cholic acid-inducible protein gene could also be important in this interaction, if the 27K proteins are indeed the 3α -HSDH. As judged from activity levels and Western analysis, the 7α -HSDH accounts for less than 0.05% of the total cell protein. The expression of the 3α -HSDH from three genetic loci could allow the production of a large amount of this enzyme by the bacterial cell. The 3α -HSDH, then, could compete for the bile acid substrate by sheer bulk of protein present. As shown in Figure 44, after bile acids are oxidized by the 3α -HSDH, they are no longer efficiently used as substrates by the 7α -HSDH (70-fold increase in K_m). Therefore, the action of the 3α -HSDH effectively commits the bile acids to the 7α -dehydroxylation pathway. It should be noted that the reduction of 3,7-dioxo-cholic acid to 3-oxo-cholic acid by the 7α -HSDH is not impaired. This permits the utilization of the 3,7-dioxo bile acid pool for 7α -dehydroxylation as well. So, although the 7α -HSDH competes with 7α -dehydroxylation for bile acid substrates, this reaction

FIGURE 44: A Model for the Interaction Between the 7 α -HSDH and 7 α -Dehydroxylation in *Eubacterium* sp. VPI 12708.



does not appear to represent a dead-end for bile acid biotransformation in this organism.

The purified 7α -HSDH absolutely required NADP(H) as the cofactor for this reaction. Although the stereospecificity of this enzyme for the cofactor (ie. 4R-H-NADPH or 4S-H-NADPH) was not determined, other related enzymes have been previously examined. Three other bile acid HSDH's, specific for 3α , 7α , and 12α hydroxy groups, have been shown to utilize the 4S-hydrogen of their respective coenzymes [62,135]. Therefore, the HSDH's appear to all be B-stereospecific dehydrogenases. This finding is not unexpected, since enzymes which catalyze similar reactions usually have the same stereospecificity (Bentley's First Rule [15]). It has been argued by some [14,131] that cofactor stereospecificity was a strongly conserved trait during evolution and may related to the functional property of the proteins. This reasoning would lead to the hypothesis that the 7α -HSDH from *Eu. sp. VPI 12708* is also a B-stereospecific enzyme. Future experiments, using specifically tritiated or deuterated 4-H-NADPH, would allow the direct determination of the 7α -HSDH's stereospecificity.

The kinetic values derived for the 7α -HSDH are lower than reported for other, partially purified, 7α -HSDH's [85]. Most previously published K_m values range from 0.048 to 0.80 mM, with dihydroxy bile acids having significantly lower (3- to 10-fold) values than trihydroxy bile acids. Although K_m values were lower for dihydroxy bile acids, using the purified 7α -HSDH, the effect was not as pronounced (less than 2-fold differences). In addition, when comparing substrate specificity (V_{max}/K_m) chenodeoxycholate was found to be a slightly better substrate than cholate.

Interestingly, apparent kinetic constants varied with respect to bile acid hydrophobicity when comparing unconjugated bile acids to their glycine and taurine conjugates. Both K_m and V_{max} were observed to increase in a linear manner with increasing hydrophobicity. This trend is opposite that observed for 7α -HSDH from *E. coli* [113], where K_m decreased with increasing hydrophobicity. Apparent kinetic constants, however, did not correlate with substrate hydrophobicity when comparing different parent bile acids. Thus, substrate utility for the 7α -HSDH seems to be a product both of substrate hydrophobicity and the presence and orientation of the hydroxy groups. Both the primary plots of saturation kinetics (Figure 15) and product inhibition patterns (Table 4) were consistent with a ordered sequential catalytic mechanism with NADP(H) binding first. This is the first report concerning the reaction mechanism of a bile acid 7α -HSDH. Similar mechanisms have been noted for 3α -HSDH from microbial [158] and mammalian [67] sources. Many bile acid hydroxysteroid dehydrogenases have been observed to be particularly sensitive to sulfhydryl-reactive compounds [4,6,67,78,171]. Thus, it was not surprising that the purified 7α -HSDH was exquisitely sensitive to p-CMB (Table 5). Other sulfhydryl-reactive compounds, although inhibiting to a lesser degree, also suggest that a sulfhydryl residue(s) may be important for this enzyme. It was interesting, then, that the deduced amino acid sequence for the 7α -HSDH possessed only two cysteine residues (positions 25 and 182). Furthermore, neither of these residues were well conserved among the nine other alcohol/polyol dehydrogenases examined. It seems unlikely, therefore, that these two cysteines are involved in catalysis. Instead, the cysteines may be involved in a structural role for this protein (possibly forming an

intra- or inter-chain disulfide bond). Chen *et al.* arrived at a similar conclusion after performing site-directed mutagenesis studies on the *DmADH* [24]. The loss of either of two "critical" cysteines from this enzyme had no effect upon enzyme activity. The inhibition detected using N-bromosuccinamide may, too, be due to interactions with reactive cysteine groups. However, this compound is also capable of modifying tryptophan, tyrosine, and histidine residues. Although the 7 α -HSDH does not contain any tryptophan residues, a strongly conserved region containing a tyrosine and several histidines was observed in the alcohol/polyol dehydrogenases examined. Further experiments will, therefore, be required to determine the exact site(s) of N-bromosuccinamide inhibition. The lack of inhibition by up to 10 mM metal ion chelators was taken as presumptive evidence for the lack of a catalytically important metal ion. No further efforts were made to determine the metal content of this enzyme.

Quantitation of free and conjugated bile acids in biological samples has attracted much attention from investigators studying the physicochemical and physiological effects of these compounds in mammalian systems. A variety of techniques have been developed for the quantitation and identification of bile acids in such samples [167]. A variety of hydroxysteroid dehydrogenases have been used to quantitate bile acids and neutral steroids using both spectrophotometry and spectrofluorometry. Purified 3 α -HSDH from *Pseudomonas testosteroni* is used to quantitate total bile acids spectrophotometrically to final concentrations of approximately 10 μ M [167]. Use of spectrofluorometry has permitted quantitation down to 0.24 μ M [129]. Urso-bile acids have been quantitated using partially purified

preparations of 7 β -HSDH from *Cl. absonum* [117]. The NAD(H)-dependent 7 α -HSDH produced by *E. coli* has been used to quantitate bile acids [71,114]. Lyophilized 7 α -HSDH from *E. coli* and *Cl. bifermentans* (strain F-6) [168] have been demonstrated to be useful in quantitating final bile acid concentrations ranging from 20 to 100 μ M. Spectrofluorometry has allowed detection of 7 α -hydroxy bile acids down to 2 to 4 μ M [71,114]. Aqueous enzyme preparations, however, are stable for only a short period (approx 2 weeks), and background fluorescence from the enzyme preparation increases over time [115]. Use of lyophilized enzyme has been shown to circumvent these problems. The purified 7 α -HSDH described in the current study possesses several characteristics which make it an excellent candidate for analytical applications. First, the enzyme may be obtained with a high yield using a relatively simple purification protocol. In addition, the purified protein has been determined to be extremely stable in the presence of 5% (v/v) glycerol and 1 mM DTT, both at 4°C and -20°C. The broad substrate range exhibited by this enzyme allows quantitation and/or modification of a variety of 7 α -hydroxy bile acids and their derivatives. The low K_m (high affinity) and high V_{max} permit use of low final concentrations of bile acid in assays and assure reaction to completion. The pH optima for oxidation (10.5) and reduction (6.0) of bile acids are disparate enough to decrease the likelihood of back-reaction and thus eliminate the need for keto-partitioning solvents such as hydrazine. We propose that the purified 7 α -HSDH may be a useful reagent in the quantitation of both 7 α -hydroxy and 7-keto bile acids in clinical and laboratory samples. The purified enzyme has been shown, using both spectrophotometry and spectrofluorometry, to be capable of quantitating free and

conjugated primary bile acids ranging from 10 nM to 100 μ M final concentration. These values are well within the levels of total bile acid present in portal and systemic venous circulation of fasting individuals (reported to be 14 μ M and 2.4 μ M, respectively [8,50]). Use of the *Ps. testosteroni* 3 α -HSDH in conjunction with the purified 7 α -HSDH would permit the direct determination of both total bile acids present and the percent of the total bile acid pool comprised by 7 α -hydroxy and/or 7-keto bile acids. Enzymatic cycling of cofactor has been reported to be capable of amplifying the fluorometric signal up to 10,000-fold [68,133]. This technique has previously been utilized to quantitate neutral steroid concentrations to sub-pmol ranges with highly purified preparations of 3 α - and 3 β -HSDH [138] and 17 β -HSDH [139]. These techniques using the purified 7 α -HSDH may permit the quantitation of minute quantities of 7 α -hydroxy and/or 7-keto bile acids and their derivatives in biological samples.

The successful purification of the 7 α -HSDH is also important in possibly understanding the evolution and physiological significance of this class of enzymes. It is of particular interest that the N-terminal amino acid sequence derived from the purified 7 α -HSDH is homologous to several non-zinc polyol/alcohol dehydrogenases [90-92]. Subunit molecular mass and lack of inhibition by metal ion chelators are consistent with the properties of other members the dehydrogenase superfamily. The best alignment of the N-terminal sequence was achieved with the 7 α -HSDH from *Cl. absonum*. The close resemblance between the purified 7 α -HSDH and 27-1 is also intriguing. This finding is in agreement with the previous assertion that 27-1 may be a cholate-inducible bile acid oxidoreductase [28]. These preliminary results suggest

that the HSDH's, in general, may all belong to the same class (short-chain, non-zinc) of dehydrogenases. This may also be interpreted as indicating that the HSDH's all have descended from a common, secondary alcohol dehydrogenase precursor.

Cloning and Sequencing the 7 α -HSDH Gene: The gene encoding the 7 α -HSDH was cloned, as a 3.8 kb *KpnI-PstI* restriction fragment, into pUC19, giving the recombinant plasmid pBH51. *E. coli* cultures harboring pBH51 were found to over-express the 7 α -HSDH activity by approx 30-fold. Several lines of evidence indicate that the protein produced in *E. coli* is indeed authentic 7 α -HSDH. The subunit molecular mass, as determined by SDS-PAGE, was identical to enzyme purified from *Eu. sp. VPI 12708*. However, a second band, of about 32 kDa, was also present in the *E. coli* preparation. The native molecular masses, judged by native gel electrophoresis, were also identical. Furthermore, Western analysis revealed that both the 31 and 32 kDa proteins produced in pBH51 transformants were recognized by rabbit polyclonal antiserum raised against 7 α -HSDH purified from *Eu. sp. VPI 12708*. This antiserum was demonstrated to inhibit 7 α -HSDH enzymatic activity when pre-incubated with purified enzyme. In addition, the enzyme's specific activity and kinetic constants for several bile acids (cholic acid, glycochenodeoxycholic acid, and 12-oxo-cholic acid) were found to be essentially the same for 7 α -HSDH purified from either *Eu. sp. VPI 12708* or a pBH51 transformant. The size of the RNA transcript, as determined by Northern blot analysis, was the same in both *Eu. sp. VPI 12708* and *E. coli*. Furthermore, the 5' ends of these transcripts were essentially the same, suggesting that both *Eu. sp. VPI 12708* and *E. coli* DNA-dependent RNA polymerases may be recognizing the same promoter sequence for this gene. Indeed,

upstream from the 7α -HSDH open reading frame are at least three regions which possess substantial homology to the canonical *E. coli* promoter sequence as defined previously [146]. These enticing results represent the first data pertaining to the sequence of constitutive promoters in this organism. The definitive determination of the promoter sequence, however, will require further experiments (eg. DNA footprinting with purified polymerase).

The ability to over-express this protein in *E. coli* as an active enzyme opens several avenues for possible future investigation and application. As indicated above, this 7α -HSDH has potential utility for the quantitation of bile acids in clinical samples. The ability to overexpress this enzyme, allowing the preparation of gram quantities of purified enzyme, then, has obvious commercial importance. Virtually nothing is known about the structure of bile acid binding domains of proteins or the structure of their catalytic sites. Since the 7α -HSDH is well expressed in *E. coli*, the pBH51 clone may be used for the analysis of the 7α -HSDH structure through linker-scanning and site directed mutagenesis. In this manner, residues involved in bile acid binding and enzymatic catalysis may be determined. The ability to obtain large amounts of this pure enzyme may also permit future work on its crystallization and determination of the protein structure.

The deduced amino acid sequence for the 7α -HSDH confirmed the homology observed between the N-terminal amino acid sequence and several alcohol/polyol dehydrogenases of the short-chain, non-zinc superfamily. The homology to the 27 kDa cholic acid-inducible protein strongly implies that this protein is the 3α -HSDH postulated to be involved in 7α -dehydroxylation. Interestingly, the homology between

the 7 α -HSDH and both the 27 kDa proteins and glucose dehydrogenases extended throughout the entire length of the proteins (Figure 29A-D). Although the region involved in cofactor binding is well conserved amongst these dehydrogenases, it is not yet possible to determine any regions specifically involved in bile acid binding. Alignment of the 7 α -HSDH with the nine other alcohol/polyol dehydrogenases did, however, reveal six perfectly conserved amino acid residues (Figures 27 and 28). Of these, three were glycines, and are probably involved in β -turns important for the tertiary structure of the proteins. This was shown to be true for one of the conserved glycines in *DmADH* [24]. The replacement of glycine-14 in this protein with either alanine or valine resulted in a loss of enzymatic activity and thermal stability. The remaining three consisted of an aspartic acid, an asparagine, and a tyrosine. Although the precise roles of these residues are yet unknown, this tyrosine has previously been postulated to be catalytically important for other alcohol/polyol dehydrogenases [103]. These residues are obvious targets for future site-directed mutagenesis studies.

Sequence analysis of the 3' untranslated portion of the 7 α -HSDH mRNA revealed a complex potential secondary structure (Figure 21). The Gibb's free energy (approx -50 kCal) suggests that this is a physiologically significant conformation. Although it is assumed that this structure acts as a transcriptional terminator, the actual location of the 7 α -HSDH mRNA 3' end has not yet been determined. Thus, the exact sequences within this region involved in termination are not yet known. This region may also be important for other gene(s) downstream from the 7 α -HSDH reading in the opposite direction. Additional sequence data will

be required to determine the location and orientation of any such genes.

It is not yet possible to determine if the hydroxysteroid dehydrogenases comprise one or more classes of enzymes. The striking homology between the N-terminal amino acid sequences of the 7α -HSDH from *Eu. sp. VPI 12708* and *Cl. absonum* suggest the possibility of a common ancestor. The apparent conservation of cofactor stereo-specificity, discussed above, is also in accord with this hypothesis. However, the widely disparate subunit sizes of some purified HSDH's (eg. 7α -HSDH from *E. coli* 54 kDa [143], and 7β -HSDH from *Peptostreptococcus productus* 64 kDa [123] as compared to 31 kDa for the *Eu. sp. VPI 12708* 7α -HSDH) may indicate of the existence more than one type of HSDH subunit. Purification and sequence analysis of a larger number of these proteins will be required to clarify the relationships between the HSDH's.

Purification and Characterization of the NADH:FOR: The cholic acid-inducible NADH:FOR was also purified from *Eu. sp. VPI 12708*. Using a five step protocol, over a 370-fold purification with a 10% final yield was obtained. Of the affinity resins tested, only Cibacron Blue A bound the NADH:FOR activity. Even this resin bound the protein poorly, necessitating multiple loadings to achieve acceptable recoveries. The nature of the interaction of NADH:FOR with Cibacron Blue A appears to be non-specific, since cofactor was not effective in releasing the activity. This enzymatic activity was released from the affinity column, non-specifically, with 1 M KCl. Other investigators have also employed batch elution with KCl to recover enzymes from affinity columns. The reason for the apparent inability of 2 M NaCl to elute this protein, however, is not clear. The detection of more than one peak of

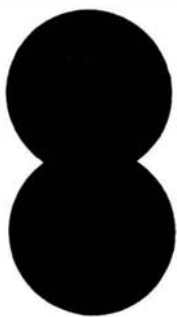
activity in the DEAE-HPLC elution profile was perhaps the most surprising result of this study. The existence of more than one form of NADH:FOR was hinted at by Lipsky and Hylemon [108], who reported that two peaks of activity were occasionally found after DEAE-cellulose chromatography. During this study, the incomplete equilibration of DE-52 was observed to result in similar elution profiles. The presence of multiple peaks of activity resulted in a great reduction in enzyme recovery from any one of the peaks. This effect stymied enzyme purification until conditions were found at which one of the forms predominated. Phenyl-HPLC was one of the best purification steps employed, giving a 7-fold purification with a 32% yield. The NADH:FOR exhibited substantial hydrophobic character on this column. The enzymatic activity was only effectively released from the resin after injecting 10% ethanol over the column (Figure 33). The purified protein had a subunit molecular mass of 72 kDa. The native molecular mass was estimated to be 210 kDa, and 150 kDa by gel filtration and native gel electrophoresis, respectively. These results are somewhat lower than previously reported (260 kDa) [108]. Based upon these size estimates, the NADH:FOR probably exists either as a dimer or trimer of identical subunits.

Further experiments were performed to discern the reason for the segregation of NADH:FOR activity into multiple peaks on DEAE-HPLC. The elution pattern for this activity was observed to change with respect to the purification protocol employed (Figure 35). Thus, the presence of multiple peaks did not appear to be due to the presence of several different cholic acid-inducible proteins. The presence of a similar, 72 kDa, band in both forms was confirmed both by SDS-PAGE and

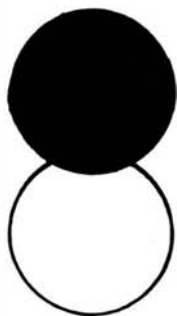
Western analysis. Instead, this enzyme appeared to be modified as a result of the conditions employed during the purification process. Since a similar effect could not be produced by a change in pH alone, the interaction with the column resins is important for this modification. Purified form III (the predominant form found in crude material) was found to possess a dark yellow color while form I (the predominant form after purification) was clear. This suggested that the flavin contents of these forms were different. Spectral analysis of the two NADH:FOR preparations confirmed the presence of flavin in form III, but not form I (Figure 36). Therefore, the cumulative loss of flavin during the purification process may have been, at least in part, responsible for the presence of multiple peaks of activity on DEAE-HPLC. The presence of three peaks may be explained if the NADH:FOR exists as a dimer. Form I would represent a dimer of enzyme with each subunit containing a flavin. In form II, only one of the subunits would possess a flavin, while form III would have no flavin molecules. Since form II was never observed to accumulate, there may be allosteric interaction between the subunits in the dimer such that the loss of flavin from one subunit results in the loss from both. This model is shown diagrammatically in Figure 45. Attempts to reconstitute FAD into form I were unsuccessful. This may be due to the aerobic conditions under which the experiments were performed. Alternatively, additional components, such as specific metals, may be required for successful reconstitution.

The purified NADH:FOR (form I) was found to be susceptible to inhibition by a variety of different compounds. The partially purified enzyme was previously reported to be somewhat sensitive to p-CMB (1 mM = 25% inhibition). In contrast,

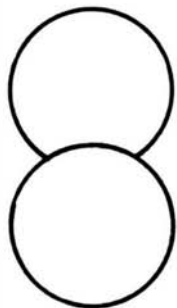
FIGURE 45: A Possible Model for the Presence of Multiple Forms of the NADH:FOR Upon Elution From DEAE-HPLC. The protein subunits for the NADH-FOR are illustrated as circles and the native enzyme is assumed to form a homodimer. Filled circles represent subunits with bound flavin, while the open circles indicate a subunit from which the flavin has been removed.



Form III



Form II



Form I

the purified enzyme was nearly completely inhibited by 1 mM p-CMS, CuCl_2 , HgCl_2 , and NEM. Additionally, 1 mM ZnCl_2 gave 73% inhibition. Iodoacetate and iodoacetamide, however, did not appreciably affect this activity. The purified enzyme was also exquisitely sensitive to N-bromosuccinamide. This may reflect its ability to interact with sulfhydryl groups. The reaction with tryptophan, tyrosine or histidine as well, though, cannot be excluded. The NADH:FOR was also inhibited by the metal ion chelators o-phenanthroline and EDTA. Interestingly, EGTA and NaN_3 did not inhibit this enzyme. The inhibition of NADH:FOR activity by o-phenanthroline has previously been reported [108]. The inhibition by EDTA may explain the failure of previous attempts to purify this enzyme. During his purification attempts, Lipsky reportedly included 0.1 mM EDTA in all of the buffers [108]. The inhibition by chelating compounds may be indicative of a catalytically important metal in this protein. O-phenanthroline is generally known as a non-heme iron chelator. Therefore, the NADH:FOR may possess a iron-sulfur center. This would be consistent both with the strong inhibition seen with the sulfhydryl-reactive compounds and an apparent irreversible inactivation of the protein at pH values less than 5.0. Acriflavine, a flavin analog, was also shown to be a potent inhibitor of the NADH:FOR activity. This is also in agreement with previous studies [108]. It is not apparent, then, why acriflavine agarose failed to bind NADH:FOR when it was screen as a possible affinity chromatography resin.

The NADH:FOR was initially reported to be a cholic acid-inducible activity in *Eu. sp.* VPI 12708 [108]. This was confirmed both by Ochterlony plate and Western analysis of protein expression as well as activity stains of native slab gels.

Although Northern analysis of NADH:FOR transcription was not performed in this study, this too, is likely to be cholic-acid inducible, as has been found for the other proteins examined from this organism [28,178].

The first 25 N-terminal amino acids of the purified NADH:FOR were also determined. This sequence was found to exhibit a significant homology to the enoate reductase expressed by *Clostridium kluyveri* [104]. It was interesting that the two amino acids which could not be determined from the NADH:FOR sequence were also not sequencable in the enoate reductase N-terminus [104]. This may indicate the presence of similar residues in both proteins which are difficult to sequence using Edman degradation. Furthermore, this apparent homology is strengthened by the other similarities between these two proteins. The subunit molecular masses of the purified proteins are very similar [104], as determined by SDS-PAGE. Both enzymes, in addition, are flavoproteins and may contain an iron-sulfur centers. Interestingly, the structural conformation of the enoate reductase has also been demonstrated to be sensitive to loss of a flavin during purification. Based upon these similarities, it may be proposed that the reactions performed by these enzymes are also alike. The enoate reductase catalyzes the stereospecific reduction of a variety of α/β unsaturated short-chained carboxylates [21]. This flavin-dependent reaction is illustrated in Figure 42B. A homologous reaction in the 7α -dehydroxylation of bile acids is the reduction of 3-oxo- $\Delta^{4,6}$ -deoxycholic acid to 3-oxo- Δ^4 -deoxycholic acid. The reduction of this bond by cell-free extracts has previously been demonstrated to be stimulated by the addition of free reduced flavins [174]. However, attempts to detect an accumulation of the $\Delta^{4,6}$ -precursor after inhibiting the NADH:FOR with either

polyclonal antiserum or acriflavine gave inconclusive results. TLC analysis of the bile acid product(s) formed from radiolabelled 3-oxo- $\Delta^{4,6}$ -deoxycholic acid by the purified NADH:FOR will be required to unambiguously prove this function. Although both form I and III possessed NADH:FOR activity *in vitro*, probably only form III, which still contains a flavin, will be capable of reducing the Δ^6 bond.

A synthetic oligonucleotide was created which was complementary for a portion the N-terminal amino acid sequence of the NADH:FOR. Using this as a probe a chromosomal restriction map for the NADH:FOR gene was determined. Based upon this map, the entire open reading frame was predicted to be contained on both a 5.9 Kb *KpnI* and a 8.9 Kb *PstI* restriction fragment. The derived map was not substantially different from that of the 3' end of the large cholic acid-inducible operon. Therefore, it is not yet possible to determine if this protein is transcribed as part of this operon, or if it is part of yet another, heretofore unknown, transcript. Since FOR-2 seemed to anneal specifically to the NADH:FOR gene, the future cloning and sequencing of this region should be relatively easily accomplished. In addition, since this probe is the reverse complement for the mRNA, it may also be used in future Northern analysis of NADH:FOR transcription. The results of these experiments could help to determine whether or not the NADH:FOR is indeed transcribed as part of the large operon.

LITERATURE CITED

LITERATURE CITED

1. Abrams, G.D., H. Bauer, and H. Sprinz. (1963) Influences of the Normal Flora on Mucosal Morphology and Cellular Renewal in the Ileum: A Comparison of Germfree and Conventional Mice. *Lab. Invest.* **12**: 355-364.
2. Abrams, G.D., and G.E. Bishop. (1967) Effect of the Normal Microbial Flora on Gastrointestinal Motility. *Proc. Soc. Exp. Biol. Med.* **126**: 301-304.
3. Akao, T., T. Akao, M. Hattori, T. Namba, and K. Kobashi. (1986) 3β -Hydroxysteroid Dehydrogenase of *Ruminococcus* sp. from Human Intestinal Bacteria. *J. Biochem.* **99**: 1425-1431.
4. Akao, T., T. Akao, and K. Kobashi. (1987) Purification and Characterization of 7β -Hydroxysteroid Dehydrogenase from *Ruminococcus* Species of Human Intestine. *J. Biochem.* **102**: 613-619.
5. Alexander, M. (1971) *Microbial Ecology*, pp. 3-21. Wiley, New York.
6. Amuro, Y., W. Yamdu, T. Yamamoto, A. Maebo, T. Hada, and K. Higashino. (1987) Partial Purification and Characterization of 7α -Hydroxysteroid Dehydrogenase from Rat Liver Microsomes. *Biochim. Biophys. Acta* **917**: 101-107.
7. Andrews, P. (1964) Estimation of the Molecular Weights of Proteins by Sephadex Gel-Filtration. *Biochem. J.* **91**: 222-232.
8. Angelin, B., I. Bjökhem, K. Einersson, and S. Ewerth. (1982) Hepatic Uptake of Bile Acids in Man. Fasting and Postprandial Concentrations of Individual Bile Acids in Portal Venous and Systemic Blood Serum. *J. Clin. Invest.* **70**: 724-731.
9. Aries, V., and M.J. Hill. (1970) Degradation of Steroids by Intestinal Bacteria. II. Enzymes Catalysing the Oxidoreduction of the 3α -, 7α -, and 12α -Hydroxyl Groups in Cholic Acid, and the Dehydroxylation of the 7-Hydroxyl Group. *Biochim. Biophys. Acta* **202**: 535-543.

10. Aries, V., and M.J. Hill. (1971) Degradation of Steroids by Intestinal Bacteria. III. 3-oxo-5 β - Δ^1 -Dehydrogenase and 3-oxo-5 β - Δ^4 -Dehydrogenase. *Biochim. Biophys. Acta.* **248**: 482-488.
11. Ausubel, F.M., R. Brent, R.E. Kingston, D.D. Moore, J.G. Seideman, J.A. Smith, and K. Struhl. (eds.) *Current Protocols in Molecular Biology*. Wiley & Sons, New York.
12. Bauer, J., R.E. Horowitz, S.M. Levenson, and H. Popper (1963) Responses of the Lymphatic Tissue to the Microbial Flora. Studies on Germfree Mice. *Am. J. Pathol.* **42**: 471-483.
13. Bealmeair, P.M., and R. Wilson. (1967) Homograft Rejection by Neonatally Thymectomized Germfree Mice. *Cancer Res.* **27**: 358-361.
14. Benner, S.A., and K.P. Nambiar. (1986) Functional Explanations for Stereoselectivity in Dehydrogenases. pp. 29-43. In: P.A. Frey (ed.) *Mechanisms of Enzymatic Reactions: Stereochemistry*. Elsevier Science Publishing Co., Amsterdam.
15. Bentley, R. (1970) *Molecular Asymmetry in Biology*. Vol. 2 pp. 1-89.
16. Bernhardsson, D., I. Björkhem, H. Danielsson and K. Wikvall. (1973) 12 α -Hydroxylation of 7 α -Hydroxy-4-cholesten-3-one by a Reconstituted System From Rat Liver Microsomes. *Biochem. Biophys. Res. Commun.* **54**: 1030-1038.
17. Björkhem, I, K. Einarsson, P. Melone, and P. Hylemon. (1989) Mechanism of Intestinal Formation of Deoxycholic Acid from Cholic Acid in Humans: Evidence for a 3-oxo- Δ^4 -Steroid Intermediate. *J. Lipid Res.* **30**: 1033-1039.
18. Bohnhoff, M., and C.P. Miller. (1962) Enhanced Susceptibility to *Salmonella* Infection in Streptomycin-Treated Mice. *J. Infect. Dis.* **111**: 117-127.
19. Bokkenheuser, V.D., and J. Winter. (1983) Biotransformation of Steroids. pp. 215-239. In D.J. Hentges (ed.), *Human Intestinal Microflora in Health and Disease*. Academic Press, New York.
20. Bradford, M.M. (1976) A Rapid and Sensitive Method for the Quantitation of Microgram Quantities of Protein Utilizing the Principle of Protein-Dye Binding. *Anal. Biochem.* **72**: 248-254.
21. Buhler, M., and J. Simon. (1982) On the Kinetics and Mechanism of Enolate Reductase. *Hoppe-Seyler's Z. Physiol. Chem.* **363**: 609-625.

22. Carey, M.C. (1985) Physical-Chemical Properties of Bile Acids and Their Salts. pp. 345-403. *In*: H. Danielsson and J. Sjövall (eds.) *Sterols and Bile Acids*. Elsevier Science Publishers, Amsterdam.
23. Carey, M.C., and M.J. Cahalane. (1988) The Enterohepatic Circulation. *In*: Arias I., and H. Popper (eds.) *The Liver: Biology and Pathobiology*. Raven Press, New York.
24. Chen, Z., L. Lu, M. Shirley, W.R. Lee, and S.H. Chang. (1990) Site-Directed Mutagenesis of Glycine-14 and Two "Critical" Cysteiny Residues in *Drosophila* Alcohol Dehydrogenase. *Biochemistry* **29**: 1112-1118.
25. Cohen, B.I., R.F. Raicht, E.E. Deschener, M. Takahashi, A.M. Sarwal, and E. Fazzini. (1980) The Effect of Cholic Acid Feeding on N-Methyl-N-Nitrosourea Colon Tumors and Cell Kinetics in Rats. *JNCI, J. Natl. Cancer Inst.* **64**: 573-578.
26. Coleman, J.P., W.B. White, and P.B. Hylemon (1987) Molecular Cloning of Bile Acid 7-Dehydroxylase from *Eubacterium* sp. Strain VPI 12708. *J. Bacteriol.* **169**: 1516-1521.
27. Coleman, J.P., W.B. White, B. Egestad, J. Sjövall, and P.B. Hylemon (1987) Biosynthesis of a Novel Bile Acid Nucleotide and Mechanism of 7 α -Dehydroxylation by an Intestinal *Eubacterium* Species. *J. Biol. Chem.* **262**: 4701-4707.
28. Coleman, J.P., W.B. White, M. Lijewski, and P.B. Hylemon. (1988) Nucleotide Sequence and Regulation of a Gene Involved in Bile Acid 7-Dehydroxylation by *Eubacterium* sp. Strain VPI 12708. *J. Bacteriol.* **170**: 2070-2077.
29. Cornish-Bowden, A. (1976) *Principles of Enzyme Kinetics*. pp. 71-100. Butterworths, London.
30. Crabbé, P.A., H. Bazin, H. Eyssen, and H.F. Heremans. (1968) The Normal Microbial Flora as a Major Stimulus for Proliferation of Plasma Cells Synthesizing IgA in the Gut. *Int. Arch. Allergy Appl. Immunol.* **34**: 362-375.
31. Dean, P.D.G., and D.H. Watson. (1979) Protein Purification Using Immobilized Triazine Dyes. *J. Chromatogr.* **165**: 301-319.
32. DeBoth, N.J., and H. Plaiser. (1974) The Influence of Changing Cell Kinetics on Functional Differentiation in the Small Intestine of the Rat. A Study of Enzymes Involved in Carbohydrate Metabolism. *J. Histochem. Cytochem.* **22**: 352-360.

33. Decker, K., K. Jungermann, and R.K. Thauer. (1970) Energy Production in Anaerobic Organisms. *Angew. Chem. Int. Ed. Engl.* **9**: 138-158.
34. Dempsey, M.E. (1974) Regulation of Steroid Biosynthesis. *Ann. Rev. Biochem.* **43**: 967-990.
35. Devereux, J., P. Haerberli, and O. Smithies. (1984) A Comprehensive Set of Sequence Analysis Programs for the VAX. *Nucleic Acid Res.* **12**: 387-395.
36. Dothie, J.M., J.R. Giglio, C.B. Moore, S.S. Taylor, and B.S. Hartley. (1985) Ribitol Dehydrogenase of *Klebsiella aerogenes*. *Biochem. J.* **230**: 569-578.
37. Drasar, B.S., and P.A. Barrow. (1985) Aspects of Microbiology Vol. 10. *Intestinal Microbiology*. American Society for Microbiology, Washington, D.C.
38. Drasar, B.S., and M.J. Hill (1974) *The Human Intestinal Flora*, pp. 1-263. Academic Press, London.
39. Drasar, B.S., A.G. Renwick, and R.T. Williams. (1972) The Role of the Gut Flora in Metabolism of Cyclamate. *Biochem. J.* **129**: 881-890.
40. Dubos, R., R.W. Schaedler, R. Costello, and P. Hoet. (1965) Indigenous, Normal, and Autochthonous Flora of the Gastrointestinal Tract. *J. Exp. Med.* **122**: 67-76.
41. Edenharder, R. (1984) Dehydroxylation of Cholic Acid at C₁₂ and Epimerization at C₅ and C₇ by *Bacteroides* species. *J. Steroid Biochem.* **21**: 413-420.
42. Edenharder, R., and T. Knafllic. (1981) Epimerization of Chenodeoxycholic Acid to Ursodeoxycholic Acid by Human Intestinal Lecithinase-Lipase-Negative *Clostridia*. *J. Lipid Res.* **22**: 652-658.
43. Edenharder, R., and K. Mielek (1984) Epimerization, Oxidation, and Reduction of Bile Acids by *Eubacterium lentum*. *Syst. Appl. Microbiol.* **5**: 287-298.
44. Edenharder, R., and A. Pfutzner. (1988) Characterization of NADP-Dependent 12 β -Hydroxysteroid Dehydrogenase from *Clostridium paraputrificum*. *Biochim. Biophys. Acta.* **962**: 362-370.
45. Edenharder, R., and M. Pfutzner. (1989) Partial Purification and Characterization of an NAD-Dependent 3 β -Hydroxysteroid Dehydrogenase from *Clostridium innocuum*. *Appl. Environ. Microbiol.* **55**: 1656-1659.

46. Edenharder, R., A. Pfutzner, and R. Hammann. (1989) NADP-Dependent 3β -, 7α -, and 7β -Hydroxysteroid Dehydrogenase Activities from Lecithinase-Lipase-Negative *Clostridium* Species 25.11.C. *Biochim. Biophys. Acta* **1002**: 37-44.
47. Edenharder, R., A. Pfutzner, and R. Hammann. (1989) Characterization of NAD-Dependent 3α - and 3β -Hydroxysteroid Dehydrogenase and of NADP-Dependent 7β -Hydroxysteroid Dehydrogenase from *Peptostreptococcus productus*. *Biochim. Biophys. Acta* **1004**: 230-238.
48. Elliot, W.H. (1971) Allo Bile Acids. pp. 47-92. In: P.P. Nair and D. Kritchevsky (eds.) *The Bile Acids: Chemistry, Physiology, and Metabolism, Vol. 1*. Plenum Press, New York.
49. Eneroth, P. (1963) Thin-Layer Chromatography of Bile Acids. *J. Lipid Res.* **4**: 11-16.
50. Everson, G.T. (1987) Steady State Kinetics of Serum Bile Acids in Healthy Human Subjects: Single and Dual Isotope Techniques Using Stable Isotopes and Mass Spectroscopy. *J. Lipid Res.* **28**: 238-252.
51. Eyssen, H., G. DePauw, J. Stragier, and S. Verhulst. (1983) Cooperative Formation of ω -Muricholic Acid by Intestinal Microorganisms. *Appl. Environ. Microbiol.* **45**: 141-147.
52. Fedorowski, T., G. Salen, G.S. Tint, and E.J. Mosbach. (1979) Transformation of Chenodeoxycholic Acid and Ursodeoxycholic Acid by Human Intestinal Bacteria. *Gastroenterology.* **77**: 1068-1073.
53. Ferrari, A., N. Pacini, and E. Canzi. (1980) A Note on Bile Acids Transformations by Strains of *Bifidobacterium*. *J. Appl. Bacteriol.* **49**: 193-197.
54. Ferrari, A., N. Pacini, E. Canzi, and F. Brano (1980) Prevalence of O_2 -Intolerant Microorganisms in Primary Bile Acid Dehydroxylating Mouse Intestinal Microflora. *Curr. Microbiol.* **4**: 257-260.
55. Ferrari, A., C. Scolastico, and L. Beretta. (1977) On the Mechanism of Cholic Acid 7α -Dehydroxylation by a *Clostridium bifermentans* Cell-Free Extract. *FEBS Lett.* **75**: 166-168.
56. Finegold, S.M., V.L. Sutter, and G.E. Mathisen. (1983) Normal Indigenous Intestinal Flora. pp. 3-31. In: D.J. Hentges (ed.), *Human Intestinal Microflora in Health and Disease*. Academic Press, New York.
57. Floch, M.J., J.J. Binder, B. Filburn, and W. Gershengoren. (1972) The Effect of Bile Acids on Intestinal Microflora. *Am. J. Clin. Nutr.* **25**: 1418-1426.

58. Ford, D.J., and M.E. Coates. (1971) Absorption of Glucose and Vitamins of the B-Complex by Germfree and Conventional Chicks. *Proc. Nutr. Soc.* **30**: 10A-11A.
59. Friedlaender, M.J., J. Baer, and P.R.B. McMaster. (1972) Contact Sensitivity and Immunologic Tolerance in Germfree Guinea Pigs. *Proc. Soc. Exp. Biol. Med.* **141**: 522-526.
60. Gallagher, K., J. Mauskopf, J.T. Walker, and L. Lack (1976) Ionic Requirements for the Active Ileal Bile Salt Transport System. *J. Lipid Res.* **17**: 572-577.
61. Gilliland, S.E., and M.L. Speck. (1977) Deconjugation of Bile Acids by Intestinal Lactobacilli. *Appl. Environ. Microbiol.* **33**: 15-18.
62. Glasfeld, A., G.F. Leanz, and S.A. Benner. (1990) The Stereospecificities of Seven Dehydrogenases from *Acholeplasma laidlawii*. *J. Biol. Chem.* **265**: 11692-11699.
63. Gopal-Srivastava, R., and P.B. Hylemon. (1988) Purification and Characterization of Bile Salt Hydrolase from *Clostridium perfringens*. *J. Lipid Res.* **29**: 1079-1085.
64. Gopal-Srivastava, R., D.H. Mallonee, W.B. White, and P.B. Hylemon (1990) Multiple Copies of a Bile Acid-Inducible Gene in *Eubacterium* sp. Strain VPI 12708. *J. Bacteriol.* **172**: 4420-4426.
65. Gossling, J., and J.M. Slack. (1974) Predominant Gram-Positive Bacteria in Human Feces: Numbers, Variety, and Persistence. *Infect. Immun.* **9**: 719-729.
66. Hanes, C.S. (1932) CLXVII. Studies on Plant Amylases. I. The Effect of Starch Concentration Upon the Velocity of Hydrolysis by the Amylase of Germinated Barley. *Biochem J.* **26**: 1406-1421.
67. Hara, A., Y. Inoue, M. Nakajawa, F. Naganeo, and H. Sawada. (1988) Purification and Characterization of NADP⁺-Dependent 3 α -Hydroxysteroid Dehydrogenase from Mouse Liver Cytosol. *J. Biochem.* **103**: 1027-1034.
68. Härkönen, M., H. Adlercreutz, and E.V. Groman. (1974) Enzymatic Techniques in Steroid Assay. *J. Steroid Biochem.* **5**: 717-725.
69. Harris, J.N., and P.B. Hylemon. (1977) Partial Purification and Characterization of NADP-Dependent 12 α -Hydroxysteroid Dehydrogenase from *Clostridium leptum*. *Biochim Biophys Acta* **528**: 148-157.

70. Haslewood, G.A.D. (1978) The Biological Importance of Bile Salts. *In: A. Neuberger and E.L. Tatum (eds.) Frontiers of Biology Vol. 47.* North-Holland Publishing Company, Amsterdam.
71. Haslewood, G.A.D., G.M. Murphy, and J.M. Richardson. (1973) A Direct Enzymatic Assay for 7 α -Hydroxy Bile Acids and Their Conjugates. *Clin. Sci.* **44**: 95-98.
72. Hayakawa, S. (1973) Microbial Transformation of Bile Acids. *In: Adv. Lipid Res.* **11**: 143-192.
73. Heftman, E., and E. Mosettig. (1960) *In: Biochemistry of Steroids.* Reinhold Publishing Corp., New York. **1**: 79-82.
74. Heilmann, H.J., H.J. Maeger, and H.G. Gassen. (1986) Identification and Isolation of Glucose Dehydrogenase Genes of *Bacillus megaterium* M1286 and Their Expression in *Escherichia coli*. *Eur. J. Biochem.* **174**: 485-490.
75. Heneghan, J.B. (1963) Influence of the Microbial Flora on Xylose Absorption in Rats and Mice. *Am. J. Physiol.* **205**: 417-420.
76. Heuman, D.M., C.R. Hernandez, P.B. Hylemon, W.M. Kubaska, C. Hartman, and Z.R. Vlahcevic. (1988) Regulation of Bile Acid Synthesis: I. Effects of Conjugated Ursodeoxycholate and Cholate on Bile Acid Synthesis in Chronic Bile Fistula Rat. *Hepatology* **8**: 358-365.
77. Heuman, D.M., Z.R. Vlahcevic, M.L. Bailey, and P.B. Hylemon. (1988) Regulation of Bile Acid Synthesis: II. Effect of Bile Acid Feeding on Enzymes Regulating Hepatic Cholesterol and Bile Acid Synthesis in the Rat. *Hepatology* **8**: 892-897.
78. Hirano, S., and N. Masuda. (1982) Characterization of NADP-Dependent 7 β -Hydroxysteroid Dehydrogenases from *Peptostreptococcus productus* and *Eubacterium aerofaciens*. *Appl. Environ. Microbiol.* **43**: 1057-1063.
79. Hofmann, A.F. (1988) Bile Acids. pp. 553-572. *In: I.M. Arias, W.B. Jakoby, H. Popper, D. Schachter, and D.A. Shafritz (eds.) The Liver: Biology and Pathology.* Raven Press, Ltd., New York.
80. Hofmann, A.F., and A. Roda (1984) Physiological Properties of Bile Acids and Their Relationship to Biological Properties: An Overview of the Problem. *J. Lipid Res.* **25**: 1477-1489.

81. Holdeman, L.V., I.J. Good, and W.E.C. Moore. (1976) Human Fecal Flora: Variation in Bacterial Composition Within Individuals and a Possible Effect of Emotional Stress. *Appl. Environ. Microbiol.* **31**: 359-375.
82. Holt, P.R. (1964) Intestinal Absorption of Bile Salts in the Rat. *Am. J. Physiol.* **207**: 1-7.
83. Hylemon, P.B. (1985) Metabolism of Bile Acids in Intestinal Microflora. pp. 331-343. *In*: H. Danielsson and J. Sjövall (eds.) *Sterols and Bile Acids*. Elsevier Science Publishers, Amsterdam.
84. Hylemon, P.B., A.F. Cacciapuoti, B.A. White, T.R. Whitehead, and R.J. Fricke. (1980) 7α -Dehydroxylation of Cholic Acid by Cell Extracts of *Eubacterium* species V.P.I. 12708. *Am. J. Clin. Nutr.* **33**: 2507-2510.
85. Hylemon, P.B., and T.L. Glass. (1983) Biotransformation of Bile Acids and Cholesterol by the Intestinal Microflora. pp. 189-213. *In*: D.J. Hentges (ed.) *Human Intestinal Microflora in Health and Disease*. Academic Press, New York.
86. Hylemon, P.B., and J.A. Sherrod. (1975) Multiple Forms of 7α -Hydroxysteroid Dehydrogenase in Selected Strains of *Bacteroides fragilis*. *J. Bacteriol.* **122**: 418-424.
87. IUPAC - IUB Revised Tentative Rules for Nomenclature of Steroids. (1969) *Biochemistry* **8**: 2227-2242; Corrections (1971) *Biochemistry* **10**: 4494-4995.
88. IUPAC Tentative Rules for the Nomenclature of Organic Chemistry. Section E. Stereochemistry. (1970) *J. Org. Chem.* **35**: 2849-2867; (1976) *Pure Appl. Chem.* **45**: 13-30.
89. Jany, K.-D., W. Ulmer, M. Fröschle, and G. Pfeleiderer. (1983) Complete Amino Acid Sequence of Glucose Dehydrogenase from *Bacillus megaterium*. *FEBS Lett.* **165**: 6-10.
90. Jörnvall, H., J.-O. Höög, H. von Bahr-Lindstrom, and B.L. Vallee. (1987) Mammalian Alcohol Dehydrogenases of Separate Classes: Intermediates Between Different Enzymes and Intraclass Isozymes. *Proc. Natl. Acad. Sci. USA* **84**: 2580-2584.
91. Jörnvall, H., M. Perrson, and J. Jeffery. (1981) Alcohol and Polyol Dehydrogenases are Both Divided Into Two Protein Types, and Structural Properties Cross-Relate the Different Enzyme Activities Within Each Type. *Proc. Natl. Acad. Sci. USA* **78**: 4226-4230.

92. Jörnvall, H., H. von Bahr-Linstrom, K.-D. Jeny, W. Ulmer, and M. Frischle. (1984) Extended Superfamily of Short-Polyol-Sugar Dehydrogenases: Structural Similarities Between Glucose and Ribitol Dehydrogenases. *FEBS Lett.* **165**: 190-196.
93. Jungermann, K., M. Kern, V. Riebeling, and R.K. Thauer. (1976) Function and Regulation of Ferredoxin Reduction with NADH in *Clostridia*. pp. 85-94. *In*: J.G. Schlegel, G. Gottschalk, and N. Pfennig, (eds.) *Microbial Production and Utilization of Gases*. Göttingen.
94. Kalb, V.F., and R.W. Bernlohr (1977) A New Spectrophotometric Assay for Proteins in Cell Extracts. *Analyt. Biochem.* **82**: 362-371.
95. Kallner, A. (1967) The Transformation of Deoxycholic Acid into Allodeoxycholic Acid in the Rat. *Acta Chem. Scand.* **21**: 87-92.
96. Kallner, A. (1967) On the Biosynthesis and Metabolism of Allodeoxycholic Acid in the Rat. Bile Acids and Steroids, 175. *Acta Chem. Scand.* **21**: 315-321.
97. Kawamoto, K., I. Horibe, and K. Uchida. (1989) Purification and Characterization of a New Hydrolase for Conjugated Bile Acids, Chenodeoxycholytaurine Hydrolase, from *Bacteroides vulgatis*. *J. Biochem.* **106**: 1049-1053.
98. Kellogg, T.F. (1973) Bile Acid Metabolism in Gnotobiotic Animals. pp. 283-304. *In*: P.P. Nair, and D. Kritchevsky (eds.) *The Bile Acids: Chemistry, Physiology, and Metabolism*. Plenum Press, New York.
99. Kellogg, T.F., and B.S. Wostmann. (1969) Fecal Neutral Steroids and Bile Acids from Germfree Rats. *J. Lipid Res.* **10**: 495-503.
100. Klubes, P., and W.R. Jondorf. (1971) Dimethylnitrosamine Formation from Sodium Nitrite and Dimethylamine by Bacterial Flora of Rat Intestine. *Res. Commun. Chem. Pathol. Pharmacol.* **2**: 23-34.
101. Kobashi, K., I. Nishizawa, T. Yamada, and J. Jase. (1978) A New Hydrolase Specific for Taurine Conjugates of Bile Acids. *J. Biochem.* **84**: 495-497.
102. Krol, A.J.M., J.G.J. Hontelez, B. Roozendaal, and V. van Kammen (1982) On the Operon Structure of the Nitrogenase Genes of *Rhizobium leguminosarum* and *Azotobacter vinelandii*. *Nucleic Acid Res.* **10**: 4147-4157.

103. Krook, M., L. Marekov, and H. Jörnvall. (1990) Purification and Structural Characterization of Placental NAD⁺-Linked 15-Hydroxyprostaglandin Dehydrogenase. The Primary Structure Reveals the Enzyme to Belong to the Short-Chain Alcohol Dehydrogenase Family. *Biochemistry* **29**: 738-743.
104. Kuno, S., A. Bacher, and H. Simon. (1985) Structure of Enoate Reductase from a *Clostridium tyrobutyricum* (C. spec. La1). *Biol. Chem. Hoppe-Seyler* **366**: 463-472.
105. Laemmli, U.K. (1970) Cleavage of Structural Proteins During the Assembly of the Head of Bacteriophage T4. *Nature (London)* **227**: 680-685.
106. Leppik, R.A. (1989) The Genetics of Bile Acid Degradation in *Pseudomonas* ssp.: Location and Cloning of Catabolic Genes. *J. Gen. Microbiol.* **135**: 1989-1996.
107. Lindenbaum, J., D.G. Rund, V.P. Butler, D. Tse-Eng, and G.R. Saha (1981) Inactivation of Digoxin by the Gut Flora: Reversal by Antibiotic Therapy. *N. Engl. J. Med.* **305**: 789-794.
108. Lipsky, R.H., and P.B. Hylemon. (1980) Characterization of a NADH:Flavin Oxidoreductase Induced by Cholic Acid in a 7 α -Dehydroxylating Intestinal *Eubacterium* Species. *Biochim Biophys Acta.* **612**: 328-336.
109. MacDonald, I.A., N.D. Bokkenheusen, H. Winter, A.M. McLernon, and E.H. Mosbach. (1983) Degradation of Steroids in the Human Gut. *J. Lipid Res.* **24**: 675-700.
110. MacDonald, I.A., and Y.P. Rochon. (1983) Affinity Chromatography of Bile Salt 7 α -, 7 β -, and 12 α -Hydroxysteroid Dehydrogenases on Immobilized Procion Red and Cibacron Blue Sepharose 4B Columns. *J. Chromatogr.* **259**: 154-158.
111. MacDonald, I.A., Y.P. Rochon, D.M. Hutchison, and L.V. Holdeman. (1982) Formation of Ursodeoxycholic Acid From Chenodeoxycholic Acid by a 7 β -Hydroxysteroid Dehydrogenase-Elaborating *Eubacterium aerofaciens* strain Cocultured with 7 α -Hydroxysteroid Dehydrogenase-Elaborating Organisms. *Appl. Environ. Microbiol.* **44**: 1187-1195.
112. MacDonald, I.A., B.A. White, and P.B. Hylemon (1983) Separation of 7 α - and 7 β -Hydroxysteroid Dehydrogenase Activities from *Clostridium absoum* ATCC# 27555 and Cellular Response of the Organism to Bile Acid Inducers. *J. Lipid Res.* **24**: 1119-1126.

113. MacDonald, I.A., C.M. Williams, and D.G. Mahony. (1973) 7α -Hydroxysteroid Dehydrogenase from *Escherichia coli* B: Preliminary Studies. *Biochim. Biophys. Acta* **309**: 243-253.
114. MacDonald, I.A., C.M. Williams, and D.G. Mahony. (1974) A 3α -, and 7α -Hydroxysteroid Dehydrogenase Assay for Conjugated Dehydroxy-Bile Acid Mixtures. *Anal. Biochem.* **57**: 127-136.
115. MacDonald, I.A., C.M. Williams, and D.G. Mahony. (1975) Lyophilized 7α -Hydroxysteroid Dehydrogenase: A Stable Enzyme Preparation for Routine Bile Acid Analysis. *J. Lipid Res.* **16**: 244-246.
116. MacDonald, I.A., C.M. Williams, D.G. Mahony, and W.M. Christie. (1975) NAD- and NADP-Dependent 7α -Hydroxysteroid Dehydrogenases from *Bacteroides fragilis*. *Biochim. Biophys. Acta* **384**: 12-24.
117. MacDonald, I.A., C.M. Williams, J.D. Sutherland, and A.C. MacDonald. (1983) Estimation of Ursodeoxycholic Acid in Human and Bear Biles Using *Clostridium absonum* 7β -Hydroxysteroid Dehydrogenase. *Anal. Biochem.* **135**: 349-354.
118. Mahony, D.E., C.E. Neier, I.A. MacDonald, and L.V. Holdeman. (1977) Bile Salt Degradation by Nonfermentive Clostridia. *Appl. Environ. Microbiol.* **34**: 419-423.
119. Maizel, J., and R.P. Lenk (1981) Enhanced Graphic Matrix Analysis of Nucleic Acid and Protein Sequences. *Proc. Natl. Acad. Sci., USA* **78**: 7665-7669.
120. Marekov, L, M. Krook, and H. Jörnvall. (1990) Prokaryotic 20β -Hydroxysteroid Dehydrogenase is an Enzyme of the 'Short-Chain, Non-Metalloenzyme' Alcohol Dehydrogenase Type. *FEBS Lett.* **266**: 51-54.
121. Margalith, P.Z. (1986) *Steroid Microbiology*. Charles C. Thomas, Springfield.
122. Marmur, J. (1961) A Procedure for the Isolation of Deoxyribonucleic Acid from Microorganisms. *J. Mol. Biol.* **3**: 208-218.
123. Masuda, N., H. Oda, and H. Tanaka. (1983) Purification and Characterization of NADP-Dependent 7β -Hydroxysteroid Dehydrogenase from *Peptostreptococcus productus* Strain B-52. *Biochim. Biophys Acta* **755**: 65-69.
124. Midvedt, T. (1974) Microbial Bile Acid Transformation. *Am. J. Clin. Nutr.* **27**: 1341-1347.

125. Midvedt, T. and A. Norman (1967) Bile Acid Transformations by Microbial Strains Belonging to Genera Found in Intestinal Contents. *Acta Pathol. Microbiol. Scand.* **71**: 629-638.
126. Moore, W.E.C., and L.V. Holdeman. (1974) Human Fecal Flora: The Normal Flora of 20 Japanese-Hawaiians. *Appl. Microbiol.* **27**: 961-979.
127. Moore, W.E.C., L.V.H. Moore, and E.P. Cato. (1988) You and Your Flora. *U. S. Fed. Culture Collect.* **18**: 7-22.
128. Mower, H.F., R.M. Ray, R. Shoff, G.M. Stemmerman, A. Momura, G. Gloor, S. Kamiyama, A. Shimada, and H. Yamakawa. (1979) Fecal Bile Acids in Two Japanese Populations with Different Colon Cancer Risks. *Cancer Res.* **39**: 328-331.
129. Murphy, G.M., B.H. Billing, and D.H. Baron. (1970) A Fluorimetric and Enzymatic Method for the Estimation of Serum Total Bile Acids. *J. Clin. Path.* **23**: 594-598.
130. Myant, N.B., and K.A. Mitropoulos. (1977) Cholesterol 7 α -Hydroxylase. *J. Lipid Res.* **18**: 135-153.
131. Nambiar, K.P., D.M. Stauffer, P.A. Kolodziej, and S.A. Benner. (1983) A Mechanistic Basis for the Stereoselectivity of Enzymatic Transfer of Hydrogen from Nicotinamide Cofactors. *J. Am. Chem. Soc.* **105**: 5886-5890.
132. Needleman, S.B., and C.D. Wunsch. (1970) A General Method Applicable to the Search for Similarities in the Amino Acid Sequence of Two Proteins. *J. Mol. Biol.* **48**: 443-453.
133. Nicolas, J.-C., A.M. Boussioux, B. Descomps, and A.C. DePaulet. (1979) Enzymatic Determination of Estradiol and Estrone in Plasma and Urine. *Clin. Chim. Acta* **92**: 1-9.
134. Olson, G.B., and B.S. Wostmann. (1966) Lymphocytopoiesis, Plasmacytopoiesis and Cellular Proliferation in Non-antigenically Stimulated Germfree Mice. *J. Immunol.* **97**: 267-274.
135. Ottolina, G., S. Riva, G. Carrea, B. Danieli, and A.F. Buckmann. (1989) Enzymatic Synthesis of [4R-²H]HAD(P)H and [4S-²H]NAD(P)H and Determinations of the Stereospecificity of 7 α - and 12 α -Hydroxysteroid Dehydrogenase. *Biochim. Biophys. Acta* **998**: 173-178.

136. Ouchterlony, O. and L.A. Nilsson. (1973) Immunodiffusion and Immuno-electrophoresis. Chapter 19. In: D.M. Weir (ed.) *Handbook of Experimental Immunology*. Blackwell.
137. Paone, D.A.M., and P.B. Hylemon (1984) HPLC Purification and Preparation of Antibodies to Cholic Acid-Inducible Polypeptides from *Eubacterium* sp. V.P.I. 12708. *J. Lipid Res.* **25**: 1343-1349.
138. Payne, D.W., M. Shikita, and P. Talalay. (1982) Enzymatic Estimation of Steroids in Subpicomole Quantities by Hydroxysteroid Dehydrogenases and Nicotinamide Nucleotide Cycling. *J. Biol. Chem.* **257**: 633-642.
138. Payne, D.W., and P. Talalay. (1985) Isolation of Novel Microbial 3 α -, 3 β -, and 17 β -Hydroxysteroid Dehydrogenases. Purification, Characterization, and Analytical Applications of a 17 β -Hydroxysteroid Dehydrogenase from an *Alcaligenes* sp. *J. Biol. Chem.* **260**: 13648-13655.
140. Pearson, W.R., and D.J. Lipman (1988) Improved Protocol for Biological Sequence Comparison. *Proc. Natl. Acad. Sci., USA* **85**: 2444-2448.
141. Peltoketo, H., V. Isomaa, O. Mäentausta, and R. Vihko. (1988) Complete Amino Acid Sequence of Human Placental 17 β -Hydroxysteroid Dehydrogenase Deduced from cDNA. *FEBS Lett.* **239**: 73-77.
142. Peppercorn, M.A., and P. Goldman (1972) The Role of Intestinal Bacteria in the Metabolism of Salicylazosulfapyridine. *J. Pharmacol. Exp. Ther.* **181**: 555.
143. Prabha, V., M. Gupta, D. Seiffge, and K.G. Gupta. (1990) Purification of 7 α -Hydroxysteroid Dehydrogenase from *Escherichia coli* strain 080. *Can. J. Microbiol.* **36**: 131-135.
144. Reddy, B.S., and B.S. Wostmann. (1966) Intestinal Disaccharidase Activities in the Growing Germfree and Conventional Rats. *Arch. Biochem. Biophys.* **113**: 609-616.
145. Reddy, B.S., J.R. Pleasants, and B.S. Wostmann. (1969) Effect of Intestinal Microflora on Calcium, Phosphorus, and Magnesium Metabolism in Rats. *J. Nutr.* **99**: 353-362.
146. Rosenberg, M., and D. Court. (1979) Regulatory Sequences Involved in the Promotion and Termination of RNA Transcription. *Annu. Rev. Genet.* **13**: 319-353.
147. Sabine, J.R. (ed.) (1983) 3-Hydroxy-3-Methylglutaryl Coenzyme A Reductase. CRC Press, Boca Raton.

148. Samuelsson, B. (1960) Bile Acids and Steroids. (96) On the Mechanism of the Biological Formation of Deoxycholic Acid From Cholic Acid. *J. Biol. Chem.* **235**: 361-366.
149. Sanger, F., S. Nicklen, and A.R. Coulson. (1977) DNA Sequencing With Chain-Terminating Inhibitors. *Proc. Natl. Acad. Sci. U.S.A.* **74**: 5463-5467.
150. Savage, D.C. (1972) Association and Physiological Interactions of Indigenous Microorganisms and Gastrointestinal Epithelia. *Am. J. Clin. Nutr.* **25**: 1372-1379.
151. Savage, D.C. (1977) Microbial Ecology of the Gastrointestinal Tract. *Ann. Rev. Microbiol.* **31**: 107-133.
152. Scholmerich, J., M.S. Becher, K. Schmidt, R. Shubert, B. Kremer, S. Felhaus, and W. Gerok. Influence of Hydroxylation and Conjugation of Bile Salts on Their Membrane Damaging Properties. Studies on Isolated Hepatocytes and Lipid Membrane Vesicles. *Hepatology* **4**: 661-666.
153. Shaw, C.R., and R. Prasad (1970) Starch Gel Electrophoresis of Enzymes-A Compilation of Recipes. *Biochem. Genet.* **4**: 297-320.
154. Sherrod, J.A., and P.B. Hylemon. (1977) Partial Purification and Characterization of NAD-Dependent 7α -Hydroxysteroid Dehydrogenase from *Bacteroides thetaiotaomicron*. *Biochim. Biophys. Acta* **468**: 351-358.
155. Shimada, K., K.S. Bricknell, and S.M. Finegold. (1969) Deconjugation of Bile Acids by Intestinal Bacteria: Review of the Literature and Additional Studies. *J. Infect. Dis.* **119**: 273-281.
156. Shultz, R.M., E.V. Groman, and L.L. Engel. (1977) $3(17)\beta$ -Hydroxysteroid Dehydrogenase of *Pseudomonas testosteroni*. A Convenient Purification and Demonstration of Multiple Forms. *J. Biol. Chem.* **252**: 3775-3783.
157. Sjövall, J. (1960) Bile Acids in Man Under Normal and Pathological Conditions: Bile Acids and Steroids 73. *Clin. Chim. Acta* **5**: 33-41.
158. Skåljegg, B.A. (1974) 3α -Hydroxysteroid Dehydrogenase from *Pseudomonas testosteroni*: Kinetic Properties with NAD and Its Thionicotinamide Analogue. *Eur. J. Biochem.* **50**: 603-609.
159. Small, D.M. (1971) The Physical Chemistry of Cholanic Acids. pp. 249-356. In: P.P. Nair and D. Kritchevsky (eds.) *The Bile Acids*. Plenum Press, New York.

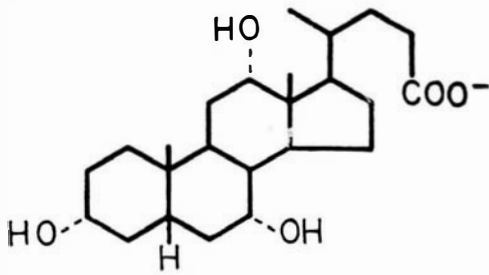
160. Smith, H.W. (1965) Observations on the Flora of the Alimentary Tract of Animals and Factors Affecting Its Composition. *J. Pathol. Bacteriol.* **89**: 95-122.
161. Smith, C.S., H.I. Pilgrim, and D. Steinmuller. (1972) The Survival of Skin Allografts and Xenografts in Germ-Free Mice. *Transplantation* **13**: 38-41.
162. Southern, E.M. (1975) Detection of Specific Sequences Among DNA Fragments Separated by Gel Electrophoresis. *J. Mol. Biol.* **98**: 503-517.
163. Stellwag, E.J., and P.B. Hylemon (1976) Purification and Characterization of Bile Salt Hydrolase from *Bacteroides fragilis* subsp. *fragilis*. *Biochim. Biophys. Acta.* **542**: 165-176.
164. Stellwag, E.J., and P.B. Hylemon (1979) 7α -Dehydroxylation of Cholic Acid and Chenodeoxycholic Acid by *Clostridium leptum*. *J. Lipid Res.* **20**: 325-333.
165. Stevens, C.E. (1977) *Comparative Physiology of the Digestive System*. Ithaca: Cornell University.
166. Stokes, N.A., and P.B. Hylemon. (1985) Characterization of Δ^4 -3-Ketosteroid 5β -Reductase and 3β -Hydroxysteroid Dehydrogenase in Cell Extracts of *Clostridium innocuum*. *Biochim. Biophys. Acta* **836**: 255-261.
167. Street, J.M., D.I.H. Trafford, and H.L.J. Makin. (1983) The Quantitative Estimation of Bile Acids and Their Conjugates in Human Biological Fluids. *J. Lipid Res.* **24**: 491-511.
168. Sutherland, J.D., D.M. Hutchinson, and C.N. Williams. (1988) Lyophilized *Clostridium perfringens* 3α - and *Clostridium bifermentans* 7α -Hydroxysteroid Dehydrogenases: Two Stable Enzyme Preparations for Routine Bile Acid Analysis. *Biochim. Biophys. Acta* **962**: 116-121.
169. Tazume, S., K. Hashimoto, and S. Sasaki. (1979) Intestinal Flora and Bile Acids Metabolism: Influence of Bile Acids on Rejection of *Shigella flexneri* 2a from the Intestine. *Nippon Saikingaku Zasshi* **34**: 745-754.
170. Thatcher, D.R. (1980) The Complete Amino Acid Sequence of 3-Alcohol Dehydrogenase Alloenzymes (Adh^{N-11} , Adh^S , and Adh^{UP}) From the Fruit Fly *Drosophila melanogaster*. *Biochem. J.* **187**: 875-883.
171. Usui, E., and K. Okuda. (1986) Identification of $7\alpha,12\alpha$ - 5β -cholestan-3-one 3α -Reductase as 3α -Hydroxysteroid Dehydrogenase. *Biochim. Biophys. Acta* **877**: 158-166.

172. Vlahcevic, Z.R., D.M. Heuman, and P.B. Hylemon. (1990) pp. 341-377. Physiology and Pathophysiology of Enterohepatic Circulation of Bile Acids. *In: D. Zakim, and T.D. Boyer (eds.) Hepatology*. W.B. Saunders Co., Philadelphia.
173. Whitaker, H.R. (1963) Determination of Molecular Weights of Proteins by Gel Filtration on Sephadex. *Anal. Chem.* **35**, 1950-1954.
174. White, B.A., A.F. Cacciapuoti, R.J. Fricke, T.R. Whitehead, E.H. Mosbach, and P.B. Hylemon. (1981) Cofactor Requirements for 7 α -Dehydroxylation of Cholic and Chenodeoxycholic Acid in Cell Extracts of the Intestinal Anaerobic Bacterium, *Eubacterium* species V.P.I. 12708. *J. Lipid Res.* **22**: 891-898.
175. White, B.A., R.J. Fricke, and P.B. Hylemon. (1982) 7 β -Dehydroxylation of Ursodeoxycholic Acid by Whole Cells and Cell Extracts of the Intestinal Anaerobic Bacterium, *Eubacterium* Species VPI 12708. *J. Lipid Res.* **23**: 145-153.
176. White, B.A., R.L. Lipsky, R.J. Fricke, and P.B. Hylemon. (1980) Bile Acid Induction Specificity of 7 α -Dehydroxylase Activity in an Intestinal *Eubacterium* Species. *Steroids* **35**: 103-109.
177. White, B.A., D.A.M. Paone, A.F. Cacciapuoti, R.J. Fricke, E.H. Mosbach, and P.B. Hylemon. (1983) Regulation of Bile Acid 7-Dehydroxylase Activity by NAD⁺ and NADH in Cell Extracts of *Eubacterium* species V.P.I. 12708. *J. Lipid Res.* **24**: 20-27.
178. White, W.B., J.P. Coleman, and P.B. Hylemon. (1988) Molecular Cloning of a Gene Encoding a 45,000-Dalton Polypeptide Associated With Bile Acid 7-Dehydroxylation in *Eubacterium* sp. Strain VPI 12708. *J. Bacteriol.* **170**: 611-616.
179. White, W.B., C.V. Franklund, J.P. Coleman, and P.B. Hylemon. (1988) Evidence for a Multigene Family Involved in Bile Acid 7-Dehydroxylation in *Eubacterium* sp. Strain VPI 12708. *J. Bacteriol.* **170**: 4555-4561.
180. Yolton, D.P., C. Stanley, and D.C. Savage (1971) Influence of the Indigenous Gastrointestinal Microbial Flora on Duodenal Alkaline Phosphatase Activity in Mice. *Infect Immun.* **3**: 768-773.
181. Zakim, D. (1990) pp. 65-96. Metabolism of Glucose and Fatty Acids by the Liver. *In: D. Zakim, and T.D. Boyer (eds.) Hepatology* W.B. Saunders Co., Philadelphia.

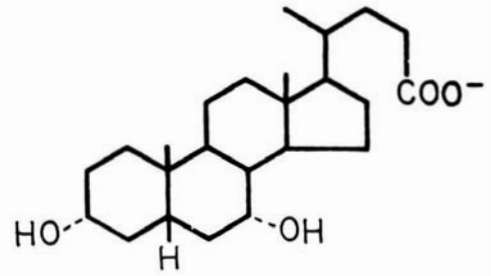
182. Zuker, M., and P. Stiegler (1981) Optimal Computer Folding of Large RNA Sequences Using Thermodynamics and Auxillary Information. *Nucl. Acids Res.* **9**: 133-148.

APPENDIX

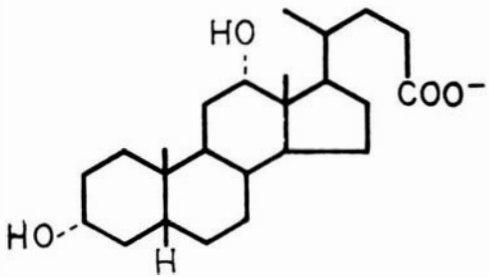
Structures of Bile Acids and Intermediates.



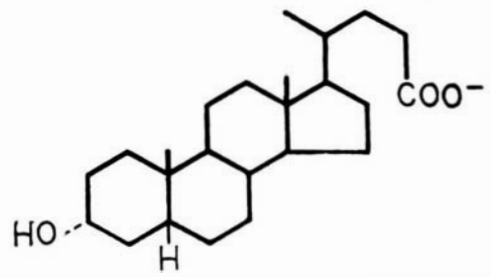
Cholic Acid



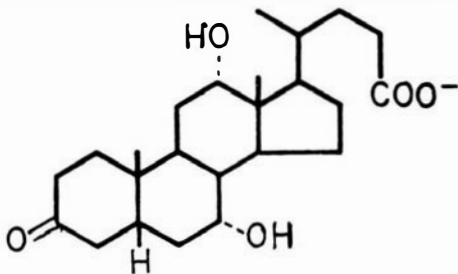
Chenodeoxycholic Acid



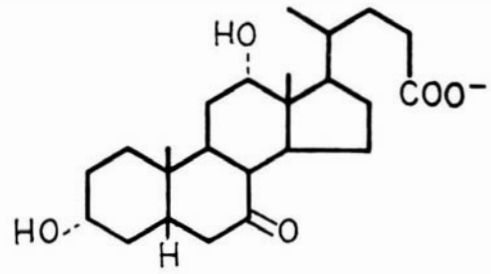
Deoxycholic Acid



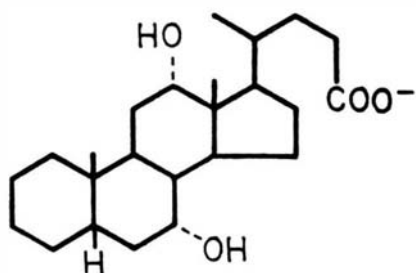
Lithocholic Acid



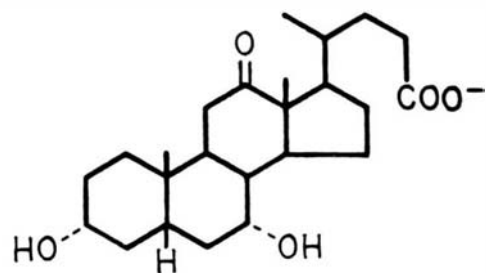
3-oxo-Cholic Acid



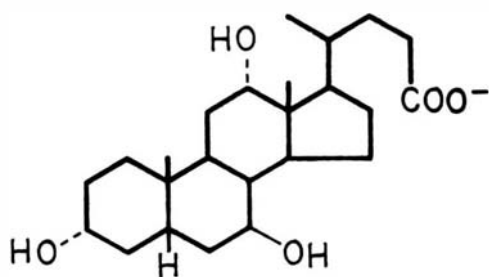
7-oxo-Cholic Acid



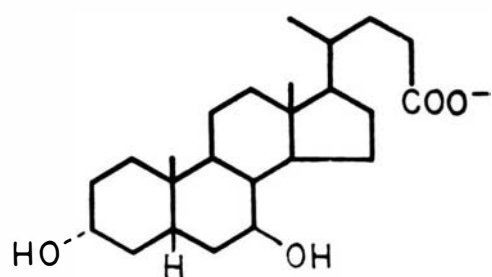
3-Deoxycholic Acid



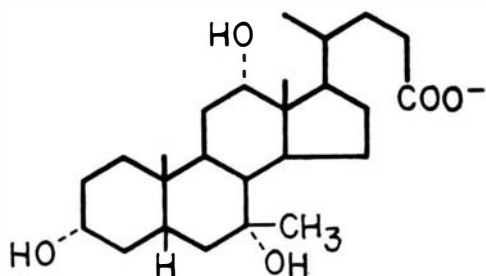
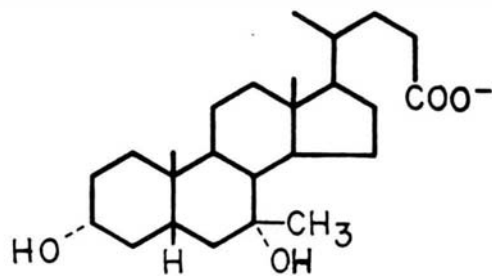
12-oxo-Cholic Acid

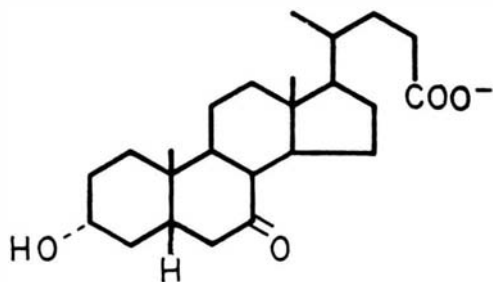


Ursocholic Acid

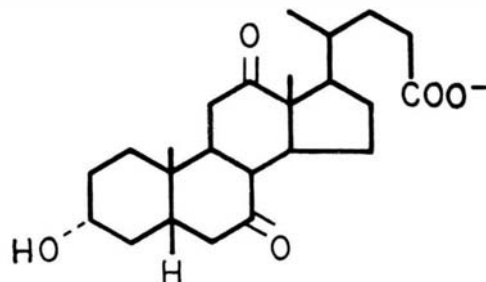


Ursodeoxycholic Acid

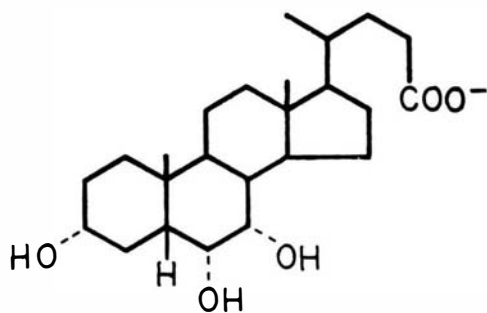
7 β -Methyl Cholic Acid7 β -Methyl Chenodeoxycholic Acid



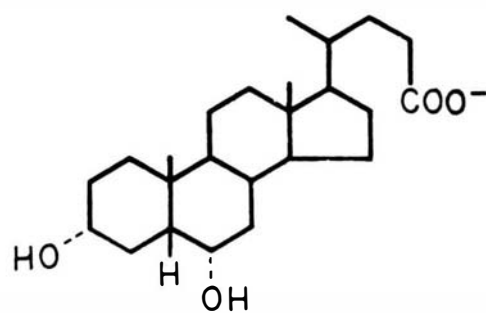
7-oxo-Chenodeoxycholic Acid



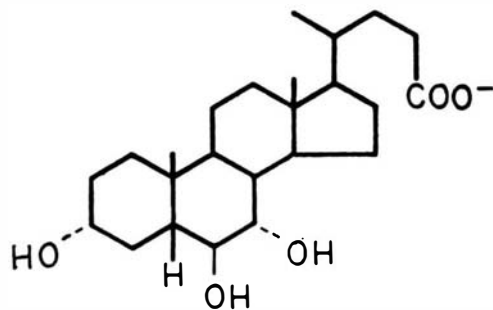
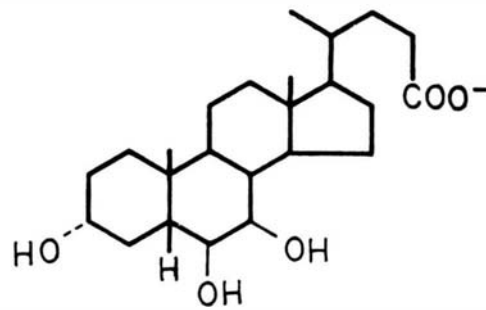
7,12-di-oxo-Cholic Acid

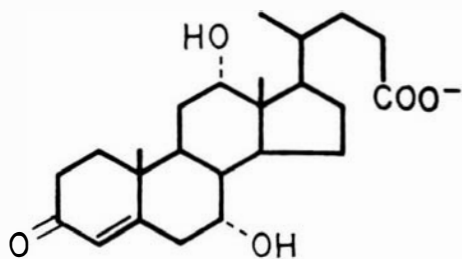
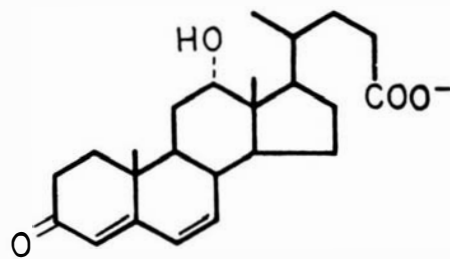
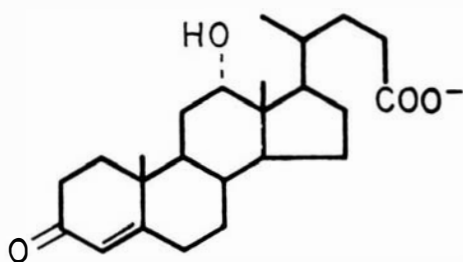
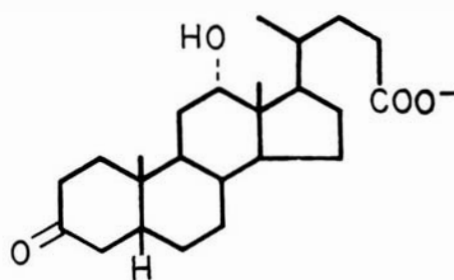


Hyocholic Acid

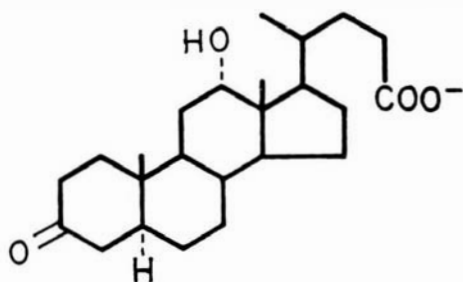


Hyodeoxycholic Acid

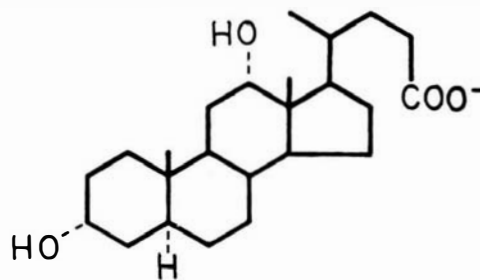
 α -Muricholic Acid β -Muricholic Acid

3-oxo- Δ^4 -Cholic Acid3-oxo- $\Delta^{4,6}$ -Deoxycholic Acid3-oxo- Δ^4 -Deoxycholic Acid

3-oxo-Deoxycholic Acid



3-oxo-Allo-Deoxycholic Acid



Allo-Deoxycholic Acid

VITA

